Chapter 4
Observations in the Ocean

Bert Rudels, Leif Anderson, Patrick Eriksson, Eberhard Fahrbach, Martin Jakobsson, E. Peter Jones, Humfrey Melling, Simon Prinsenberg, Ursula Schauer, and Tom Yao

Abstract The chapter begins with an overview of the exploratory work done in the Arctic Ocean from the mid nineteenth century to 1980, when its main features became known and a systematic study of the Arctic Ocean evolved. The following section concentrates on the decade between 1980 and 1990, when the first scientific icebreaker expeditions penetrated into the Arctic Ocean, when large international programme were launched, and the understanding of the circulation and of the processes active in the Arctic Ocean deepened. The main third section deals with the studies and the advances made during the ACSYS decade. The section has three headings: the circulation and the transformation of water masses; the changes that have been observed in the Arctic Ocean, especially during the last decades; and the transports between the Arctic Ocean and the surrounding world ocean through the different passages, Fram Strait, Barents Sea, Bering Strait and the Canadian Arctic Archipelago. In section

B. Rudels (✉)
Department of Physics, University of Helsinki, P.O. Box 64, FI-00014 Helsinki, Finland

Finnish Meteorological Institute, P.O. Box 503, FI-00101 Helsinki, Finland
e-mail: bert.rudels@helsinki.fi; bert.rudels@fmi.fi

L. Anderson
Department of Chemistry, University of Gothenburg, SE-41296 Göteborg, Sweden
e-mail: leifand@chalmers.se

P. Eriksson
Finnish Meteorological Institute, P.O. Box 503, FI-00101 Helsinki, Finland
e-mail: Patrick.Eriksson@fmi.fi

E. Fahrbach • U. Schauer
Alfred-Wegener-Institute for Polar and Marine Research, P.O. Box 120161, D-27515 Bremerhaven, Germany
e-mail: Eberhard.Fahrbach@awi.de; Ursula.schauer@awi.de

M. Jakobsson
Department of Geological Sciences, Stockholm University, SE-10691 Stockholm, Sweden
e-mail: martin.jakobsson@geo.su.se

P. Lemke and H.-W. Jacobi (eds.), *Arctic Climate Change: The ACSYS Decade and Beyond,* Atmospheric and Oceanographic Sciences Library 43,
DOI 10.1007/978-94-007-2027-5_4,

four, the Arctic Ocean is considered as a part of the Arctic Mediterranean Sea, and the impacts of possible climatic changes on the circulation in the Arctic Mediterranean and on the exchanges with the world ocean are discussed.

Keywords Arctic Ocean • Arctic Mediterranean Sea • Ocean Circulation • Water mass formation • Water mass transformation • Mixing • Open ocean convection Thermohaline circulation • Boundary convection • Intrusions • Double-diffusive convection

4.1 Mid 1800–1980: Exploration

Because of the severe high-latitude climate and the perennial ice cover, little was known about the Arctic Ocean 100 years before the beginning of the ACSYS decade. Was it an ocean, or did large, yet undetected, landmasses exist? Was open water to be found behind the forbidding ice fields? Large polynyas had been observed beyond the coastal ice cover, and the northernmost extension of the Gulf Stream was believed to transport warm water into the Arctic Ocean west of Svalbard. Because sea ice contains so little salt, it was also speculated that only freshwater freezes. Once a ship got beyond the pack ice formed in the low-salinity water influenced by runoff from the continents, it would encounter an ice-free ocean with saline water supplied by the Gulf Stream (Petermann 1865).

Driftwood, originating from Siberia, had been found on the Greenland coasts, indicating a flow of ice, or water, across the Polar Sea, exiting between Greenland and Svalbard. Finally, remnants from the wreck of the steamship *Jeanette*, crushed by the ice in the East Siberian Sea in 1881 in its attempt to reach the North Pole from Bering Strait, were found at Julianehåb in southwestern Greenland in 1884. This confirmed the existence of a rapid stream carrying ice across the Arctic Ocean from the East Siberian Sea to the East Greenland Current, flowing southward along the east coast of Greenland. This discovery was, perhaps, decisive for Nansen's plan to reach the North Pole by allowing a ship to be frozen into the ice – no open water was expected by Nansen – upstream of this transpolar stream and then drift across the Polar Sea, passing the pole.

E.P. Jones • S. Prinsenberg
Department of Fisheries and Oceans, Bedford Institute of Oceanography, P.O. Box 1006, Dartmouth NS B2Y 4A2, Canada
e-mail: Peter.Jones@dfo-mpo.gc.ca; Simon.Prinsenberg@dfo-mpo.gc.ca

H. Melling
Institute of Ocean Sciences, Fisheries and Oceans Canada, Sidney, BC, Canada, V8L 4B2
e-mail: Humfrey.Melling@dfo-mpo.gc.ca

T. Yao
3989 W 18th Ave, Vancouver, BC, Canada V6S 1B6
e-mail: tomyao@telus.net

The drift of *Fram* 1893–1896, although it never reached the pole, provided the first information of the Arctic Ocean beneath the ice (Nansen 1902). It was deep, >3,000 m, and below the ice and the cold, low-salinity surface water, the salinity was observed to increase towards the bottom, and a layer with temperatures above 0°C was found between 200 and 500 m depth. Nansen concluded that the warm layer was Atlantic water advected into the Arctic Ocean from the Norwegian Sea through the passage west of Svalbard–Petermann's Gulf Stream. Nansen also suggested that the high salinity of the deep water was caused by freezing and brine rejection on the Arctic Ocean shelves, where the brine-enriched water sinks to and accumulates at the bottom. The salinity of the shelf bottom water increases during winter, and as it eventually crosses the shelf break, it sinks into the deep Arctic Ocean basins. In a later work, largely based on Amundsen's oceanographic observations on *Gjöa* in 1901, Nansen examined the possibility to form dense, saline water in the eastern Barents Sea (Nansen 1906). In that work, he also discussed open ocean convection and deep-water formation in the Greenland Sea. The salinities determined on *Fram* were later found erroneous, and Nansen adopted the view that the deep waters of the Arctic Ocean were advected from deep-water formation area in the Greenland Sea (Nansen 1915). Nansen also noted that sea ice drifted to the right of the wind and assumed that this was an effect of the earth's rotation. This observation eventually led to the formulation of the theory of wind-driven ocean currents and to the discovery of the Ekman spiral (Ekman 1905).

During the following 80 years, up to 1980, the study of the Arctic Ocean retained much of its early exploratory character. Amundsen attempted to reach the North Pole from Bering Strait with *Maud* 1919–1925, but the vessel got trapped in the ice in the East Siberian Sea and never crossed the shelf break. An effort to enter the Arctic Ocean through Fram Strait, the passage between Greenland and Svalbard, using a discarded submarine, *Nautilus*, was attempted in 1931, but due to technical problems, *Nautilus* only reached slightly north of Svalbard. The icebreaker *Sedov*, involuntarily, repeated the drift of *Fram* 1937–1940, and the first Soviet ice drift station, North-pole 1, lead by Papanin, was established by aircraft at the North Pole in May 1937, and the research group was picked up by the icebreaker *Taymyr* in the East Greenland Current in February 1938 (Libin 1946; Buinitsky 1951). This drift station was followed by many others, most of them launched by the Soviet Union, but also other countries contributed as with e.g. T3 ice island, and the AIDJEX and LOREX ice camps. A comprehensive oceanographic survey of the entire Arctic Basin was made using aviation during two spring seasons of 1955 and 1956. In 1973–1979, seven such surveys were made following each other with a yearly interval and a total number of stations of 1,229. These data were used for preparation of charts in the Atlas of the Arctic Ocean (Gorshov 1980) and in the Atlas of the Arctic (Treshnikov 1985).

The knowledge of the bathymetry improved steadily, and the large extension of the shelves and the existence and location of the major ridges and deep basins became gradually known. More than half (53%) of the 9.5×10^{12} m^2 large Arctic Ocean is now known to consist of shelf areas (Jakobsson et al. 2004a). The deep ocean is divided into two main basins, the Eurasian Basin and the Canadian Basin,

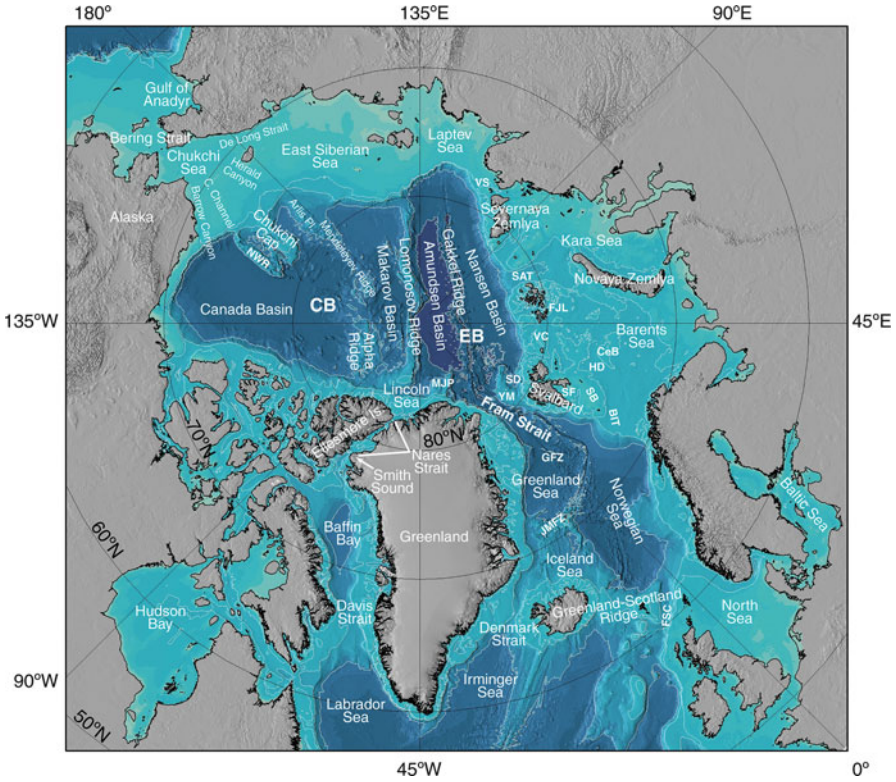

Fig. 4.1 Map of the Arctic Mediterranean Sea showing geographical and bathymetric features. The bathymetry is from IBCAO updated data base (Jakobsson et al. 2004b; Jakobson et al. 2008), and the projection is Lambert Equal Area. The 200, 500, 2,000 and 4,000 m isobaths are shown. *BIT* Bear Island Trough, *CB* Canadian Basin, *CeB* Central Bank, *EB* Eurasian Basin, *FJL* Franz Josef Land, *GFZ* Greenland Fracture Zone, *FSC* Faroe Shetland Channel, *HD* Hopen Deep, *JMFZ* Jan Mayen Fracture Zone, *MJP* Morris Jessup Plateau, *NwR* Northwind Ridge, *SAT* St. Anna Trough, *SB* Svalbrad Bank, *SD* Sofia Deep, *SF* Storfjorden, *YP* Yermak Plateau, *VC* Victoria Channel, *VS* Vilkiltskij Strait (Rudels 2009)

by the Lomonosov Ridge, sill depth ca 1,600 m. The Eurasian Basin is further separated into the deeper (4,500 m) Amundsen Basin and the somewhat shallower Nansen Basin (4,000 m) by the Gakkel Ridge. The Canadian Basin is separated by the Alpha and Mendeleyev ridges into the 4,000 m deep Makarov Basin and the shallower (3,800 m) and larger Canada Basin (Fig. 4.1). Airborne expeditions during spring allowed for hydrographic observations from the ice, covering extensive regions. Especially in the 1950s and in the mid 1970s, the Soviet airborne expeditions extended almost over the entire Arctic Ocean.

The picture of the deep Arctic Ocean, the northernmost part of the North Atlantic, that evolved was one of an ice-covered, strongly stratified ocean, whose water column was dominated by advection from the neighbouring seas and oceans. The large river runoff and the inflow of low-salinity Pacific water through Bering Strait form

the low-salinity polar surface water, with an upper, winter homogenised Polar Mixed Layer (PML) closest to the ice. In summer, seasonal ice melt creates a 10–20-m surface layer of still lower salinity (Coachman and Barnes 1961; Coachman and Aagaard 1974). The salinity starts to increase below the PML, at about 50 m, but the temperature remains close to freezing until it suddenly increases as the Atlantic layer is encountered between 100 and 250 m depth. This cold layer, between the PML and the Atlantic water, was named the Arctic Ocean halocline (Coachman and Aagaard 1974). In the Canadian Basin the PML is less saline than in the Eurasian Basin due to the inflow of low-salinity Pacific water. The Pacific water entering during winter, the Bering Sea Winter Water (BSWW), is colder and more saline and also contributes to the halocline (Coachman and Barnes 1961). In the Eurasian Basin the PML is more saline and Pacific water is practically absent, and additional sources for the halocline water had to be considered (Fig. 4.2). It was realised that it could not be created by direct mixing between the PML and the Atlantic water, and Coachman and Barnes (1962) suggested that Atlantic water is brought onto the shelves through deeper canyons, becomes cooled and diluted by less-saline surface water and eventually returns to the deep basins, intruding between the PML and the Atlantic layer.

The Atlantic layer was observed throughout the Arctic Ocean, being colder and less saline in the Canada Basin than at its entrance through Fram Strait as a part of the West Spitsbergen Current (Timofeyev 1960; Coachman and Barnes 1963). The deep water in the Arctic Ocean was assumed supplied from the Greenland Sea through Fram Strait (Nansen 1915; Wüst 1941). It is warmer than in the Greenland Sea, and the deep Canadian Basin is warmer than the deep Eurasian Basin. The latter was explained by the presence of the Lomonosov Ridge, which would prevent the densest water from the Greenland Sea to penetrate further into the Arctic Ocean. This temperature difference was in fact used as evidence for the existence of a ridge dividing the Arctic Ocean in two major basins before the Lomonosov Ridge was properly mapped (Worthington 1953). Another indication of the presence of a submarine ridge was the retarding of the tidal wave entering through Fram Strait (Harris 1911; Fjeldstad 1936).

The circulation of the ice and the surface water was found to be anti-cyclonic, centred around the Beaufort Gyre north of the North American continent, with the transpolar drift (TPD) moving across the Arctic Ocean in two branches, the Siberian branch from the Siberian shelves and the transpolar branch detaching from the western side of the Beaufort Gyre (Fig. 4.3). The movements of the Atlantic and deeper water masses, by contrast, were deduced from water mass properties, mainly temperature, to be cyclonic around the Arctic Ocean (e.g. Timofeyev 1960; Coachman and Barnes 1963; Coachman and Aagaard 1974).

The ice camps offered opportunities to measure the velocity profiles underneath the ice and Hunkins (1966) documented the existence of the Ekman spiral, the velocity at the surface was 45° to the right of the wind and decreased and turned further to the right with increasing depth. Hunkins separated the velocity into three components: a geostrophic velocity caused by the sea surface slope, a turbulent, 1–2 m thick, boundary layer just below the ice and moving in the same direction as the ice and the Ekman spiral caused by the wind as predicted by Ekman (1905).

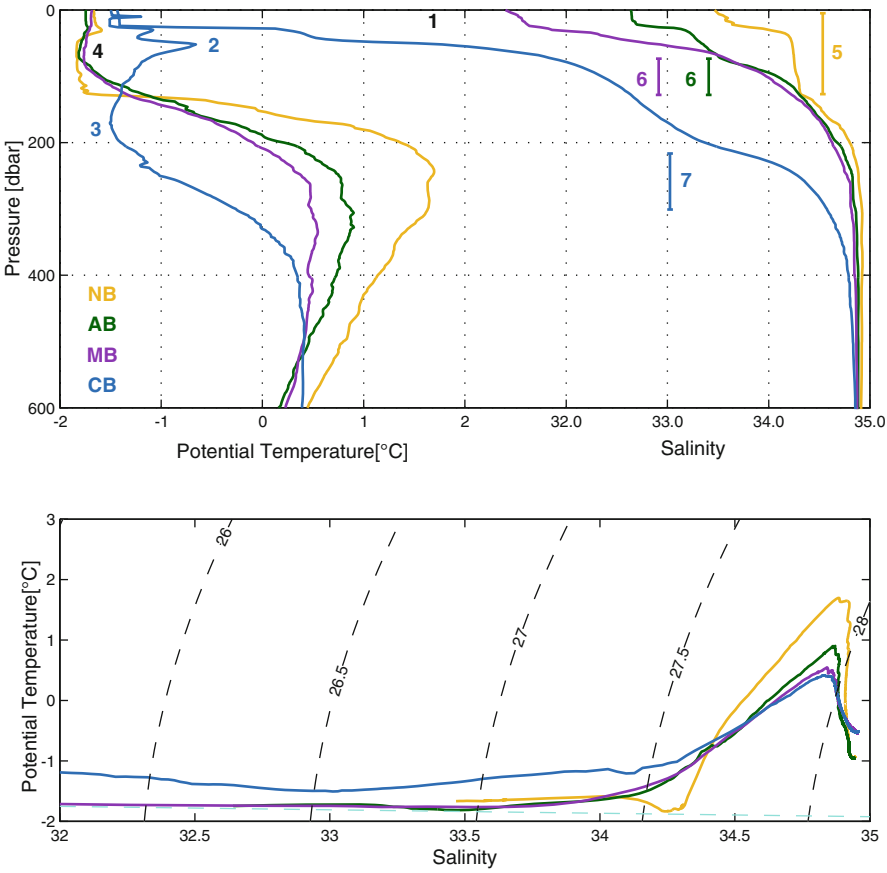

Fig. 4.2 The characteristics of the upper layers in the different basins of the Arctic Ocean. (**a**) potential temperature and salinity profiles, and (**b**) ΘS curves. *Yellow* Nansen Basin, *Green* Amundsen Basin, *Magenta* Makarov Basin, *Blue* Canada Basin. *1* Summer melt water layers, *2* Temperature maximum related to the Bering Strait summer inflow, *3* upper halocline, *4* Temperature minimum created by winter convection, marking the lower limit of the Polar Mixed Layer, *5* Winter-mixed layer in the Nansen Basin, *6* lower halocline in the Amundsen (*green*) and Makarov (*magenta*) basins, *7* lower halocline in the Canada Basin (Adapted from Rudels et al. 2004a). The positions of the stations are shown in Fig. 4.19a

High velocity events in the upper part of the water column were noticed already during the drift of the first ice station, NP-1, and were suggested to be connected with high-energy eddies (Shirshov 1944). Similar events were encountered on the later ice stations (Belyakov and Volkov 1980) and during the AIDJEX experiment (Hunkins 1974; Newton et al. 1974). The eddies were 10 to 20 km in diameter and highly energetic with the maximum azimuthal velocities located around 150 m depth and reaching 40–60 cm s^{-1}. These eddies, mostly anti-cyclonic, were mainly found in the Canada Basin and were commonly associated with anomalous Θ-S characteristics suggesting the presence of a different water mass. Hunkins (1974)

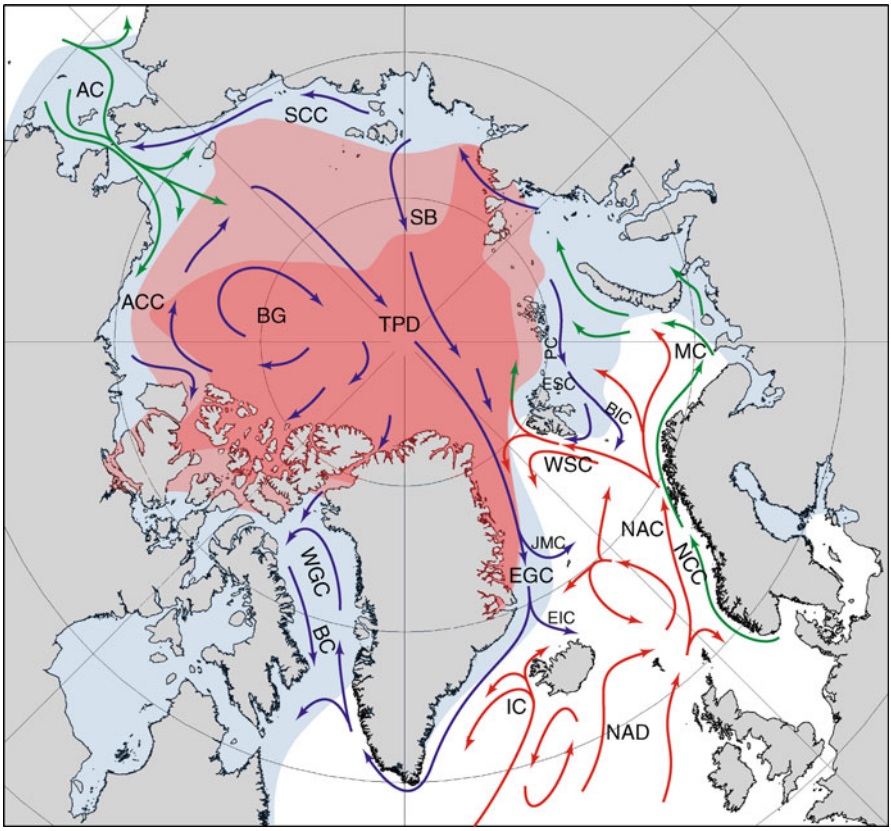

Fig. 4.3 The circulation of the upper layers of the Arctic Mediterranean Sea. Warm Atlantic currents are indicated by red arrows and cold, less-saline polar and arctic currents by *blue arrows*. Low-salinity transformed currents are shown by *green arrows*. The maximum ice extent is shown in *blue* and the minimum ice extent in *red*. The absolute minimum, to date, of 2007 is shown in *dark red*. *AC* Anadyr Current, *ACC* Alaskan Coastal Current, *BC* Baffin Current, *BIC* Bear Island Current, *BG* Beaufort Gyre, *EGS* East Greenland Current, *EIC* East Iceland Current, *ESC* East Spitsbergen Current, *IC* Irminger Current, *JMC* Jan Mayen Current, *MC* Murman Current, *NAD* North Atlantic Drift, *NAC* Norwegian Atlantic Current, *NCC* Norwegian Coastal Current, *PS* Persey Current, *SB* Siberian branch (of the Transpolar Drift), *SCC* Siberian Coastal Current, *TPD* Transpolar Drift, *WGC* West Greenland Current, *WSC* West Spitsbergen Current (Adapted from Rudels 2001)

assumed that the eddies were generated by baroclinic instability as the inflowing Pacific water entered the Canada Basin in the Barrow Canyon, north of Alaska. This idea was later supported by theoretical work by Hart and Killworth (1976).

The exchanges between the Arctic Ocean and the world ocean through the different passages were studied by hydrographic observations and by direct current measurements, and several budgets for the Arctic Ocean and for the Nordic Seas (the Greenland, Iceland and Norwegian seas) were presented (e.g. Mosby 1962; Vowinckel and Orvig 1970; Aagaard and Greisman 1975; Nikiforov and Shpaiker 1980).

Fram Strait, connecting the Arctic Ocean with the Nordic Seas, is the only deep (2,600 m) passage and the only one where steady in- and outflows occur. A second connection between the Arctic Ocean and the Nordic Seas is over the broad and fairly shallow (200–300 m) Barents Sea, where mainly an inflow to the Arctic Ocean takes place. An inflow from the Pacific Ocean occurs through the narrow and shallow (50 m) Bering Strait, while the restricted, shallow (125–230 m) passages in the Canadian Arctic Archipelago are dominated by outflow of low-salinity polar surface water.

The most cited transport estimates through the different passages around 1980 were (+ in, − out); Bering Strait; +1.5 Sv, the Canadian Arctic Archipelago; −2.1 Sv, the Barents Sea; +0.6 Sv, Fram Strait; Atlantic water +7.1 Sv, polar surface water −1.8 Sv, modified Atlantic water −5.3 Sv provided by Aagaard and Greisman (1975). In this budget, the transports through Fram Strait were assumed to balance. Such large inflow of warm Atlantic water raised the question: What will happen if the freshwater input to the Arctic Ocean diminishes? Will the heat stored in the Atlantic layer then reach the surface and melt the ice? The importance of the halocline, acting as a barrier to such vertical heat flux, was then also appreciated (Aagaard and Coachman 1975).

The knowledge of the Arctic Ocean oceanography gained during the first eight decades of the twentieth century is admirably summarised and presented in the Atlas of the Arctic Ocean (Gorshov 1980). The oceanographic observations from the Russian drifting stations continued until 1991, and during the period 1937–1991, there were 1,800 soundings. Winter oceanographic observations were conducted at 7,200 stations using airplanes. During the summers of 1950–1993, oceanographic surveys of the Siberian Arctic Sea conducted 31,000 soundings (McClimans personal communication 2010).

4.2 1980–1990: Interpretation

The period from 1980 until the early 1990s saw the, hesitant, beginnings of the scientific icebreaker expeditions to the Arctic Ocean: *Ymer* in 1980, *Polarstern* in 1984 and 1987 and *Oden* and *Polarstern* together reaching the North Pole in 1991. It also saw the first large multi-national research programmes, the Marginal Ice Zone Experiment (MIZEX) in 1983 and 1984 and a winter MIZEX in 1987; a multi-national programme to study the convection in the Greenland Sea, the Greenland Sea Project (GSP); and the first systematic effort to determine the exchanges through Fram Strait with hydrographic sections and current metre arrays extending across the entire strait, the Fram Strait Project. In spite of the wealth of observations gathered by these programmes, the perhaps most important progress was in understanding the circulation and the processes active in the Arctic Mediterranean (see Chap. 6).

The old idea, advanced by Nansen, about ice formation, brine rejection and accumulation of saline water on the shelves was revived. Aagaard et al. (1981) proposed this as a mechanism for producing the Arctic Ocean halocline. They estimated that about 2 Sv ought to be produced on the shelves and examined the potential of the different shelf areas to supply water to the halocline. The main production areas were found to be the Barents and the Kara Seas and the Chukchi Sea. Melling and

Lewis (1982) studied plumes entering the halocline in the Canada Basin, and Jones and Anderson (1986) suggested that the nutrient maximum at a salinity of 33.1 in the Canadian Basin originated from the Chukchi shelf, where dense brine-enriched bottom water becomes rich in nutrients from the re-mineralization of organic matter at the bottom before it crosses the shelf break into the deep basin and enters the halocline.

These findings had some bearing on models describing the exchanges between the Arctic Ocean and the surrounding seas as a two-layer fjord circulation, where Atlantic water enters through Fram Strait, becomes entrained into the PML and then exported, together with the Pacific water and the runoff, as low salinity Polar surface water through Fram Strait and the Canadian Arctic Archipelago in geostrophically balanced boundary flows (Stigebrandt 1981). The thickness of the ice cover and the freshwater content in the PML then depend upon the heat loss to the atmosphere and on the amount of heat entrained into the mixed layer from below, and the outflow is controlled by the depth of the mixed layer and the density difference between the PML and Atlantic water. Assuming that the heat loss to the atmosphere, the river runoff and the Pacific inflow are known, it is possible to close the system and compute the exchanges between the Arctic Ocean and the North Atlantic. If the straits are wider than the internal Rossby radius, the transports are only determined by the density difference between the layers and the depth of the upper layer, and since the Canadian Arctic Archipelago has more openings than Fram Strait, it can sustain a larger transport (Stigebrandt 1981). However, if the entrainment of Atlantic water in the interior is prevented by the halocline, this coupling disappears and the shelf processes have to be taken explicitly into account.

Björk (1989) assumed that the outflow from the Arctic Ocean was geostrophic and determined by the stratification. He computed the production of saline shelf water necessary to reproduce the stratification and maintain the exchange. He found that about 1.2 Sv had to be supplied from the shelves. Rudels (1989) took the inflow from the Bering Strait to be short-circuited to the Canadian Arctic Archipelago and only considered the exchanges with the Nordic Seas. Assuming that the river runoff that enters the shelves also enters the basins, it was possible to compute, using salinities observed on the shelves and an estimate of the ice production related to the observed heat loss, how much of the runoff is exported as ice; how much as less saline, compared to the PML, surface water and how much as brine-enriched denser water. The salt balance was closed by requiring a compensating flow from the basin onto the shelves, at the bottom in summer and at the surface in winter. Assuming geostrophic flow in Fram Strait, an Arctic Ocean water column could be constructed that was capable of exporting the created volumes, allowing for a compensating inflow of Atlantic water, divided between Fram Strait and the Barents Sea. It was found that the export from the shelves mainly freshened the PML, and additional ice formation had to occur in the basins to reach the observed salinity of the PML. Only the Barents and Kara Seas produced water dense enough to supply the halocline and only a small amount, 0.2 Sv.

The deep and bottom waters in the Arctic Ocean are warmer and more saline than the Greenland Sea deep water, and Aagaard (1980) noticed that the Canadian Basin

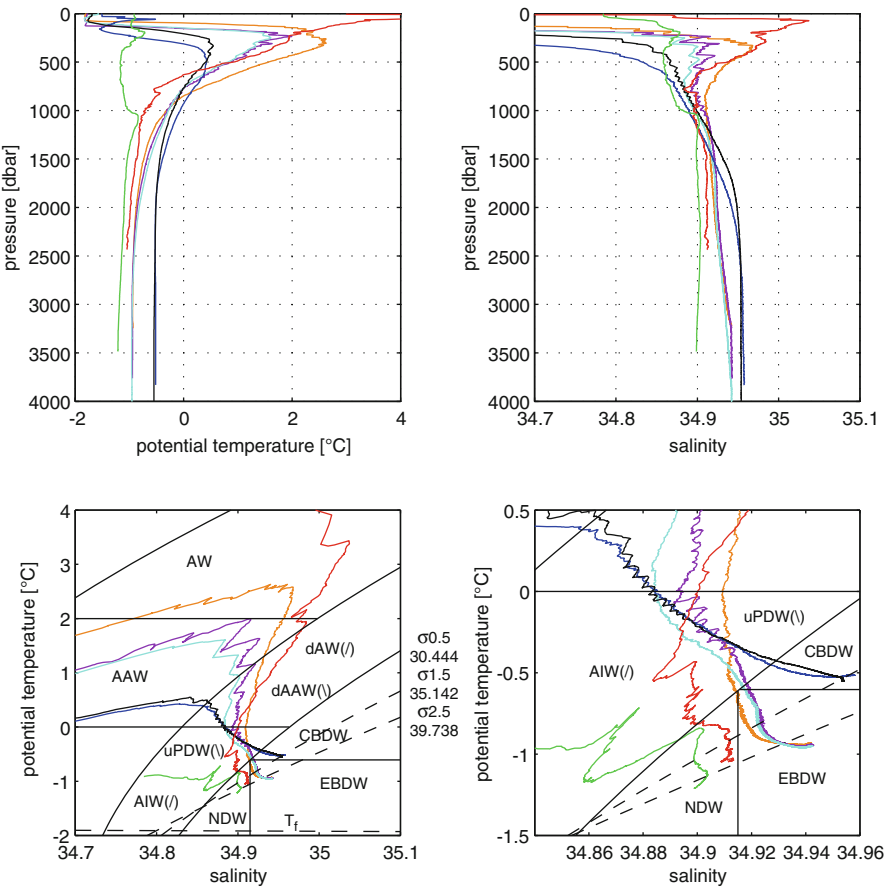

Fig. 4.4 Characteristics of the water columns in different parts of the Arctic Mediterranean. (*upper left*) potential temperature profiles, (*upper right*) salinity profiles, (*lower panel*) ΘS curves. *Green* Greenland Sea, *Red* Fram Strait (West Spitsbergen Current); *Dark yellow* Nansen Basin (Fram Strait branch), *Magenta* Nansen Basin (interior), *Cyan* Amundsen Basin, *Black* Makarov Basin, *Blue* Canada Basin (From Rudels 2009). The positions of the stations are shown in Fig. 4.19b

deep water was not only warmer but also more saline than the Eurasian Basin deep water (Fig. 4.4). This implies that some deep-water formation and convection must take place in the Arctic Ocean. The stratification is too strong for this to occur in the interior of the basins, and shelf-slope convection, as Nansen originally suggested, is the only possibility. Either entraining (Rudels 1986a) or shaving (Aagaard et al. 1985) boundary plumes was suggested as the mode of convection. Dense shelf bottom water had been observed in the eastern Barents Sea (e.g. Nansen 1906; Midttun 1985) and in Storfjorden in southern Svalbard (Midttun 1985; Anderson et al. 1988), and in 1986, a warmer, saline bottom layer was observed on the continental slope west of Svalbard, indicating a plume sinking from Storfjorden into Fram Strait entraining warm Atlantic water on its way down the slope (Quadfasel et al. 1988).

Circulation schemes for the deep waters in the Arctic Mediterranean Sea connecting the two deep water sources, the Arctic Ocean and the Greenland Sea, through Fram Strait were proposed to explain the differences in deep water characteristics in the different basins (Aagaard et al. 1985; Rudels 1986a). The more saline deep waters of the Arctic Ocean, the warmer, less-dense Canadian Basin Deep Water (CBDW) and the colder, denser Eurasian Basin Deep Water (EBDW) pass south through Fram Strait into the Nordic Seas. Part of the outflow remains at the rim of the Greenland Sea, interacting and mixing with the waters of the Greenland Sea. This mixing product then follows the Jan Mayen Fracture Zone into the Norwegian Sea to renew the Norwegian Sea Deep Water (NSDW). The NSDW then partly returns to the Arctic Ocean via Fram Strait. The other fraction of the Arctic Ocean deep waters enters the Greenland Sea, where it, together with the locally convecting waters, creates the Greenland Sea Deep Water (GSDW), the presence of the EBDW being revealed by the deep salinity maximum in the central Greenland Sea (Aagaard et al. 1985; Rudels 1986a) (Fig. 4.5).

Some efforts to quantify the circulation were made, either just from the Θ-S structures (Rudels 1986a) or using additional information from tracer observations (e.g. Smethie et al. 1988; Heinze et al. 1990; Schlosser et al. 1990). To match the transports with the observed Θ-S characteristics, Rudels (1986a, 1987) found that more deep water was exchanged through Fram Strait than was formed in the Arctic Ocean and in the Greenland Sea. This suggests that the deep exchanges between Arctic Ocean and the Nordic Seas are not driven by the deep-water formation but forced by other processes, e.g. the wind fields. Changes in the strength of the deep-water formation in one source area, e.g. the Greenland Sea, could, however, change the pathways of the circulation. A situation with a strong convection and deep-water formation in the Greenland Sea could force the Arctic Ocean deep waters to bypass the Greenland Sea and cross the Jan Mayen Fracture Zone into the Iceland Sea and perhaps also allow them to exit through Denmark Strait. Such variations in the circulation could also explain the fairly rapid changes in deep-water temperatures reported from the Greenland Sea (Aagaard 1968). Cooling is easily explained by an increased convection in the Greenland Sea, while it is more difficult to account for a rapid warming of the GSDW by local processes. However, if more Arctic Ocean deep water penetrates into the Greenland Sea in periods when the convection is weak, the heating can be explained (Rudels 1986a).

A situation with only deep-water sources is not possible, and implicit in all efforts to quantify the deep-water production is the assumption that the corresponding volume either upwells into the upper layer or is exported elsewhere. However, the circulation connecting the two deep-water sources, the Greenland Sea and the Arctic Ocean shelves, was assumed to be largely internal to the Arctic Mediterranean, and the overflow of dense water from the Arctic Mediterranean to the North Atlantic was believed to involve Arctic intermediate water formed mainly in the Iceland Sea (Swift et al. 1980; Swift and Aagaard 1981) and perhaps in the Greenland Sea (Smethie and Swift 1989).

Fram Strait was studied intensely. A large cyclonic recirculation of Atlantic water, as had been suggested already in the end of the nineteenth century (Ryder 1891),

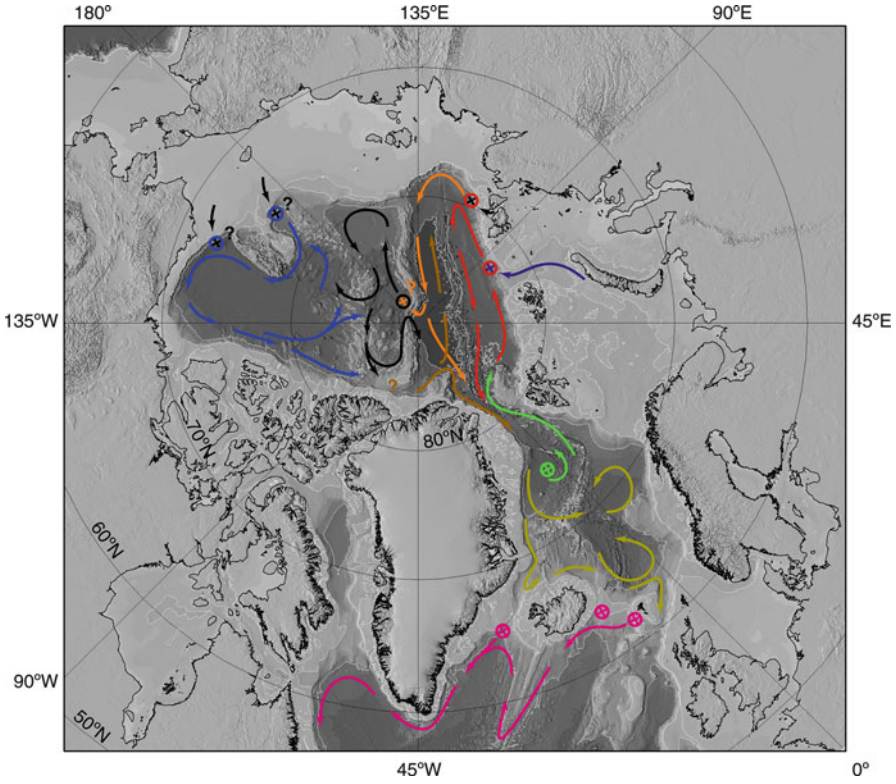

Fig. 4.5 Circulation of the deep waters. Advective exchanges through Fram Strait and advective input down the St. Anna Trough. Possible sources for slope convection are indicated by *crosses*. Crosses in the interior of the basins indicates convection or sinking from intermediate to deeper levels as for Amundsen Basin intermediate water sinking into the deep Makarov Basin. Uncertain sources and pathways are indicated by '?' (Adapted from Jones et al. 1995)

was found in the strait (Quadfasel et al. 1987; Rudels 1987; Bourke et al. 1988), and the amount of Atlantic water that really entered the Arctic Ocean was estimated, by geostrophy, to be closer to 1 or 2 Sv than to 7 Sv (e.g. Rudels 1987; Bourke et al. 1988). By contrast it was realised that the volume entering the Arctic Ocean over the Barents Sea via St. Anna Trough was as large as that passing through Fram Strait. However, the heat transport was considerably smaller because of the large heat loss taking place in the Barents Sea (Rudels 1987; Blindheim 1989).

The understanding of the role and the importance of the processes and the circulation in the Arctic Mediterranean Sea (Krümmel 1907; Wüst 1941; Sverdrup et al. 1942) for the global climate 100 years after the drift of *Fram* were summarised by Aagaard at the Nansen Centennial Meeting in Bergen 1993 (Aagaard and Carmack 1994). In 1997–1998, information collected by that time in the AARI database was used for generating climatic atlases of the Arctic Ocean for the winter (EWG 1997) and summer (EWG 1998) seasons.

4.3 The ACSYS Decade: New Insights, Variability and Change

4.3.1 Circulation and Transformation of Water Masses

4.3.1.1 Atlantic and Intermediate Water Circulation

The movement of the Atlantic water in the Arctic Ocean was known to be cyclonic but mainly thought of as a broad stream slowly moving around the central basin (e.g. Timofeyev 1960; Coachman and Barnes 1963), with perhaps a smaller anticyclonic gyre in the Beaufort Sea. The icebreaker expeditions to the Arctic Ocean in the late 1980s and early 1990s provided several new observational clues, and a more detailed picture of the circulation could be constructed. On hydrographic sections across the Eurasian Basin, signs of intrusive mixing and of a freshening of the Atlantic layer from the Nansen Basin to the Amundsen Basin were observed. Based upon XBT observations from the icebreaker *Rossia*, Quadfasel et al. (1993) proposed that the intrusions were created north of the Laptev Sea, as cold, brine-enriched water sinks off the shelf into the Atlantic layer. The intrusions were then assumed advected with the mean flow along the Gakkel Ridge toward Fram Strait. This interpretation is contrary to the one suggested by Perkin and Lewis (1984), who observed similar intrusions north of the Yermak Plateau during the EUBEX experiment in 1981 and assumed that these were created as the inflowing warm Atlantic water of the West Spitsbergen Current encountered and interacted with the 'old' Atlantic water of the Arctic Ocean water column north of Svalbard.

On the *Oden* 1991 expedition, intrusions and interleaving structures were observed in the northern Nansen Basin, in the Amundsen Basin and at the Lomonosov Ridge. The structures extended over too large depth interval and were too regular to be the result of occasional plumes leaving the Laptev shelf, and a more likely source would be the encounter between the inflow of Atlantic water through Fram Strait and the inflow of Atlantic water from the Norwegian Sea across the Barents Sea, which has been cooled and freshened in the Barents Sea before it enters the Arctic Ocean via the St. Anna Trough. Not having any observations from the continental slope, Rudels et al. (1994) postulated that the two inflow branches, the warmer Fram Strait branch and the colder, less-saline Barents Sea branch, meet at the continental slope east of the St. Anna Trough and that intense mixing takes place creating interleaving structures, which, once formed, would penetrate further across the front between the two branches, probably driven by the potential energy released by double-diffusive convection. When the driving property contrasts have been removed, the intrusions would remain as fossil structures and become advected with the mean circulation. These intrusive layers could then be used as tracers, marking the flow of the now combined branches, especially their return flow in the Eurasian Basin towards Fram Strait. As the two branches return towards Fram Strait, the Barents Sea branch water dominates in the Amundsen Basin and over the Lomonosov Ridge, while the Fram Strait branch water makes a tighter turn and is more prominent over the Gakkel Ridge and in the northern Nansen Basin.

The *Oden* 1991 observations also showed abrupt, and large, changes in water mass properties across the Lomonosov Ridge (Anderson et al. 1994; Rudels et al. 1994). The temperature in the Atlantic layer was much lower, while the intermediate water below the Atlantic layer was warmer and more saline in the Makarov Basin than in the Amundsen Basin. These differences were found at levels shallower than the sill depth of the Lomonosov Ridge and were interpreted as the result of shelf-slope convection acting on the boundary current flowing along the continental slope (Rudels et al. 1994).

Cold, saline and dense shelf water plumes sink down the slope, and the plumes merge with their surroundings when they reach their appropriate density level, entering, or bypassing, the Atlantic layer. The less-dense plumes thus cool and freshen the Atlantic layer, while denser, deeper sinking plumes entrain warm Atlantic water during their descent, and their temperature increases and, as they merge into the water column, they make the deeper layers warmer and more saline (Fig. 4.4; Rudels 1986a; Rudels et al. 1994). To attain the characteristic Θ-S properties of the upper Polar Deep Water (uPDW), with temperature decreasing and salinity increasing with depth, forming a straight line in the Θ-S diagram (Rudels et al. 1994), which are observed below the Atlantic layer on the Makarov Basin side of the Lomonosov Ridge, the water column must have moved a considerable distance along the continental slope, after it has crossed the Lomonosov Ridge (Fig. 4.4 and Table 4.1). This implies that the water on the Makarov Basin side of the Lomonosov Ridge flows along the ridge from the American side of the basin, which suggested that the boundary current splits at the Mendeleyev Ridge and makes a loop in the Makarov Basin and then flows along the Lomonosov Ridge in opposite direction as the flow on the Amundsen Basin side (Rudels et al. 1994).

The intermediate water in the Amundsen Basin is colder and less saline than that in both the Nansen and the Makarov basins, indicating that the Amundsen Basin intermediate layers are dominated by water from the Barents Sea branch, which has been less affected by slope convection. In the Atlantic layer, the temperature maximum found over the Lomonosov Ridge on the Amundsen Basin side of the front was warmer than in both the Amundsen Basin and the Makarov Basin, which could be due to a more rapid return flow along the ridge than in the interior Amundsen Basin (Rudels et al. 1994), taking into account the higher temperatures of the Fram Strait Atlantic water observed in the early 1990s (Quadfasel et al. 1991) (see Sect. 4.3.2.1).

Silicate and CFC concentrations on the Oden stations in the outflow area between the Morris Jesup Plateau and the Yermak Plateau showed differences between the intermediate waters closer to Greenland and those farther offshore. This implied that the boundary current here consists of streams from the different basins that still can be distinguished as the boundary current approaches Fram Strait. A higher silicate concentration closer to Greenland indicates the presence of water that has circulated around the Canada Basin, receiving its higher silicate content by incorporating Pacific water. Farther from Greenland, the water column became more similar to that of the Makarov Basin, while the waters from the loops in the Amundsen and Nansen basins were found closer to the Yermak Plateau (Rudels et al. 1994) (Fig. 4.6).

Table 4.1 Water mass definitions originally derived for Fram Strait (Friedrich et al. 1995; Rudels et al. 1999c) modified to include the less-dense Polar waters. The separation of water masses in the Nordic Seas is rudimentary

Water mass boundaries	Water masses	Origins, remarks
$\sigma_\theta \leq 27.70$ Upper waters		
$\sigma_\theta \leq 27.20$, $\Theta \leq 0$	Polar Water I (PWI)	Includes the Pacific inflow, the PML, shelf water and the upper halocline
$27.20 < \sigma_\theta \leq 27.70$, $\Theta \leq 0$	Polar Water II (PWII)	Includes the Atlantic-derived lower halocline and the winter-mixed layer in the Nansen Basin and the Barents Sea
$27.70 < \sigma_\theta \leq 27.97$ Atlantic waters		
(a) $27.70 < \sigma_\theta \leq 27.97$, $2 < \Theta$;	Atlantic Water (AW), and Re-circulating Atlantic Water	Norwegian Sea and West Spitsbergen Current
(a) $27.70 < \sigma_\theta \leq 29.97$, $0 < \Theta \leq 2$ (b) $27.70 < \sigma_\theta \leq 27.97$, $\Theta \leq 0$, $S \leq 34.676 + 0.232\Theta$	Arctic Atlantic Water (AAW)	Arctic Ocean: (b) includes the Arctic Ocean thermocline
$27.97 < \sigma_\theta$, $\sigma_{0,5} \leq 30.444$ Intermediate waters		
$27.97 < \sigma_\theta$, $\sigma_{0,5} \leq 30.444$, $0 < \Theta$	Dense Atlantic (DAW) (/) and Re-circulating dense Atlantic Water	Θ decreasing, S decreasing with depth
$27.97 < \sigma_\theta$, $\sigma_{0,5} \leq 30.444$, $0 < \Theta$;	Dense Arctic Atlantic Water (DAAW) (\)	S increasing, Θ decreasing with depth
$27.97 < \sigma_\theta$, $\sigma_{0,5} \leq 30.444$, $\Theta \leq 0$;	Arctic Intermediate Water AIW (/)	Greenland Sea: Includes a salinity minimum, in the Greenland Sea also a temperature minimum
$27.97 < \sigma_\theta$, $\sigma_{0,5} \leq 30.444$, $\Theta \leq 0$	Upper Polar Deep Water (uPDW) (\)	Arctic Ocean: S increasing, Θ decreasing with depth
$30.444 < \sigma_{0,5}$ Deep Waters		
$30.444 < \sigma_{0,5}$, $S \leq 34.915$	Nordic seas Deep Water (NDW)	Greenland Sea: Includes GSDW, ISDW, NSDW
$30.444 < \sigma_{0,5}$, $-0.6 < \Theta$, $34.915 < S$	Canadian Basin Deep Water (CBDW)	Canadian Basin
$30.444 < \sigma_{0,5}$, $\Theta \leq -0.6$, $34.915 < S$	Eurasian Basin Deep Water (EBDW)	Eurasian Basin

The $\sigma_{1,5}$ and $\sigma_{2,5}$ isopycnals shown in the ΘS diagrams correspond to the densities at the sill depth of the Lomonosov Ridges and Fram Strait, respectively. For an alternative water mass classification see Carmack (1990)

Several of these conjectures regarding the circulation were vindicated in the following years. In 1993, *Polarstern* studied the Laptev Sea shelf and slope. The less-saline Barents Sea branch water column was observed: the maximum temperature and salinity in the Atlantic layer were distinctly lower north of the Laptev Sea than at stations taken west of Franz Josef Land, and at some stations, strong interleaving between the two branches was observed (Schauer et al. 1997). At the slope

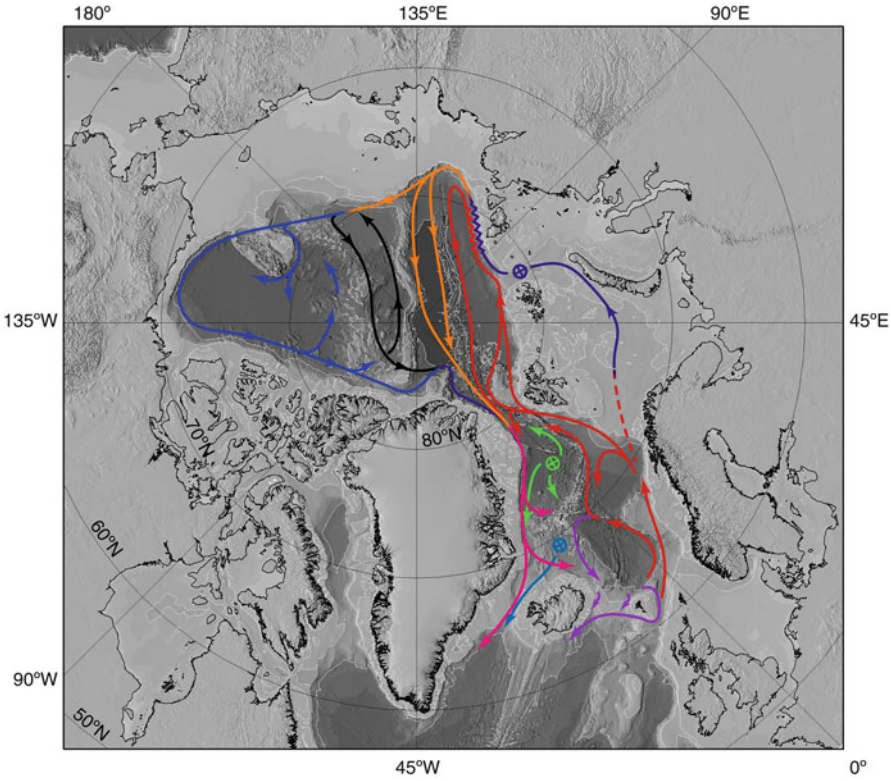

Fig. 4.6 Schematics showing the circulation in the subsurface Atlantic and intermediate layers of the Arctic Ocean and the Nordic Seas. The interactions between the Barents Sea and Fram Strait inflow branches north of the Kara Sea as well as the recirculation and different inflow streams in Fram Strait and the overflows across the Greenland–Scotland Ridge are indicated (Adapted from Rudels et al. 1994)

north of Severnaya Zemlya, the expected strong interleaving between the two inflow branches was observed in 1995 (Rudels et al. 2000a). The interleaving extended over several hundred metres depth and was present in all kinds of background stratifications: saltfinger unstable, diffusively unstable and also when the water column was stable in both properties. The thickness of the individual layers ranged from 5 to 50 m (Fig. 4.7).

In 1996, *Polarstern* occupied a section across the St. Anna Trough. It showed, as had the *Northwind* observations in 1965 (Hanzlick and Aagaard 1980), the colder, less-saline Barents Sea branch water entering the Nansen Basin in the deepest part and along the eastern flank of the trough (Schauer et al. 2002a, b). The 1996 *Polarstern* cruise then continued with a section from the eastern Kara Sea, across the Nansen and Amundsen basins, over the Lomonosov Ridge and into to the Makarov Basin (Schauer et al. 2002a). The Barents Sea branch was observed at the slope, but the mixing between the branches appeared somewhat weaker than in 1995. Farther from

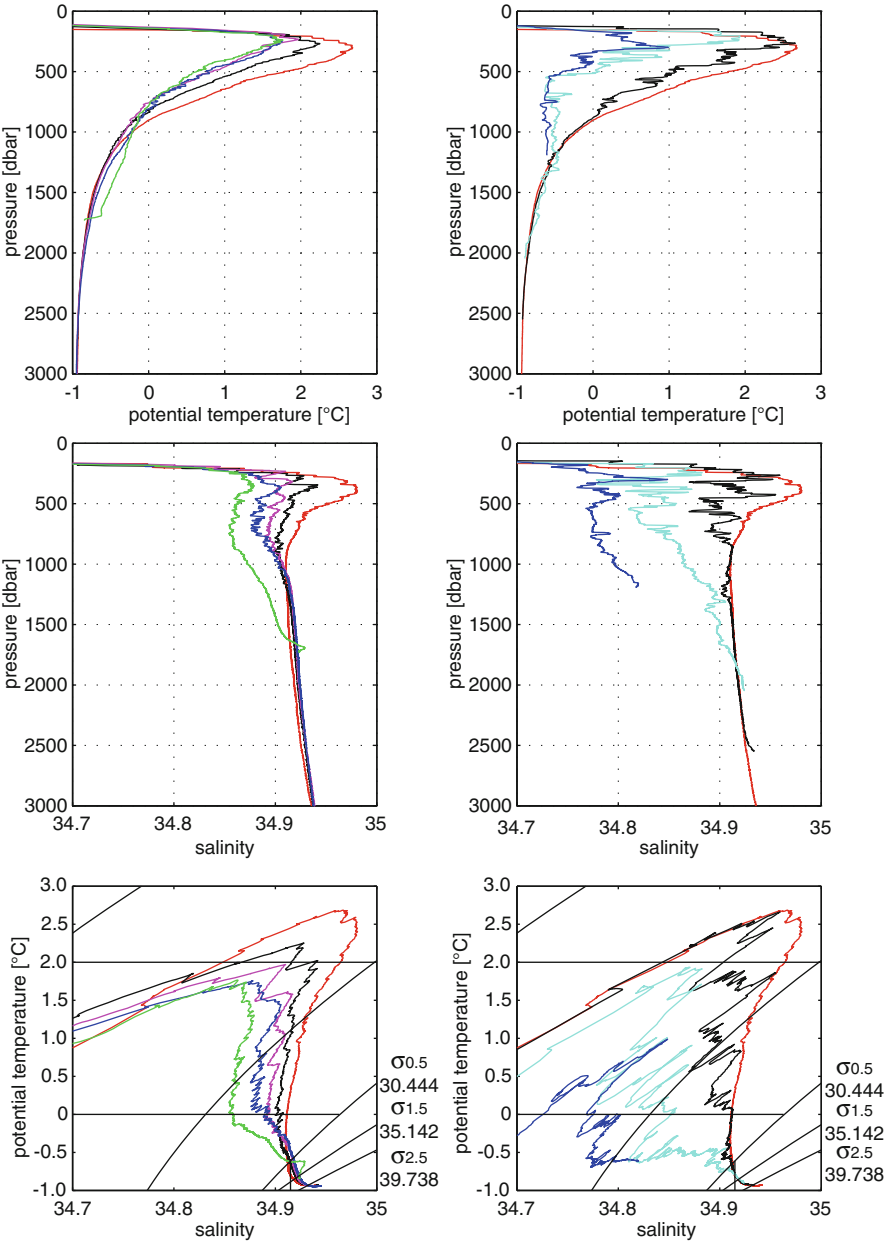

Fig. 4.7 Potential temperature and salinity profiles and ΘS curves showing the interaction and interleaving between the Fram Strait branch and the Barents Sea branch north of Severnaya Zemlya (*right column*) and the water mass properties in the Nansen and Amundsen basins seaward of the Fram Strait branch (*left column*). *Red station* Fram Strait branch, *blue station* Barents Sea branch, *black* and *cyan stations* show mixing between the branches. Note that the interleaving is present not only in the Atlantic layer but also in the intermediate levels (~1,000 m). Seaward of the Fram Strait branch (*left column*, *red station*), the warm, saline interleaving in the Nansen Basin (*black* and *magenta stations*) suggests a close recirculation of the Fram Strait branch in the Nansen Basin while the colder interleaving in the Amundsen Basin (*green* and *blue stations*) indicates that the intermediate part of the water column here is dominated by Barents Sea branch water (From Rudels 2009). Station positions are shown in Fig. 4.19c

the slope, an almost undisturbed, warm Fram Strait branch Atlantic core was observed, while on the basin side of this core, regular inversions and extensive layer structures were encountered in the Atlantic layer as well as in the intermediate water below. These inversions were similar to those observed on the *Oden* sections but with larger layer thickness and with overall higher temperature and salinity. Also these layers were interpreted as created by interactions between Barents Sea branch and Fram Strait branch waters (Rudels et al. 1999a) (Fig. 4.7).

The Barents Sea branch water was prominent in the Amundsen Basin and at the Lomonosov Ridge, consistent with a flow of Barents Sea branch, and to a lesser degree Farm Strait branch, waters towards Fram Strait in the Amundsen Basin and at the Lomonosov Ridge. However, the interleaving structures present on the offshore side of the warmer Fram Strait branch water may not only be an indication of intruding Barents Sea branch water but could also, as suggested by Rudels et al. (1994), be a sign that a major fraction of the Fram Strait branch is returning towards Fram Strait in the northern Nansen Basin and over the Gakkel Ridge, advecting intrusions already formed as the two branches flowed eastward along the continental slope. However, the hypotheses of the formation, dynamics and movements of the intrusions in the Arctic Ocean diverge and we shall return to this below.

In 1994, on the transpolar section taken by the icebreaker *Louis S. St-Laurent*, the stations in the Makarov Basin close to the Mendeleyev Ridge showed warm cores in the Atlantic layer and colder, less-saline water at 1,200–1,600 m depth. This is consistent with the picture of the boundary current crossing the Lomonosov Ridge and then being partly deflected into the Makarov Basin at the Mendeleyev Ridge. No stations were obtained at the continental slope in the Makarov Basin during the AO94 expedition, and it was not possible to determine, with certainty, the origin of the intermediate depth, cold, low-salinity lenses. Were they outflows from a nearby shelf, or did they derive from the Barents Sea branch (Aagaard et al. 1996; Carmack et al. 1997; Swift et al. 1997)? In 1995, *Polarstern* worked on the slope from the eastern Kara Sea to the western East Siberian Sea. Less-saline intermediate water could then be followed along the slope from the Kara Sea to the East Siberian Sea, where it extended down to 1,600 m, indicating the sill depth at the Lomonosov Ridge encountered by the boundary current. This is in agreement with less-saline intermediate Barents Sea branch water entering the Canadian Basin and the interior of the Makarov Basin (Rudels et al. 2000a).

No large property contrasts between the waters above sill level on each side of the Lomonosov Ridge were seen close to the continental slope as were found at the *Oden* section further into the basins. This suggests that the boundary current broadens, or makes a loop along the ridge, before it splits into one part flowing northward along the ridge and the rest entering the Canadian Basin (Rudels et al. 2000a; Schauer et al. 2002a).

During the *Polarstern* cruises in 1995 and 1996, three moorings were deployed in 1995 and recovered the following year. Two of the moorings were located at the 1,700 m isobath on the continental slope, north of the Laptev Sea and north of the East Siberian Sea and close to the Lomonosov Ridge, while the third was deployed at the same bottom depth on the Amundsen Basin side of the ridge. The flow in the

boundary current was found to be largely barotropic, and the calculated transports indicated 5 Sv flowing eastward above the Laptev Sea slope. The current then bifurcated with about 2.5 Sv moving north along the Lomonosov Ridge and 2.5 Sv crossing the ridge into the Makarov Basin (Woodgate et al. 2001).

Further to the east, in the Canada Basin, analysis of hydrographic and tracer data from the SCICEX-96 expedition together with data obtained from the AO94 and the *Polarstern* expeditions indicated that a further bifurcation of the boundary current occurred in the Canada Basin west of the Chukchi Cap (Smith et al. 1999; Smethie et al. 2000). The boundary current in the Canadian Basin thus separates into 3 loops, a splitting occurring at each topographic feature present at the slope. Similar bifurcations are then to be expected on the American side of the basin, at the Alpha Ridge and at the Lomonosov Ridge, bringing older and more transformed Atlantic and intermediate layer waters into the interior Canada and Makarov basins forming, at least rudimentary, gyres in these basins.

4.3.1.2 Formation of the 'Lower Halocline'

The origin of the more saline, nutrient-poor lower halocline has been found more elusive than that of the upper halocline (Jones and Anderson 1986; Jones et al. 1991; Anderson and Jones 1992). The low nutrient content indicates that the contact with bottom sediments is brief or non-existent, and an accumulation of brine-enriched water at the bottom of the shelves appears less likely. Rudels et al. (1991) proposed that the haline convection in the northern Barents Sea and north of Svalbard was limited, not by the shelf bottom but by the pycnocline above the Atlantic water and that it was strong enough to homogenise the less-saline upper layer, which would continue into the Arctic Ocean, eventually supplying water to the lower halocline. Steele et al. (1995) suggested that the melting of sea ice, as the Atlantic water meets the ice in the marginal ice zone in the northern Barents Sea, would lead to the formation of water with the characteristics of the lower halocline. Rudels et al. (1996) proposed that as the West Spitsbergen Current enters the Arctic Ocean through Fram Strait, the Atlantic water encounters, and melts, sea ice. The melt water is mixed into the upper part of the Atlantic water, cooling it and reducing its salinity. A less-saline upper layer is created that is homogenised in winter by convection. Close to Fram Strait, this convection is initially thermal, but when the upper layer reaches freezing temperature, the convection becomes haline, driven by freezing and brine rejection.

This upper layer extends down to the thermocline above the Atlantic layer and is advected eastward together with, and above, the main part of the Fram Strait branch. In summer, a low-salinity melt water layer develops at the surface, which again is removed by ice formation the following winter. This situation extends over the entire Nansen Basin, and the cold halocline, present elsewhere in the Arctic Ocean, is missing. Rudels et al. (1996) proposed that this 'winter-mixed layer' reaching down to a pycnocline with coinciding thermocline and halocline is the embryo of the 'lower' halocline water found in the other Arctic Ocean basins.

Steele et al. (1995), following Moore and Wallace (1988), assumed that the salinity, S_1, of the upper 'melt water' layer should be close to $S_1 = S_A(1 - c\Delta T L^{-1})$, where S_A is the salinity of the Atlantic water and ΔT the temperature difference between the upper layer and the Atlantic water. L is the latent heat of melting and c the heat capacity of sea water. The minimum salinity is reached when the surface water is at the freezing point, and all available heat of the Atlantic water has been used to melt sea ice. This results in lower salinities than those observed in the lower halocline (34.2–34.4), unless the Atlantic water has been cooled considerably before it encounters the ice.

Rudels et al. (1999b) proposed that cooling in the presence of sea ice always leads to a loss of oceanic sensible heat both to the atmosphere and to ice melt and proposed that the fraction, f, going to ice melt is such that the ice melt rate is a minimum. A larger fraction evidently leads to more ice melt, but so does also a smaller fraction, since the stability at the base of the mixed layer becomes weaker, allowing for stronger entrainment and larger transport of heat into the mixed layer from below. The fraction was found to be $f \approx 2\alpha L(c\beta S_A,)^{-1}$ where α is the coefficient of heat expansion and β the coefficient of salinity contraction. The salinity of the upper layer becomes $S_1 = S_A(1 + 2\alpha\Delta T(\beta S_A)^{-1})^{-1}$, and with the temperatures and salinities observed in the Atlantic water north of Svalbard, this expression gives a salinity range of 34.2–34.4, close to that observed in the upper layer north of Svalbard and in the lower halocline. The salinity minimum is attained when the surface layer reaches freezing temperature. Once ice starts to form, the salinity again rises above this value.

The winter-mixed layer remains in contact with the sea surface and is ventilated down to the thermocline each winter, until it is overrun by shelf water of still lower salinity that crosses the shelf break. A massive outflow of low-salinity shelf water commonly occurs from the Laptev Sea and is, in reality, a further interaction between the two inflow branches. The Barents Sea branch does not just supply water to the Atlantic, intermediate and deeper layers of the Arctic Ocean via the St. Anna Trough. One part, comprising much of the water of the Norwegian Coastal Current, enters the Kara Sea through the Kara Gate south of Novaya Zemlya. In the Kara Sea, it receives the runoff from Ob and Yenisey and its salinity decreases. Most of the shelf water appears to continue eastward through the Vilkiltskij Strait into the Laptev Sea, and only a smaller fraction crosses the Kara Sea shelf break into the Nansen Basin. Once in the Laptev Sea, the runoff from the Lena, Yana and Khatanga rivers is added to the shelf water before it crosses the shelf break and enters the deep Arctic Ocean basins.

The inflow of less-saline shelf water on top of the winter-mixed layer in the Nansen Basin creates a 'cold' salinity gradient between the shelf water and the winter-mixed layer. Winter convection becomes limited to the 'shelf water', which evolves into the PML, while the now isolated 'winter-mixed layer' becomes the halocline water mass commonly referred to as the lower halocline (Rudels et al. 1996). This implies that the lower halocline initially is a mode water (McCartney 1977), a halostad with vertically almost constant temperature and salinity, which, after it has been isolated from the surface convection, becomes stratified by internal turbulent

mixing. The fact that the term halocline in the Arctic Ocean is used to signify both a distinct water mass between the Polar Mixed Layer and the Atlantic layer and a sharp salinity gradient may cause some confusion (see below Sect. 4.3.2.2).

This mechanism for halocline formation differs from the shelf scenarios previously proposed (Coachman and Barnes 1962; Aagaard et al. 1981). The mechanisms do not exclude each other. In the Eurasian Basin, the waters crossing the shelf break are either dense enough to enter, or sink below, the Atlantic layer (see e.g. Schauer et al. 1997; Rudels and Friedrich 2000) or are less dense and enter at the surface. There, they either become stirred into the mixed layer in winter or, if the volumes are large, evolve into the PML. As the PML and the halocline both enter the Canadian Basin, the density difference between them is large enough for water of intermediate density to sink off the shelves and penetrate between the PML and the lower halocline, as e.g. the upper halocline water discussed by Jones and Anderson (1986).

A similar homogenisation of melt water above the Atlantic layer also takes place in the northern and eastern Barents Sea, and Rudels et al. (2001, 2004a) traced the part of the Barents Sea winter-mixed layer, which enters the Arctic Ocean with the Barents Sea branch in the St. Anna Trough, along the Eurasian continental slope into the Canada Basin. The halocline water deriving from the Barents Sea branch is more saline and becomes warmer than that of the Fram Strait branch due to stronger mixing with underlying Atlantic water at the continental slope (Rudels et al. 2004a) (Fig. 4.8).

At the mooring deployed on 1995/1996 north of the Laptev Sea, halocline water from either the Fram Strait branch or from the Barents Sea branch was observed at any particular time (Woodgate et al. 2001). This suggests that the two branches move side by side at least as far as the Lomonosov Ridge. The Fram Strait branch supplies the colder, and slightly less-saline, halocline observed in the Amundsen Basin but also contributes to the lower halocline in Makarov basins and in the Canada Basin west of the Chukchi Cap. The Barents Sea branch halocline remains at the slope until it crosses the Chukchi Cap. Beyond the Chukchi Cap, it appears to leave the slope to flow into the basin, supplying the warmer, more saline lower halocline water in the remotest (seen from the Atlantic) part of the Canada Basin. Some of the Barents Sea branch halocline water passes through Nares strait into Baffin Bay, but most of it exits the Arctic Ocean together with the Fram Strait branch halocline water in the East Greenland Current, where strong isopycnal mixing between the two halocline water masses has been observed in the temperature profiles (Rudels et al. 2005).

4.3.1.3 Pacific Water

Pacific water in the Arctic Ocean is distinguished from the Atlantic-derived waters by its lower salinity and density. This implies that it mostly contributes to the upper layers of the Arctic Ocean water column – the PML and the halocline. The Pacific water enters through the shallow Bering Strait and starts as three separate water

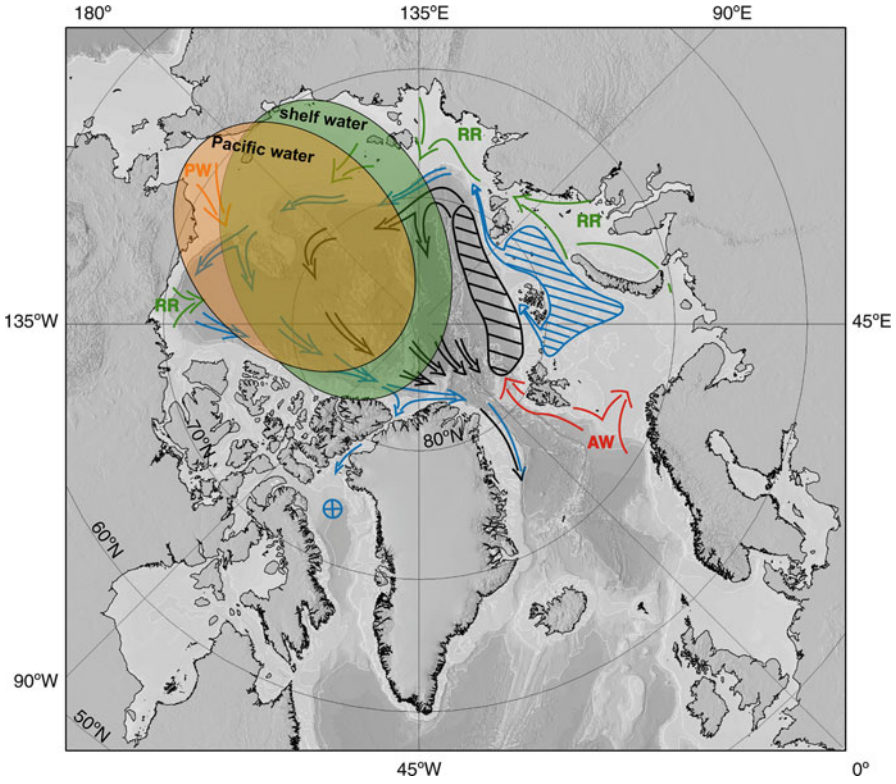

Fig. 4.8 Circulation of the Atlantic-derived halocline waters. The proposed source areas for the Fram Strait branch lower halocline water (*black*) and the Barents Sea branch lower halocline water (*blue*) are shown by diagonals and the circulation of these halocline waters in the Arctic Ocean is indicated. *RR* river runoff, *PW* Pacific water, *AW* Atlantic water. The *green* and *yellow* transparent ovals show the distributions of the Eurasian Basin shelf input and the Pacific water, respectively. The cross indicates possible contribution of Barents Sea branch lower halocline water to the Baffin Bay bottom water (Adapted from Rudels et al. 2004)

masses; farthest to the west is the more saline Gulf of Anadyr water, $32.8 < S < 33.2$, then the Bering Shelf water, $32.5 < S < 32.8$ and Alaskan Coastal Water $S \approx 32$ to the east (Coachman et al. 1975). Once these waters enter the Chukchi Sea, the two westernmost waters merge in the central part to form the Bering Strait Water (BSW), while the Alaskan Coastal Water (ACW) remains close to the Alaskan coast in the Alaskan Coastal Current (ACC). It becomes further diluted by runoff and enters the southern Canada Basin along the Barrow Canyon. The Bering Strait Water mainly flows northward and enters the Arctic Ocean primarily down the Herald Canyon (Coachman et al. 1975) (see also Fig. 4.3 above).

The characteristics of the Pacific water depend upon season, and Coachman and Barnes (1961) distinguished between the Bering Strait Summer Water (BSSW) with temperature clearly above the freezing point and salinity around 32.5, which shows

up as a temperature maximum around 75 m in the Canada Basin, and Bering Strait Winter Water (BSWW) with temperature at the freezing point and salinity around 33.1 and located between 150 and 200 m in the Canada Basin water column.

Steele et al. (2004) identified two temperature maxima, one less dense deriving from the Alaskan Coastal Water (ACW) and one denser originating from the BSSW. Since these two water masses enter the Arctic Ocean by different paths, down the Barrow Canyon and down the Herald Canyon respectively, the salinity of the upper temperature maximum can be used to determine which water mass is present and thus trace the circulation of the less-dense part of the Pacific water in the interior of the Arctic Ocean (see Sect. 4.3.2 below).

The denser and colder BSWW mainly enters the Canada Basin west of the Chukchi Cap (Coachman et al. 1975), but recent studies have suggested that a less-dense fraction of BSWW also reaches the Canada Basin east of the Chukchi Cap (McLaughlin et al. 2004). The temperature minimum is also associated with an oxygen minimum and a nutrient, especially a silicate, maximum. Jones and Anderson (1986) proposed that this nutrient maximum was the result of remineralisation of organic matter from the shelf bottom, which implies convection of brine-enriched water to the shelf bottom that subsequently leaves the shelf, sinking into the deep Canada Basin forming the upper halocline.

The Pacific water differs from the Atlantic water also in other parameters. The nutrient concentrations are generally higher, and the ratio of nitrate and phosphate concentrations is different from that in the Atlantic water. This is because the oxygen concentration in the North Pacific, and especially in the Bering Sea, is low, and nitrate is used to oxidise organic matter, which results in a deviation from the Redfield ratio (Redfield et al. 1963) and changes the nitrate–phosphate ratio. The nitrate–phosphate ratio has therefore been used, often together with the silicate concentration, to determine the Pacific fraction in the water masses both within the Arctic Ocean and in the outflows through Fram Strait and the Canadian Arctic Archipelago (Jones et al. 1998; Jones et al. 2003).

That the Pacific water dominates the upper layers in the Canada Basin is rather obvious, considering its proximity to Bering Strait, but also the upper layers of the entire Canadian Basin during the early ice camp expeditions were found to exhibit Pacific water characteristics (Kinney et al. 1970; Gorshov 1980; Moore et al. 1983). This situation has presently changed (see Sect. 4.3.3 below). The Pacific water dominates in the western channels of the Canadian Arctic Archipelago (Jones and Coote 1980), and only in the deeper (230 m) Nares Strait is Atlantic water found in the deeper layers (Jones et al. 2003). Pacific water has also been observed leaving the Arctic Ocean through Fram Strait (e.g. Anderson and Dyrssen 1981; Jones et al. 1998, 2003).

Elevated silicate concentrations have been found in the lower halocline for salinities at least as high as 33.6 (Salmon and McRoy 1994), and the nitrate and phosphate concentrations and also the vertical gradient in I^{129} concentration (Swift et al. 1997; McLaughlin et al. 2002) show that Pacific water penetrates deeper than the 33.1 of the upper halocline (Jones and Anderson 1986). This could be due to excessive brine release, especially in polynyas on the Chukchi shelf close to the

Alaskan coast, leading to salinities above 34 (Weingartner et al. 1998) occasionally above 36 (Aagaard et al. 1985), high enough for the Pacific water to sink into the lower halocline. The difference between the deeper parts of the water columns in the Eurasian and Canadian basins, from the Atlantic layer to the bottom, has also been interpreted as sign of deep-reaching shelf-slope convection occurring in the Canadian Basin, which, by necessity, would involve Pacific water (Aagaard et al. 1985; Rudels 1986a). These volumes of Pacific water would, however, be small < 0.1 Sv (Rudels et al. 1994; Jones et al. 1995).

Another possibility could be that large amplitude vertical displacements observed at upwelling events (Carmack and Kulikov 1998; Kulikov et al. 1998) bring lower halocline and Atlantic water onto the shelf. Atlantic water has been observed moving along the bottom of the Barrow Canyon towards the Chukchi shelf (Weingartner et al. 1998), and it could occur also elsewhere. This situation, similar to the mechanism suggested by Coachman and Barnes (1962) for the formation of the lower halocline in the Eurasian Basin (see Sect. 4.2), would enhance the mixing between the Atlantic and Pacific water and stir Pacific waters into the lower halocline.

4.3.1.4 Shelf Processes, River Runoff, Ice Melt, Freezing and Brine Rejection

The atmospheric meridional transport of water vapour leads to net precipitation in the Arctic. The low air temperatures limit the vapour content, and the net precipitation over the Arctic Ocean is small. But because of its large catchment area, the Arctic Ocean, comprising 2.5% of the area of the world ocean, receives 7% of the runoff of the earth's rivers (Baumgartner and Reichel 1975). The runoff is strongly seasonal with the largest discharge in spring and early summer. The river runoff forms low-salinity surface plumes that commonly flow eastward along the coast. The runoff from Ob and Yenisey in the Kara Sea mostly passes through the Vilkiltskij Strait into the Laptev Sea before it, together with the runoff from the Lena and Yana rivers, crosses the shelf break into the Amundsen Basin. The rivers discharging into the East Siberian Sea contribute to the Siberian Coastal Current, which may reach as far east as Bering Strait, before it becomes mixed into the northward-flowing Pacific water; occasionally, it even passes through the strait into the Bering Sea (Roach et al. 1995). The runoff from the Yukon enters the Arctic Ocean in the Alaskan Coastal Current (ACC) via Bering Strait, and more runoff is added as the ACC moves towards the Mackenzie delta. The river plumes may easily become disrupted by offshore winds, which spread the water from the coast, thinning the low-salinity layer and thus preventing e.g. the shallow Siberian Coastal Current from developing (Münchow et al. 1999; Weingartner et al. 1999). Changes in the large-scale atmospheric circulation pattern such as the Arctic Oscillation (AO) (or the Northern Annular Mode (NAM)) (Thompson and Wallace 1998) and the North Atlantic Oscillation (NAO) (Hurrell 1995) may also affect the paths of the larger runoff volumes from the Ob, Yenisey and Lena rivers, making them enter either the

Amundsen Basin or flow eastward into the East Siberian Sea (Proshutinsky and Johnson 1997) (see Sect. 4.3.2 below).

The river water enters the deep Arctic Ocean basins as the low-salinity shelf waters cross the shelf break. River water can be distinguished from sea ice melt water by its higher total alkalinity and different ^{18}O concentrations, which can be used to track the river water across the Arctic Ocean (Anderson et al. 1994; Anderson et al. 2004). Tracers like barium may be used to identify water from different rivers (Guay et al. 2001). ^{18}O makes it possible to separate river runoff, ice melt and ice formation (Östlund and Hut 1984) (see below, Sects. 4.3.1.5 and 4.3.2).

The shore-fast ice and the grounded ridges 'stamukhies' outside the coast prevent the river water from easily escaping to the outer shelf areas, and large, under ice, freshwater lakes may form seasonally as in the Mackenzie delta (Carmack and MacDonald 2002). The ice formation and the ice melt, since the ice moves differently than the water, add a further path for the freshwater to circulate and become redistributed in the Arctic Ocean surface layer (Macdonald 2000). On occasion the melting and the northward retreat of the drift ice may act as a buoyancy source that creates a low-salinity surface flow. This has been observed in the East Siberian and eastern Chukchi Sea where, in 1995, instead of the expected eastward-flowing Siberian Coastal Current, a westward surface flow was observed (Münchow et al. 1999; Weingartner et al. 1999).

The interaction between sea ice and the underlying ocean is simple in most parts of the deep Arctic Ocean. Ice melts in summer, mostly from above, due to the strong solar radiation. In autumn and winter, the freshwater is removed by freezing, and released brine homogenises the PML. Since the PML is located above the cold halocline, no heat is added by entrainment from below during winter, and the ice grows as a response to the heat loss to the atmosphere and to space. Only in the marginal ice zone does the ice come in direct contact with warmer water and melts from below. The formation of a melt water layer below the ice will, however, reduce the heat transfer and the melting unless the ice is drifting very rapidly, keeping the melt water layer thin, and continuously forcing contact with new, warm water (McPhee 1990; Boyd and D'Asaro 1994).

A somewhat similar situation occurs in the Nansen Basin, where the cold halocline is absent and, during winter, warm Atlantic water may be entrained into the winter-mixed layer, influencing the ice formation rate as well as supplying heat to the atmosphere. In the Nansen Basin, the stratification and the deep winter-mixed layer will limit the entrainment, and the only effect is a slightly reduced ice formation. However, in less-stratified waters like the Greenland Sea and the Weddell Sea in Antarctica, this vertical heat flux from below could lead to the disappearance of the ice already in midwinter, when the cooling is the strongest (Martinson 1990; Lemke 1993; Walin 1993; Rudels et al. 1999b).

As it became clear that sinking of cold, saline water from the shelves down the slope was the one process that could explain not only the formation of water in the density range of the halocline but also the transformations of the deeper layers of the Arctic Ocean basins (Nansen 1906; Aagaard et al. 1985; Rudels 1986a) and after the observation of dense bottom water sinking from Storfjorden into Fram

Strait (Quadfasel et al. 1988), the studies of freezing, brine rejection and the accumulation of cold saline water on the shelves and of the sinking of dense water down the continental slopes were intensified. The ice production and the corresponding formation of saline water in polynyas were estimated from satellite observations of polynya extent and the wind and temperature fields (Martin and Cavalieri 1989; Cavalieri and Martin 1994; Winsor and Björk 2000). Winsor and Björk examined 28 different polynya areas forced by 39 years of reanalysed meteorological data. Using a polynya model originally developed by Pease (1987), they obtained a much lower (0.2 Sv) estimate of halocline water formation than Björk (1989), Martin and Cavalieri (1989) and Cavalieri and Martin (1994) (around 1.2 Sv), but similar to the estimate by Rudels (1989) (0.2 Sv). They concluded that the areas most likely to form dense water, capable of renewing the deeper layers of the Eurasian Basin and the Canadian Basin, were the Barents Sea and the Chukchi Sea, respectively.

In numerical studies of dense water production in polynyas, Gawarkiewicz and Chapman (1995) found that water was transported across the shelf in small-scale eddies formed by baroclinic instabilities around the polynya. The production of dense water and large density anomalies were thus limited by the eddy flux (Chapman and Gawarkiewicz 1997; Gawarkiewicz et al. 1998), and Gawarkiewicz (2000) found that eddies could transport dense water across the shelf break and down the slope, giving another mechanism in addition to baroclinic instability (Hart and Killworth 1976) and frictional spin-up (D'Asaro 1988a, b) for forming and injecting eddies into the upper Arctic Ocean. Winsor and Chapman (2002) combined the polynya model used by Winsor and Björk (2000) with a primitive equation ocean model to estimate the production and export of dense water from the Chukchi shelf. They found that the amount of dense water production, halocline water and denser, was small and that the density anomalies were as much due to the initial conditions, set by the inflowing Pacific water, as to the ice formation in the polynya. This is in agreement with the observations by Roach et al. (1995) and Weingartner at al. (1998).

Convection, thermal and haline, and the formation and spreading of dense water over the shelf and down the slope were modelled by Backhaus et al. (1997), using different process models. Especially the outflow from Storfjorden was examined and compared with observations (Jungclaus et al. 1995; Backhaus et al. 1997). The path of the plume was well simulated as was the change of properties caused by the entrainment. The Storfjorden polynya and the outflow of dense water from Storfjorden into Fram Strait have been thoroughly investigated during the ACSYS period (e.g. Schauer 1995; Haarpainter 1999; Haarpainter et al. 2001; Schauer and Fahrbach 1999; Fer et al. 2003a; Fer et al. 2003b; Skogseth et al. 2005). The 1990s was a period when little highly dense water was observed in Storfjorden, but in 2002, salinities above 35.8 were observed in Storfjorden from *Oden* during the Arctic Ocean 2002 expedition. This was perhaps the highest salinity reported from Storfjorden to that date (Rudels et al. 2005).

Sinking of dense water from the shelves into the deep Arctic basins was not noticed until 1995 (Rudels et al. 2000a), when thin layers of saline, denser but warmer bottom water was found deeper than 2,000 m on the continental slope north

of Severnaya Zemlya. Similar bottom layers were also seen north of the eastern Kara Sea in 1996 and were actually present also on some *Polarstern* stations taken north of the Laptev Sea in 1993 (Fig. 4.9). The origin of these dense bottom layers has, so far, not been determined, and the paths of the water have not been reconstructed. Detailed plume models, taking into account the bathymetry and the origins and paths of the plumes, have therefore not yet been used to describe the deepest reaching boundary convection within the Arctic Ocean.

Some efforts have been made to use simple balance models to estimate the properties the shelf water initially must have and the rate of entrainment into the plume that is necessary to reproduce the characteristics observed in the deep Arctic Ocean basins. In the Eurasian Basin, the intermediate waters are dominated by the two inflow branches, and the effects of shelf–slope convection are mainly seen in the deepest part of the water column, where the temperature is almost constant with depth and the salinity increases towards the bottom. In the Canadian Basin, however, the changes in the Atlantic and intermediate waters that cross the Lomonosov Ridge are due to slope convection. Rudels et al. (1994) assumed that the entrainment rate of ambient water into the plumes was constant with depth and added for every 150 m of descent a volume of entrained water corresponding to the initial volume passing the 200 m isobath. Since the dense shelf water is formed by brine rejection, the initial temperature of all plumes should be the same, and the depths the plumes reach would only depend upon their salinity. The assumptions made by Rudels et al. (1994) did not lead to contradiction with the observed water mass properties in the interior of the Canadian (Makarov) Basin. The entrained water quickly dominated the characteristics of the plumes, making them warmer than their surroundings once they had passed the Atlantic layer. To reach the deeper parts of the water column, the initial salinity had to be high, close to or above 36, but perhaps not inconceivable. The volume of shelf water contributing to the ventilation of the deeper layers was very small, around 0.02 Sv (Rudels et al. 1994).

Goldner (1999a, 1999b) examined slope convection using an inverse box model to determine the transport from the boxes and the renewal from the shelves necessary to maintain the mass, heat and salt balances in the boxes. He separated the Canadian Basin and the Eurasian Basin and found that the Canadian Basin shelves could supply about 0.2 Sv and the Eurasian Basin shelves 1.4 Sv, including the Barents Sea inflow, to the deep basins. In these models, there is no balance of the transport across the shelf break as in Björk (1989) and Rudels (1989), and the mass and salt budgets were assumed closed by inflows from behind, through Bering Strait, over the Barents Sea and by river runoff. For the Bering Strait inflow, this is obvious, but considering how especially the Norwegian Coastal Water of the Barents Sea branch spreads from one shelf sea to the next (see e.g. Rudels et al. 1999c), this is probably realistic also for the Eurasian Basin. In Goldner (1999a), the shelves were found to supply mainly dense water to the deep basins, while in Goldner (1999b), the input of freshwater from the shelves was larger. The first result is likely due to the inclusion of the Barents Sea branch as a shelf outflow rather than a direct inflow from the Norwegian Sea to the Nansen Basin. The second result, which implies a net ice formation in the deep basins, appears more realistic.

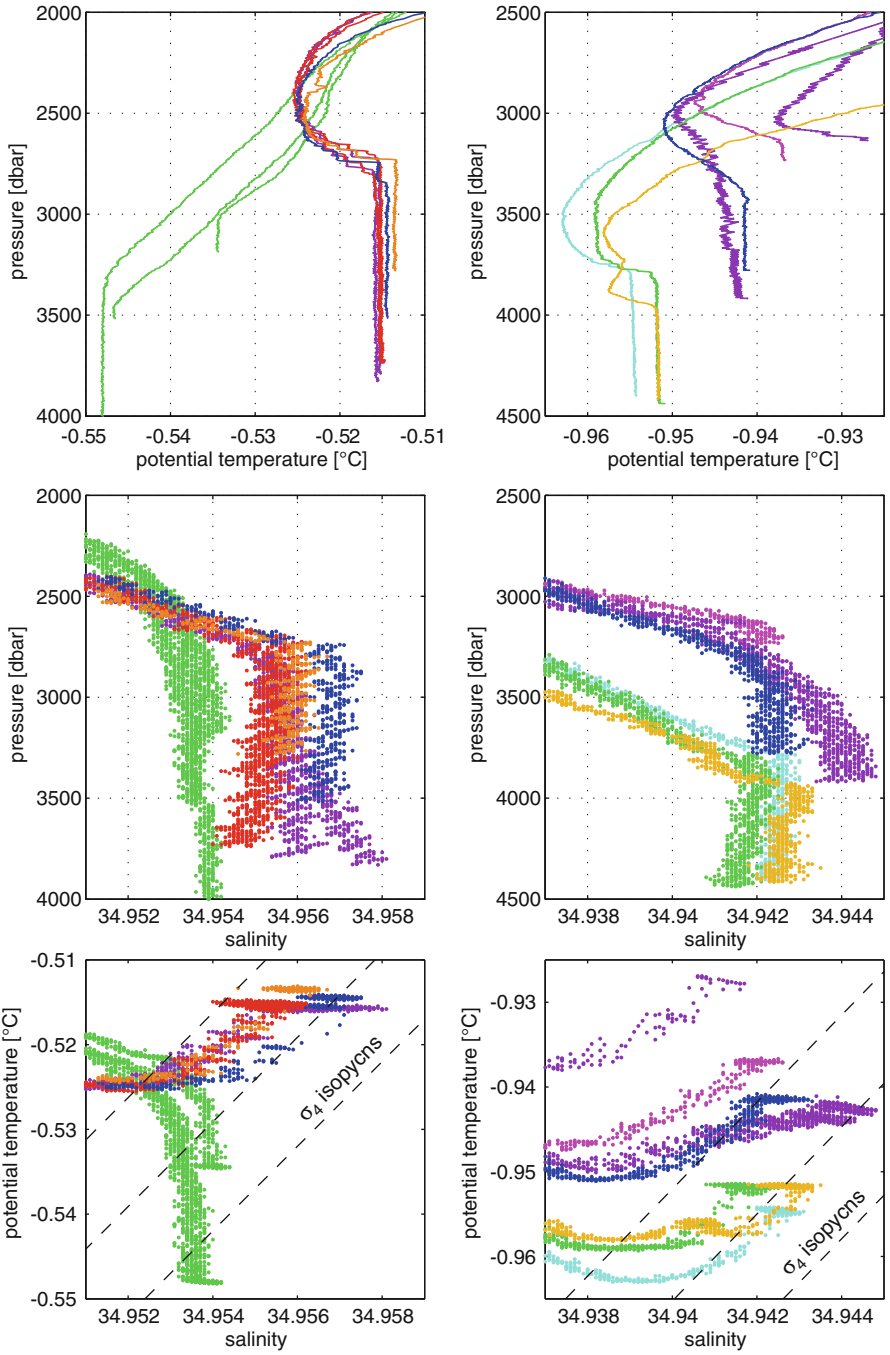
pressure [dbar]
potential temperature [°C]
salinity
σ4 isopycns

4.3.1.5 Tracking the Waters: Insights from Tracers

The chemical signature is useful to trace the source, distribution and circulation of most Arctic Ocean water masses. Chemical tracers can be separated into the three groups, conservative (e.g. ^{18}O), bioactive (e.g. oxygen and nutrients) and transient (e.g. CFCs, ^{3}H, ^{14}C), contributing different information.

Two freshwater sources dominate in the PML, sea ice melt and river runoff, and they have very distinct chemical signatures. Sea ice melt has a signature that is a function of salinity and the composition of the seawater from which it was formed. Runoff, on the other hand, has low fraction of $^{18}O/^{16}O$ ($\delta^{18}O$) and high barium (Ba) and total alkalinity (A_T) concentrations. The low $\delta^{18}O$ signal is a signature of meteoric water, while the high Ba and A_T concentrations are caused by weathering of minerals in the drainage basins. The latter often results in high, but variable, concentrations of Ba and A_T in the waters of individual rivers.

When applying $\delta^{18}O$ or A_T to evaluate the freshwater sources, one also gets negative sea ice melt water, and this is an indication of brine being added to the water during sea ice production. Already in the beginning of the 1980s, $\delta^{18}O$ was used to evaluate the distribution of sea ice melt water (Tan and Strain 1980) and to make balances of mass (volume) and freshwaters for the Arctic (Östlund and Hut 1984). Since then, $\delta^{18}O$ has been a commonly used tracer, often in combination with others, to evaluate the water mass composition of the Arctic Ocean (e.g. Schlosser et al. 1994a; Bauch et al. 1995; Melling and Moore 1995; Macdonald et al. 1995; Macdonald et al. 1999; Ekwurzel et al. 2001).

By combining data from five cruises performed in 1987, 1991, 1993, 1994 and 1995, Ekwurzel et al. (2001) show that the runoff is fairly evenly distributed, adding ~10 m of freshwater over the whole central Arctic Ocean except for the Nansen Basin, where much less is found. This estimate includes freshwater removed as sea ice.

Fig. 4.9 *Left column*, deep-water characteristics in the Makarov Basin (*green*) and the Canada Basin (*red* and *violet*). *Right column* deep-water characteristics in the Amundsen Basin (*cyan* (1991), *green* and *yellow* (1996)) and Nansen Basin (*blue* (1996)). *Violet* (1995) and *magenta* (1993) indicate stations taken at the slope of the Nansen and Amundsen basins. The deepest of these stations is at the base of the slope north of the Laptev Sea. The higher temperatures and salinities at the bottom suggest that the bottom water is created by slope convection and entraining plumes. The variability in salinity and temperature in the Amundsen Basin bottom water could either be due to geothermal heating or to varying characteristics of the waters derived from the slope convection, as is seen by the high temperature and salinity found at the base of the Laptev Sea slope (deepest *violet station*). The temperature minimum in the Nansen and Amundsen basins could be due to less-saline inflow from the St. Anna Trough. In the Canada Basin, the temperature minimum could be explained by the advection of deep waters from the Makarov Basin across the sill between the Alpha and the Mendeleyev ridges. The Makarov Basin is the only basin with no deep temperature minimum. The salinity first reaches a maximum value in a 1,200 m deep layer while the temperature decreases for another 400 m before the isothermal and isohaline bottom water is reached. This is in agreement with the densest water mostly deriving from a spillover of intermediate water from the Amundsen Basin across the Lomonosov Ridge (Jones et al. 1995), a process yet to be confirmed. Stations positions are shown in Fig. 4.19d

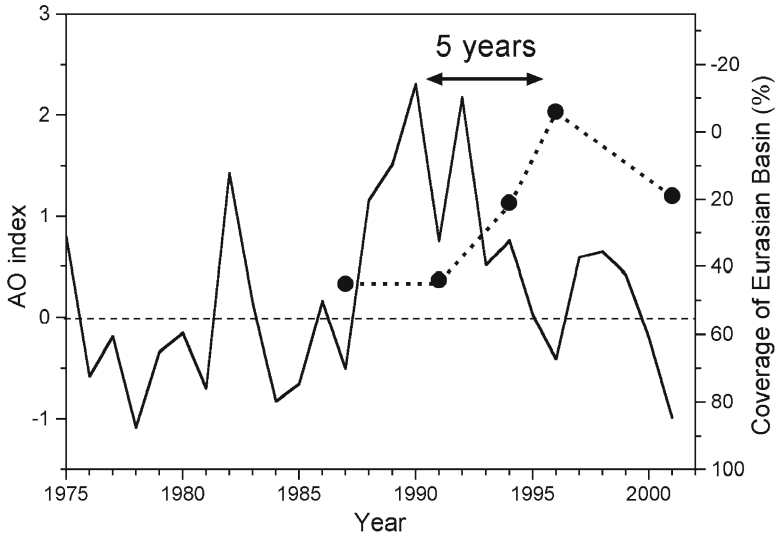

Fig. 4.10 Changes in the shelf (river) water front. The *solid line* represents the winter (November–February) values of the Arctic Oscillation, and the *dots* show the percentage of the deep Eurasian Basin covered by low-salinity shelf water (river runoff) (Adapted from Anderson et al. 2004)

The sea ice melt is mainly found north of the Barents Sea, where the warm inflowing Atlantic Water meets and melts the exiting sea ice, while brine equivalent to ~6 m sea ice production is found over the Canadian and western Amundsen Basins, with little north of the Laptev Sea, where much of the ice in the Arctic initially is formed. The distribution of sea ice melt and brine reflects a combination of ice dynamics and circulation of the upper waters.

Total alkalinity is an almost conservative tracer in the Arctic Ocean, and high concentrations are found in river runoff as a result of a combination of decay of organic matter and dissolution of metal carbonates. It has been used to trace the river runoff front within the Eurasian Basin (e.g. Anderson and Jones 1992), which reflects the extent of the 'cold halocline' as further discussed under 4.3.2.3. By applying the variability of the front during five cruises between 1987 and 2001, it was shown that the runoff has a minimum coverage over the Eurasian Basin during years of high AO indexes, but with a lag of ~5 years (Anderson et al. 2004) (Fig. 4.10).

Dissolved barium concentrations in the upper Arctic Ocean (<200 m) range between 19 and 168 nmol L^{-1} in a manner geographically consistent with sources and sinks. The sources are runoff, with the highest concentrations from the American continent, and sinks are biological removals (Guay and Falkner 1998). As a result of these variable sources and sinks, barium has to be used more as a qualitative than as a quantitative tracer.

One of the most useful bioactive chemical tracers of Arctic Ocean water masses is silicate, which is high in the Pacific water entering over the Bering and Chukchi shelves. Through fixation by marine plankton with subsequent sedimentation and decay at the sediment surface, very high concentrations are found in waters of

salinities around 33.1 flowing off the Chukchi shelf (Jones and Anderson 1986). Furthermore, elevated silicate concentrations are found at all depths below the 33.1 isohaline at the Chukchi shelf slope, suggesting the penetration of high-density plumes of high salinity from the Chukchi Sea.

The distribution of the silicate concentration in the intermediate depth waters (from the upper halocline all the way to below the Atlantic layer) collected during the *Oden*-91 expedition was one of the key signatures behind the circulation pattern suggested by Rudels et al. (1994). This circulation pattern was supported by the silicate concentration distribution as observed from ice camps during the 1980s (Jones and Anderson 1986; Jones et al. 1991; Anderson and Jones 1992), suggesting a steady-state situation with a consistent circulation pattern. However, during the ACSYS, decade changes have been observed in the silicate concentration distribution, especially within the Canadian Basin, with decreasing concentrations in the Makarov Basin and central Canada Basin (McLaughlin et al. 1996). These changes have been accompanied by a penetration of warmer Atlantic Layer water into the Makarov Basin (e.g. Morison et al. 1998) (see Sect. 4.3.2.1 below).

The time history of water masses can be deduced from transient tracer distribution and an appropriate model approach. One of the first estimates of Arctic Ocean water mass residence times was made for the freshwater component using observed seawater tritium concentrations compared to tritium in precipitation (Östlund 1982). At most observational sites, a linear relationship between salinity and tritium concentration was found, indicating mixtures of Atlantic layer water and freshwater. The resulting freshwater tritium concentration points to an average residence time of 11 ± 1 years since the freshwater left the river mouth for the data collected in the Nansen Basin and somewhat higher for those collected in the Canada Basin (Östlund 1982). This approach was extended by Schlosser et al. (1994a) by adding ^{3}He and ^{18}O tracer data to those of tritium. With this extra information, it is possible to estimate the residence time of the river runoff on the shelf as well as the time since the halocline water left the shelf. This is possible since the tritium/^{3}He age is set to zero as long as ^{3}He can be lost to the atmosphere by gas exchange. When correcting for the limited exchange of ^{3}He on the shelf, the mean residence time of the runoff component on the shelf becomes 3.5 ± 2 years (Schlosser et al. 1994a). The tritium/^{3}He age along a section crossing the Nansen Basin at about 30°E shows low surface water age (~1 year) at the Barents Sea shelf break, increasing to about 5 years over the Gakkel Ridge. Over the Gakkel Ridge, the tritium/^{3}He age increases with depth to a maximum of about 15 years in the lower halocline (Schlosser et al. 1994a, b). A similar age distribution was also found in the upper and intermediate waters using CFCs (Wallace et al. 1992).

The transient tracer distribution was used by Frank et al. (1998) to investigate the subsurface flow along the continental slope of the Eurasian Basin. The observed tritium/^{3}He age distribution in the Atlantic Layer was found to be 2 years along the continental slope north of the Barents Sea, while it increased to 6 years at the Laptev Sea continental margin for both the Fram Strait and Barents Sea branches. The transit time of the Fram Strait branch of 4 years from the Barents Sea continental margin to that of the Laptev Sea estimated from the tritium/^{3}He age was consistent with the

CFC ages of 4–5 years (Frank et al. 1998). The comparably high tritium/^{3}He age of the Barents Sea branch at the Laptev Sea continental margin was explained by a combination of a 'non-zero' age when the water left the Barents Sea and mixed with older water along the Kara Sea continental slope. Smethie et al. (2000) expanded the transient tracer study of the intermediate waters into the Canadian Basin using samples collected from the Lomonosov Ridge (88°N, 44°W) to the Alaskan North slope (71°N, 145°W) on the SCICEX 96 cruise. Their results show tritium/^{3}He ages in the Barents Sea branch of the Atlantic Layer of 14.5 years over the Lomonosov Ridge, 18.5 years at 78°N off the Chukchi Cap and at the Alaskan North slope, and older water between 78°N and 88°N. They suggest that a fraction of the Barents Sea branch follows the Lomonosov Ridge from the Laptev Sea, while some follows the Siberian continental margin, where a fraction flows off the Chukchi Cap into the Canada Basin with some flow continuing along the boundary to the southern Canada Basin (Smethie et al. 2000). This flow path is consistent with that described in Sect. 4.3.1.1 but adds a time perspective to the flow.

The most common use of transient tracers in Arctic Ocean research has been to deduce the deep-water ventilation (Smethie et al. 1988; Heinze et al. 1990; Schlosser et al. 1990; Schlosser et al. 1994b; Jones et al. 1995; Schlosser et al. 1995; Schlosser et al. 1997; Anderson et al. 1999). Different approaches (model formulations) are used to evaluate the 'ages' of the deep and bottom waters of the different Arctic basins, but with consistent results considering the different approaches. In general, the results give mean residence times and ventilation times in the order of 100–250 years for the Eurasian Basin Deep Water, 200–350 years for the Eurasian Basin Bottom Water and 300–360 years for the Canadian Basin Deep and Bottom Waters. One investigation of special interest is that of Livingston et al. (1984), which used the artificial radionuclide signal from the Sellafield (at that time Windscale) reprocessing plant on the Irish Sea to find a transit time of 8–10 years from the source to 1,500 m depth near the North Pole (LOREX site). This is a remarkable short transit time but cannot be ruled out in light of the flow path of Atlantic water over the Lomonosov Ridge and the very high current speeds observed over the ridge close to the Laptev Sea (Woodgate et al. 2001).

4.3.1.6 Mixing in the Interior

The deep, interior Arctic Ocean is a low-energy environment, where processes normally overwhelmed by mechanical stirring and turbulence may be of importance (Carmack 1986; Padman 1995). The thermocline, where the temperature is unstably stratified, is a region where molecular processes such as double-diffusive convection through diffusive interfaces could occur. In the Canadian Basin, regular staircases with homogenous layers, 5–10 m thick, separated by thin interfaces with steps in temperature and salinity, have been observed (Neal et al. 1969; Neshyba et al. 1971; Padman and Dillon 1987, 1988, 1989). These staircases may extend over depth intervals of 100–200 m and could be instrumental in cooling the Atlantic layer in the deep Canada Basin. In the Eurasian Basin, the thermocline is stronger

but has smaller vertical extent, and the observed steps are larger than those in the Canadian Basin and often appear to be connected with weak inversions. Merryfield (2000) has suggested that horizontal advection, similar but weaker than the advection that creates interleaving and inversions, might operate in the formation of step structures. Extensive layers and step structures have also been observed closer to the bottom in the deep Canada Basin (Timmermans et al. 2003). These layers will be discussed further in connection with the deep-water formation and transformation (Sect. 4.3.1.7).

The intermediate layers of the Arctic Ocean are often characterised by large, regular intrusions, mainly in the Atlantic layer but also deeper in the water column (see Sect. 4.3.1.1 and Fig. 4.4). These layers pose several questions: How do they form? Do they have dynamics of their own? How important are they for the transfer of heat, for example, from the warm Atlantic water in the boundary current into the interior of the basins and for the mixing and transformation of the Arctic Ocean water masses?

Carmack et al. (1995) noticed that the anomalously high temperatures (see discussion in 4.3.2.1) observed in the Atlantic layer in the Makarov Basin in 1993 were associated with prominent intrusions and postulated that the intrusions were formed as the warmer Atlantic water of the boundary current interacted with the colder, and older, Atlantic layer in the Makarov Basin. This explanation is akin to the one offered by Perkin and Lewis (1984), when they observed inversions in the Atlantic layer north of Svalbard during the EUBEX expedition. Similar interleaving structures were found in the Makarov, Amundsen and Nansen basins on the AO94 expedition (Carmack et al. 1997) and had been seen in the Nansen and Amundsen basins on the *Oden*-91 expedition and on the *Polarstern* expeditions to the Eurasian Basin in the 1990s (e.g. Rudels et al. 1994; Rudels et al. 1999a). The layers appeared to reach across the basins, implying a horizontal extension of 100–1,000 km, and Carmack et al. (1997) suggested that the layers were self-propelled, formed at frontal zones, especially as the Atlantic water enters through Fram Strait, and then expanded, driven by double-diffusive processes, into the interior of the basins. The formation and expansion of interleaving layers could then be a major process in bringing heat from the boundary current into the interior of the basins (Carmack et al. 1997).

The observed interleaving structures often have alternating diffusive and saltfinger interfaces, and double-diffusive transports are likely to be present. Layers are observed in all kinds of background stratifications, diffusively unstable (cold and fresh on top), saltfinger unstable (warm and saline on top) and stable-stable (temperature decreasing, salinity increasing with depth). Stability analyses show that layers may form at thermohaline fronts, when one of the components is unstably stratified (Stern 1967; Toole and Georgi 1981; Ruddick 1992; Ruddick and Walsh 1995), but with both component stably stratified, finite disturbances are needed to carry water parcels across, or at least sufficiently far into, the front to form inversions and allow double-diffusive convection to commence.

Walsh and Carmack (2002) explored the spreading of the intrusions encountered in the upper part of the water column, above the Atlantic layer, where the temperature stratification is unstable, and double-diffusive transports due through diffusive

interfaces could occur. They examined the possibility that the non-linear equation of state, which would lead to contraction of mixing, or cabbeling, could reduce the density changes of the warmer intrusions penetrating into colder surroundings. The reduced density changes would then slow down the spreading of the intrusions and limit their extent. Considering the suggested basin-wide coherence of the individual layers, this effect, should it be present, does not seem to prevent the layer structures of the Arctic Ocean to reach the, perhaps largest, horizontal extent and the largest ratio of horizontal to vertical scale found in the world ocean.

May and Kelley (2001) examined the older data from the EUBEX expedition north of Svalbard in 1981 (Perkin and Lewis 1984) and proposed that the baroclinicity of the flow field is important, and perhaps necessary, for intrusions to develop. In the inflow region close to Svalbard, such dynamic situation could exist. However, inversions and layers are also observed in the stable-stable stratified upper Polar Deep Water (uPDW) around 1,000 m depth. These layers are in the Nansen, Amundsen and Makarov basins associated with the presence of less-saline Barents Sea branch water. Merryfield (2002) suggested that the deep layer structures could be caused by differential diffusion due to the faster diffusivity of heat. This effect could lead to the formation of layers even when both components are stably stratified. The time for the layers to form by this process is of the order of years, which appears long, since similar layers are found further to the east in the Nansen and Amundsen Basin, closer to the input of the Barents Sea branch (Rudels et al. 1999a) and at the Mendeleyev Ridge as the deeper part of the boundary current penetrates into the Makarov Basin (Swift et al. 1997). It is, however, shorter than the residence time of the uPDW.

These interpretations are all different from the one offered by Rudels et al. (1994) and discussed earlier in connection with the circulation of the Atlantic water. Rudels et al. (1994) also assumed that the interleaving structures were formed in frontal zones, in the Eurasian Basin primarily in the confluence area of the Barents Sea and in the Fram Strait branches, but expected the intrusions to evolve and expand only during a short period, running down the potential energy stored in the unstably distributed component. Afterward, fossil intrusions would remain and be passively advected by the mean circulation around the basins. Interleaving structures could also form, when there are changes in the characteristics of the boundary current, which create larger property contrasts and intrusions within the boundary current. These intrusions are then carried along by the boundary current and become reinforced as the boundary current enters the different basins and encounters different water properties. Such interpretation would be consistent with the similar shape of the intrusions seen in the boundary current as the warm pulse of Atlantic water penetrates further into the Canada Basin (see e.g. McLaughlin et al. 2004 and also Sect. 4.3.2.1 below).

The formation and the dynamics of the interleaving layers, and their importance for the mixing, heat balance and water mass transformations in the Arctic Ocean, are thus questions far from solved. Are they as extensive as they appear, or do they belong to several distinct water bodies? If interleaving structures are created in different areas, they will, because of the small layer thickness, nevertheless appear to

be connected when looked upon in a Θ-S diagram. These layer structures may, in the end, be found less important than prominent, but they do pose intriguing theoretical and observational challenges.

4.3.1.7 The Bottom Water: Stagnant or Ventilated?

Because of the higher salinities and temperatures found in the deep Arctic Ocean basins, as compared to the Greenland Sea, the renewal of the deep and bottom waters in the different basins has been assumed due to slope convection that brings cold, brine-enriched shelf water into the deep (e.g. Nansen 1906). In the Nansen Basin, this process is modified by the inflow of Nordic Sea deep water through Fram Strait and the input of denser water of the Barents Sea branch, sinking down the St. Anna Trough. In the Canadian Basin, no such deep inflows occur, and differences between the water characteristics in the Amundsen Basin at the sill depth of the Lomonosov Ridge and in the deep Makarov Basin, the Makarov Basin being warmer and more saline must be caused by slope convection. Jones et al. (1995) estimated the ventilation time of the deeper (>1,700 m) layers of the Makarov Basin using potential temperature and salinity profiles and C^{14} concentrations and the plume model applied by Rudels et al. (1994) for the intermediate layers. The deeper layers in the Makarov Basin do not exhibit an increasing salinity and constant temperature with depth, as do the other Arctic Ocean basins. Instead, the salinity reaches a constant value, while the temperature continues to decrease with depth until an 800 m deep isothermal and isohaline bottom layer is encountered. No temperature minimum is present above this layer (Fig. 4.9).

This is not what to expect from slope convection, where the temperature would attain a constant value as the plumes eventually reach the same temperature as their surroundings, and the plumes with the highest salinity (density) will reach the bottom and fill up the deepest layers, leading to increasing salinity with depth. The explanation offered by Jones et al. (1995) was that a spillover of colder water from the Amundsen Basin could take place through deeper, undetected gaps in the central Lomonosov Ridge. Once colder Amundsen Basin water enters the warmer Makarov Basin, it would sink due to its higher compressibility (the thermobaric effect). Although newer bathymetry (Jakobsson et al. 2004b) indicated a narrow, deep (2,500 m) passage through the central part of the Lomonosov Ridge, no oceanographic observations had so far been 'knowingly' made in this passage. The ventilation times determined by Jones et al. (1995) for the deep Makarov Basin were of the same order, 200–300 years, as was found independently by Schlosser et al. (1994b).

However, on the *Healy–Oden* crossing of the Arctic Ocean in 2005, the HOTRAX expedition, this area was closely examined. A 2,700-m deep depression referred to as the *intra-basin* was found in the Lomonosov Ridge with a sill depth of 2,400 m to the Amundsen Basin but a sill depth of only 1870 m to the Makarov Basin (Björk et al. 2007). The layers in the intra-basin between 1,700 and 2,300 m were dominated by deep water from the Makarov Basin overlaying colder, denser Amundsen Basin deep water. No continuous flow from the Amundsen Basin to the Makarov

Basin was observed. Should such flow exist, it must be intermittent and perhaps depend upon external forcing. The Canadian Basin Deep Water (CBDW) was present not only in the intra-basin but also beyond the sill in the Amundsen Basin, implying that CBDW passes from the Makarov Basin through the intra-basin into the Amundsen Basin. The CBDW did not spread into the Amundsen Basin but appeared to follow the Lomonosov Ridge towards Greenland. The passage through the intra-basin might thus be an important, perhaps the most important, passage for CBDW to the Eurasian Basin and to Fram Strait (Björk et al. 2007).

In the Canada, Amundsen and Nansen basins, the salinity increases, and the temperature in the deep waters decreases with depth until a weak, deep temperature minimum is encountered. Below the minimum, both the temperature and the salinity increase with depth until a thick (800 m in the Amundsen Basin, >1,000 m in the Canada Basin) isothermal and isohaline bottom layer is reached (Fig. 4.9). The salinity increase towards the bottom suggests bottom water renewal by slope convection. However, the temperature minimum above the homogenous bottom layer cannot be explained by slope convection.

Extrema often indicate advective features. The minimum present in the Canada Basin can be explained by an inflow of colder, less-saline and less-dense deep water from the Makarov Basin, passing the sill between the Mendeleyev Ridge and the Alpha Ridge (Fig. 4.9). In contrast to the situation in the Makarov Basin, the slope convection in the Canada Basin then creates water denser than that crossing the sill, and the inflow from the Makarov Basin stays above the bottom layer. The similar structure in the Amundsen and Nansen basins is more difficult to understand. One possibility would be that very dense Barents Sea branch water is formed intermittently and sinks along the bottom of the St. Anna Trough, reaching a sufficiently large 'initial' depth at the slope that it avoids entraining warmer, less-dense intermediate water. A smaller salinity excess would then be sufficient for dense plumes originating from the Barents Sea branch to sink deep into the basin, and the temperature increase would be less if they start to entrain higher up on the slope, as would be the case for the high-salinity water formed around Severnaya Zemlya (Rudels et al. 2000a).

However, another interpretation has been proposed. Timmermans et al. (2003) assume that the deepest layer in the Canada Basin is a remnant from a convection event occurring several hundred years ago (MacDonald and Carmack 1991). The temperature in the bottom layer is slowly increasing due to geothermal heating, which stirs and homogenises the bottom layer. The heat is transferred out of the bottom layer, perhaps by double-diffusive convection through the diffusive interfaces, which form an extensive step structure extending over most of the Canada Basin (see Fig. 4.9), or by increased diapycnal mixing at the lateral boundaries at the continental slopes. This transfer prevents the temperature of the bottom layer from increasing, and the density from decreasing, too rapidly. However, in the next decade or so, the density of the bottom layer might have decreased sufficiently for the bottom layer to overturn and mix with the overlying water (Timmermans et al. 2003).

Björk and Winsor (2006) noticed a temperature change in the bottom layer in the Amundsen Basin between 1991, 1996 and 2001, which they interpreted as an effect

of geothermal heating. However, the temperature and salinity in the bottom layers in the Amundsen and Nansen basins also vary along the basins, and higher temperatures and salinities were observed closer to the Laptev Sea in 1995 than in the central part of the basin in 1996. This is where dense water, formed by slope convection, is expected to enter the deep Amundsen Basin. It is thus at least conceivable that the observed changes are due to advection of water with higher temperatures and salinities recently created by slope convection (Fig. 4.9). However, the bottom layers are likely to be influenced by geothermal heating. The earth is losing heat, and it is to be expected that this heat is stored in a stagnant layer. The deep and homogenous layer also suggests that a mixing agent such as a weak thermal convection stirs the bottom water. Geothermal heating and boundary convection are two completely independent processes and can well operate simultaneously, together forming the characteristics and the controlling evolution of the bottom waters in the deep basins. The slope convection would supply the high-salinity water, causing part of the temperature increase in the deep and bottom waters, while the geothermal heating adds further heat and also stirs the bottom layers.

The Canadian and Eurasian basins are different below mid-depth because of the presence of the Lomonosov Ridge, but within the Eurasian Basin, the Nansen and Amundsen basins also exhibit differences below the sill depth of the Lomonosov Ridge. The Nansen Basin has a lower salinity between 1,500 and 2,500 m due to the inflow of less-saline Arctic Intermediate Water (AIW) and Nordic Seas Deep Water (NDW) through Fram Strait. This is the inflow of deep water from the Greenland Sea postulated by Nansen (1915). The lower salinity extends upward almost to the Atlantic layer in the Nansen Basin, but the Amundsen Basin becomes less saline than the Nansen Basin above 1,500 m because of the presence of the even less-saline Barents Sea inflow branch at these levels in the Amundsen Basin. Below the Barents Sea branch water, the Amundsen Basin has a salinity maximum around 1,500 m (Fig. 4.4) due to returning, saline deep water from the Canadian Basin, which, after crossing the Lomonosov Ridge, perhaps mainly through the intra-basin (Björk et al. 2007), bifurcates at the Morris Jesup Plateau with one part penetrating into the Amundsen and along the Gakkel Ridge but not entering the Nansen Basin. The rest joins the East Greenland Current and exit the Arctic Ocean through Fram Strait (Jones et al. 1995; Fig. 5). Warm saline Canadian Basin Deep Water (CBDW) has also been observed on the Amundsen Basin side of the Lomonosov Ridge close to the Laptev Sea. These volumes appear to be much smaller than those involved in the exchanges through the intra-basin (Rudels et al. 2000a; Woodgate et al. 2001).

4.3.1.8 Eddies

The description of the circulation presented above gives the impression that the water movements below the halocline all occur as streams, or rivers, moving around the basins. However, just as eddies have been observed in the upper layers of the Canadian Basin (e.g. Hunkins 1974, Newton et al. 1974; see Sect. 4.2 above), eddies have also been seen in the deeper layers. The low-salinity lens observed in the

Makarov Basin from *Louis S. St-Laurent* in 1994 (Swift et al. 1997) might well have been an eddy, and on the *Polarstern* 96 section across the Eurasian Basin, 4 or 5 eddies were observed. They were found at different depths and displayed different Θ-S characteristics with respect to the neighbouring stations (Fig. 4.11). The origin of the different eddies could therefore be determined (Schauer et al. 2002a).

The eddy with the largest vertical extent was observed over the Gakkel Ridge and was centred at 1,700 m depth, and its presence was detected vertically over more than 2,000 m. It was a warm and saline anomaly implying the presence of Canadian Basin Deep Water (CBDW) (Fig. 4.11). In the Amundsen Basin, a cold, less-saline eddy was found at 1,000 m depth, showing the presence of almost undiluted Barents Sea branch water. The deeper interleaving thermohaline layers present in the Nansen Basin did not show a continuous change across the front but had a station with extreme properties in the centre, suggesting layers evolving out of (or into) a lens of Barents Sea branch water, just as layers are forming around 'meddies' in the North Atlantic. Two eddies were also found in the Atlantic layer. One was identified in the interleaving structure on the basin side of the Fram Strait branch by having much weaker intrusions, suggesting inflowing rather than returning Fram Strait branch water. The second was a warm, saline fairly deep eddy of Fram Strait branch water in the Amundsen Basin. The CBDW eddy made an especially large impact on the water column, displacing the isolines downward, giving the impression that the homogenous bottom layer thickness had been reduced compared with the neighbouring stations (Fig. 4.9). The eddies, except the one surrounded by interleaving layers, were only observed at single stations and thus had a horizontal extent of less than 30 nautical miles.

How numerous are these eddies and what is their impact on the observed property distributions? How much of the deep salinity maximum in the Amundsen Basin is due to eddies moving from Greenland towards the Laptev Sea, slowly losing their properties, compared to a continuous, direct flow? The eddies appear to move differently than the mean circulation, as is suggested by their passing through ambient water masses without affecting the interleaving thermohaline layers, creating unexpected water mass characteristics in far-off areas (Schauer et al. 2002a).

4.3.2 Change

An appreciation of the variability of Arctic Ocean water masses was implicit in the rhetoric question asked by Quadfasel et al. (1991) 'Is the Arctic warming?' This question was based upon comparison between the climatological temperature field found in the Atlas of the Arctic Ocean (Gorshov 1980) and XBT observations made from the icebreaker *Rossia* in 1990. These indications have been followed by many others during the 'ACSYS' decade. First, the changes were mainly considered as possible evidence that the Arctic now was showing signs of what climate models long have been implying – the global climate is getting warmer and the largest changes are expected at high northern latitudes. While this may well be the case, the

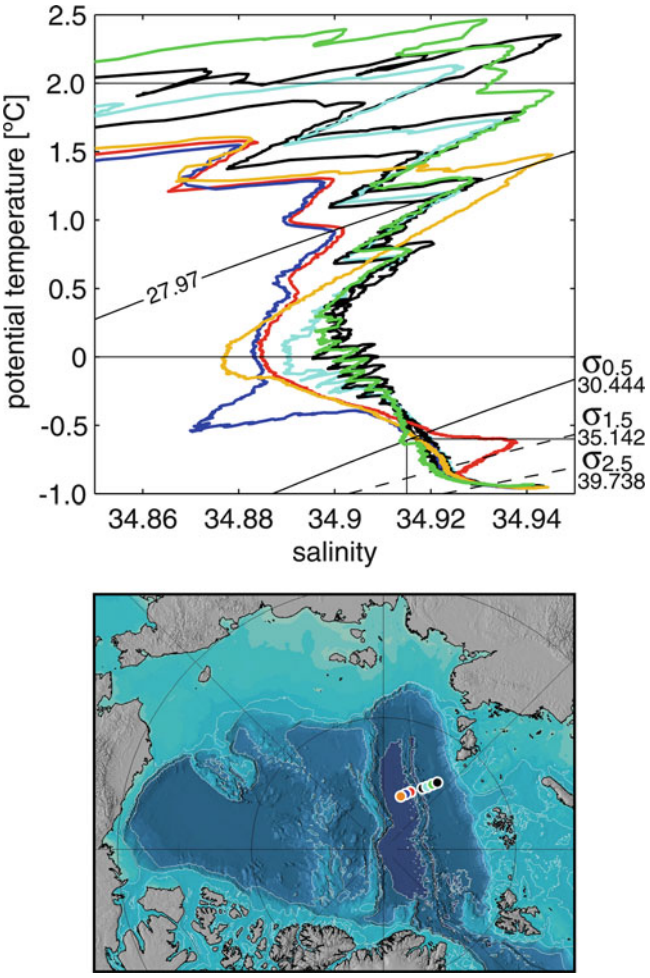

Fig. 4.11 (*Top*) ΘS diagram showing eddies present in the Intermediate and deep layers on the *Polarstern* 96 section across the Eurasian Basin. The *red station* shows the warm and saline Canadian Basin Deep Water; the *blue station* indicates an isolated lens of cold, low-salinity Barents Sea branch water. The *cyan* and *black stations* show an eddy of Barents Sea branch water with warmer and more saline water in both the slope and the basin directions and surrounded by interleaving structures like a 'meddy'. This is in contrast to the slope to basin decrease in salinity and temperature seen in the interleaving in the Atlantic layer, although also here an eddy of warm Atlantic water was detected (*green station* located in space between the *black* and *cyan stations*). Finally, an eddy of warm, saline Fram Strait branch water, *yellow station*, was present in the colder, Barents Sea branch-dominated Atlantic layer in the Amundsen Basin (Adapted from Rudels 2009). (*Bottom*) Blow-up map showing the positions of the stations

awareness that conditions in the deep Arctic Ocean could change initiated a search for variability in the Arctic Ocean and lead to efforts to relate this variability to changes in the forcing. These investigations have also gone back in time, examining older data. Did similar changes occur earlier but pass unnoticed? Intense study of

the different meteorological conditions has revealed changing, and alternating, dominant climatic regimes in the Arctic, e.g. the Arctic Oscillation (AO) (Thompson and Wallace 1998) and the North Atlantic Oscillation (NAO) (Hurrell 1995), and imposed the question how the different regimes in these oscillations influence and interact with the oceanic circulation regimes in the Arctic Mediterranean (Proshutinsky and Johnson 1997). The strength and importance of the recent changes have also lead to reanalyses of earlier, historic observations to find if similar rapid changes in the water mass characteristics had occurred (e.g. Swift et al. 2005; Polyakov et al. 2004).

4.3.2.1 The Atlantic Layer

An increase in temperature in the Atlantic layer as the one observed by Quadfasel et al. (1991) could be due to a stronger and/or warmer inflow of Atlantic water through Fram Strait. Probably, it is a consequence of both. The higher temperatures were first observed at the continental slope in the Nansen Basin in 1990 (Quadfasel et al. 1991), north of the Laptev Sea in 1993 (Schauer et al. 1997), at the Arlis Plateau in 1993 (Carmack et al. 1995), in the interior of the Makarov Basin and at the Lomonosov Ridge close to the pole in 1993 during the SCICEX-93 expedition with *USS Pago* (Morison et al. 1998), in 1994 from *CCGS Louis S. St Laurent* (Aagaard et al. 1996; Swift et al. 1997) and in the eastern Amundsen Basin from *RV Polarstern* in 1995 (Rudels et al. 2000a) and 1996 (Schauer et al. 2002a). In 1997, a warmer Atlantic layer with intrusions of less-saline and colder Barents Sea branch water was seen north of Fram Strait, returning from, presumably, the Nansen Basin (Rudels et al. 2000b).

The eastward spreading in the boundary current in the Canada Basin has taken longer time, and only in 1998 was warmer Atlantic water observed north of the Chukchi Cap and the Northwind Ridge (McLaughlin et al. 2004). The ‘pulse’ of warm Atlantic water thus works as a Lagrangian tracer delineating the paths of the Atlantic water in the Arctic Ocean. The warm Atlantic core was here, as almost everywhere else, characterised by inversions in temperature and salinity in the vertical profiles. This indicates mixing with ambient waters, or since the intrusions are very similar to those observed upstream in the boundary current, they could also have formed at the first encounter between the different waters, and these initial, advected, intrusions might precondition the further evolution of the interleaving (see Sect. 4.3.1.6 above).

After a short period of colder Atlantic water entering the Arctic Ocean in the late 1990s, the temperature of the inflowing Atlantic water has again increased. The new inflow pulses have been traced both upstream through the Norwegian Sea and downstream along the continental slope and ridges in the Arctic Ocean (Polyakov et al. 2005; Walczowski and Piechura 2006). Long-term changes in the Atlantic water are examined further in Chap. 6.

4.3.2.2 Redistribution of Water Masses in the Upper Layers

In connection with the presence of warmer Atlantic water in the Eurasian Basin, it was also found that the thickness of the upper, low-salinity surface layer had been reduced, and the Atlantic layer was closer to the sea surface and the ice (Morison et al. 1998). This vertical shift of the temperature and salinity profiles accounts for a large part of the change relative to the climatology. A similar change was also seen in the Makarov Basin (Carmack et al. 1995; Morison et al. 1998), where both the salinity and the temperature were higher than the climatological values. Changes were also seen in the nutrient and oxygen distributions. The high nutrient and low oxygen concentrations observed from the ice camps in the 1960s and 1970s (e.g. Kinney et al. 1970; Jones and Anderson 1986) were largely absent, when the icebreakers in the 1990s started to penetrate into the Makarov Basin. Excess of low-salinity surface water, by contrast, was found in the Canada Basin (McPhee et al. 1998; MacDonald et al. 1999), where the salinity of the upper layer was reduced. Carmack et al. (1995), McLaughlin et al. (1996) and Morison et al. (1998) explained this as a shift of the front between upper waters deriving from the Atlantic and the Pacific Oceans. The Pacific upper water lens no longer extended to the Lomonosov Ridge but was confined to the Canada Basin, and the Atlantic derived upper layer was in contact with the surface up to the Mendeleyev Ridge. The Pacific water, being forced into the Beaufort Sea and towards the North American slope and shelf, was becoming more prominent in the Lincoln Sea north of Ellesmere Island (Newton and Sotirin 1997). This could indicate an increased eastward boundary flow along the continental slope towards Nares Strait and Fram Strait, compensating the shift in Pacific water on the Siberian side of the Arctic Ocean. The draining of the Pacific water through the western channels of the Canadian Arctic Archipelago might also have increased.

The frontal shift is a manifestation of the contraction of the anti-cyclonic Beaufort Gyre, which is maintained by the high-pressure cell that develops during winter over the Beaufort Sea. When the advection of warmer air from lower latitudes is strong, especially through the Atlantic sector, the high-pressure cell weakens, and the oceanic anticyclone diminishes and is forced closer to the American continent, while the cyclonic circulation is strengthened. This leads to changes in the circulation of the low-salinity shelf waters on the Eurasian shelves (Proshutinsky and Johnson 1997; Polyakov et al. 1999; Polyakov and Johnson 2000; Maslowski et al. 2000).

In the anti-cyclonic regimes, the shelf water crosses the shelf break in the eastern Laptev Sea and enters the Amundsen Basin, but in the cyclonic regime (Proshutinsky and Johnson 1997) that has dominated during the 1990s, the shelf water has instead moved into the East Siberian Sea and then entered either the Makarov Basin or the Canada Basin (Maslowski et al. 2000). Since the Siberian shelves receive the runoff from the large rivers, this has led to increased salinities in the upper layers of the Amundsen and partly in the Makarov Basin and, likely, to lower salinities in the Canada Basin. The latter effect is enhanced by the closer confinement of the low-salinity Pacific water to the Canada Basin.

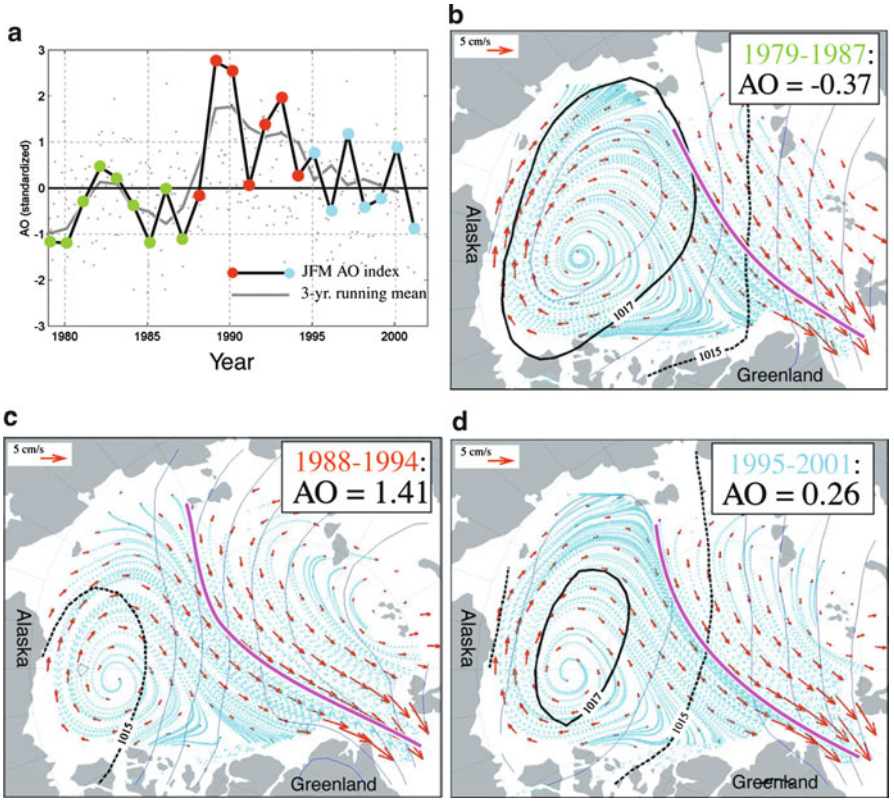

Fig. 4.12 Different circulation modes in the Pacific water. (**a**) Time series of the Arctic Oscillation (*AO*) index for January–March and its running means. Monthly values are shown as *grey dots*. Three periods are distinguished, 1979–1987 (*green*, AO negative), 1988–1994 (*red*, AO positive) and 1995–2001 (*blue*, AO weakly positive). (**b**, **c**, and **d**) show the mean sea-ice motion (vectors) and sea level pressure (contours). The *blue streaks* are the Lagrangian paths forced by the mean vector fields. The magenta line indicates the zero vorticity contour (From Steele et al. 2004)

Steele et al. (2004) traced the distribution of the upper temperature maxima of the Pacific water, deriving from the Alaskan Coastal Water (ACW) and Bering Sea Summer Water (BSSW), respectively (see above Sect. 4.3.1.3). They concluded that during a negative or weakly positive AO state with a well-developed Beaufort Gyre, the BSSW becomes trapped in the Beaufort Gyre and the upper waters north of Ellesmere Island and Greenland derive from the Siberian branch of the Transpolar Drift. In the strong positive AO state with a diminished Beaufort Gyre, the Siberian branch starts farther to the east, and the BSSW becomes incorporated into the Transpolar Drift and passes directly to the Lincoln Sea. It is also possible that the shifting of the low-salinity Beaufort Gyre surface water lens towards the North American continent strengthens the boundary flow of the Alaskan Coastal Current (ACC) to the Lincoln Sea (Steele et al. 2004) (Fig. 4.12).

4.3.2.3 Changes in the Halocline

The deflection of the low-salinity shelf water occurring in the cyclonic regime has caused a weakening and even occasional disappearance of the two-layer Polar Mixed Layer – halocline structure in parts of the Amundsen Basin. This was first noted by Steele and Boyd (1998), who compared observations close to the North Pole from SCICEX cruises in 1993 and 1995 and from *Louis S. St-Laurent* 1994 with the measurements from *Oden* in 1991. This change implies that warm water of the Atlantic layer is in direct contact with and could be entrained into the winter-mixed layer in the Amundsen Basin as well as in the Nansen Basin, which might lead to melting of ice, or rather, could reduce the ice formation rate (Martinson and Steele 2001). Whether this important implication takes place or not, depends upon the mixing mechanisms. If the main stirring is due to mechanically generated turbulence, heat can continuously be brought to the surface. Some heat would be used to melt ice; the rest would be lost to the atmosphere (Walin 1993; Rudels et al. 1999b). If the mixing is due to haline convection, as a consequence of ice formation, the heat brought into the winter-mixed layer causes ice to melt or at least lowers the ice formation rate. This reduces the convection (Martinson 1990; Martinson and Steele 2001). This in turn weakens the entrainment and the vertical heat transfer from the Atlantic layer to the mixed layer and to the ice. In either case, mechanical mixing or convection, the vertical heat flux to the ice only occurs in winter, when the strong stratification induced by summer ice melt has been removed by freezing.

The presence of the ice cover and the heat advected to the Arctic Ocean by the Atlantic water are both important components in the heat balance of the Arctic, and the formation and maintenance of the halocline as an insulating layer has therefore drawn some attention. The change in the upper layer Θ-S distribution has been described as 'the retreat of the cold halocline *layer*' (Steele and Boyd 1998) This, perhaps, to take into consideration that the halocline in the Arctic Ocean is a water mass in its own right, having a vertical extension of 50–200 m, not being just a salinity gradient (Coachman and Aagaard 1974) (see Sect. 4.2 above). To speak of the retreat of the halocline layer might then suggest that the formation of halocline water has diminished. This is not the case. In the 1990s, a winter-mixed layer has been present not only in the Nansen Basin but also in the central Amundsen Basin up to the Lomonosov Ridge, and perhaps also in the Makarov Basin. What was missing was the upper, cold low-salinity shelf water because it had been deflected farther to the east, and no cold salinity gradient had formed above the winter-mixed layer. This prevents the winter-mixed layer from becoming a halocline water mass, but it does not mean that the production of potential halocline water has diminished. The 'retreat of the cold halocline layer' had thus perhaps better been rendered 'the diversion of the low-salinity surface water'.

Recent observations have shown the return of the low-salinity shelf water to the central Amundsen Basin, and a cold halocline has again been established between the shelf water layer (the Polar Mixed Layer) and the winter-mixed layer (Björk et al. 2002; Boyd et al. 2002). Anderson et al. (2004) determined from total alkalinity the presence of river water and sea ice melt water in the upper layers of the

Eurasian Basin between 1987 and 2001 using data from 5 icebreaker cruises (see also Sect. 4.3.1.5 above). They found that in 1987 (Anderson et al. 1989) the river water front, defined as the line along which 5% of the surface water was river water, reached to the Gakkel Ridge. The extent of the river water layer then diminished from 1991 and 1994 to a minimum in 1996, when the front was located over the Lomonosov Ridge and river water was practically absent in the Amundsen Basin. In 2001, the front again had moved into the Amundsen Basin but not as far as the Gakkel Ridge (Fig. 4.10).

Another feature, which may be connected with the changed distribution of the river water, was observed in 1998 in the Canada Basin. At this time, a cold, close to freezing, highly oxygenised temperature minimum with salinity 33.9 was found close to the northern part of the Chukchi Cap (McLaughlin et al. 2004). McLaughlin et al. (2004) suggest that this halocline water mass derives from a new source of lower halocline water, the East Siberian Sea. Before 1990, the East Siberian Sea had been ignored as a possible source of halocline water because of its low salinity (Aagaard et al. 1981). During the 1990s, when most of the runoff from the western Siberian rivers entered the East Siberian Sea and not the Amundsen Basin, the salinity could be even less, and the East Siberian Sea as a source for lower halocline water appears unlikely. However, the change in the river water distribution might have caused the low-salinity surface water to be absent also from parts of the Makarov Basin. This would extend the area without a cold halocline and with convection down to the thermocline from the Nansen Basin and parts of the Amundsen Basin into the Makarov Basin, and it would maintain the cold winter-mixed layer that is the embryo of the Fram Strait branch halocline in these basins (Rudels et al. 1996; Rudels et al. 2004a). The location of the saline temperature minimum north of the Chukchi Cap rather than between the Chukchi Cap and the continental slope is in agreement with the different paths of the Barents Sea branch and the Fram Strait branch halocline waters as suggested by Rudels et al. (2001, 2004a).

In the Nansen Basin, the Polar Mixed Layer – halocline structure is absent during both the anti-cyclonic and the cyclonic regimes. Consequently, the area where the Atlantic layer and the ice cover were in contact did not increase dramatically during the 1990s and therefore probably did not contribute much to the reported reduction of the ice cover extent and thickness in the Arctic Ocean (McPhee et al. 1998; Rothrock et al. 1999; Winsor 2001; Holloway 2001; Holloway and Sou 2002).

4.3.2.4 The Intermediate Layers

The variability observed in the 1990s was not confined to the upper and Atlantic layers. Changes were also seen at intermediate depths. The less-saline Barents Sea inflow branch became more prominent in the Eurasian Basin between 1991 and 1995/1996, and a distinct salinity minimum was present below the Atlantic layer in 1995 (see e.g. Fig. 4.7). This change could have several causes. A larger precipitation in the Norwegian Sea and the Barents Sea, as a result of the strong positive NAO state dominating in the early 1990s, would lower the salinity of the Barents

Sea branch, and the warmer Atlantic water of the Fram Strait branch could be less dense than before, leading to a, relatively, deeper input from the St. Anna Trough that penetrated below rather than into the Atlantic layer, creating the mid-depth salinity minimum (Rudels and Friedrich 2000). The low-salinity Barents Sea branch water mass could be traced in the interior Nansen Basin and Amundsen Basin and along the Lomonosov Ridge. It was also seen entering the Makarov Basin in the boundary current (Rudels et al. 2000a).

The cold, less-saline intermediate water found in the Makarov Basin during AO94 expedition (Swift et al. 1997) and the cooling and freshening of the intermediate waters observed in the Canada Basin between 1989 and 1995 (McLaughlin et al. 2002, 2004) indicate an inflow of Barents Sea branch intermediate water into the interior of the Makarov and Canada basins. However, this colder, less-saline water must have left the Barents Sea earlier than the low-salinity water observed at the Lomonosov Ridge and north of the East Siberian Sea in 1995. Are we then observing a trend in decreasing salinities in the intermediate waters supplied by the Barents Sea, or are we just beginning to observe the variability of the Barents Sea branch inflow characteristics?

A lower salinity at the Lomonosov Ridge and in the boundary current changes the characteristics of the intermediate water of the Makarov and Canada basins by lateral advection and mixing. It will also affect the slope convection, since the entrained water will be colder and less saline. This gradually leads to different characteristics of the intermediate and deep waters in the Canadian Basin, even if the formation of dense shelf water and the entrainment rate do not change (Rudels et al. 2000a). Most likely they do, and the deep Makarov and Canada Basin water columns will never attain a state, where the advection in the boundary current, the slope convection and the exchanges between slope and basin interior are in equilibrium.

4.3.3 Exchanges

The exchanges, not just of volume but also of heat and freshwater (salt), have a significance extending beyond pure bookkeeping. The oceanic transports of heat have impact on the Arctic climate, and the freshwater balance of the Arctic Ocean is important for the existence of the ice cover as well as for the dense water formation, in the Arctic Ocean and in the downstream convection sites: the Greenland Sea, the Iceland Sea and the Labrador Sea. Through its influence on the deep-water formation, the freshwater transport affects the Meridional Overturning Circulation and thus the global climate. Much of the recent work on the exchanges between the Arctic Ocean and the world ocean has been carried out within the international Arctic–Subarctic Ocean Fluxes (ASOF) programme, which has acted as an umbrella for several international and national studies. Results of these efforts have now been published in the volume ‘Arctic–Subarctic Ocean Fluxes’ edited by Dickson, Meincke and Rhines (Dickson et al. 2008a). The summary of the transport estimates through the different passages given below represents the state of knowledge at the

early stage of ASOF. Rather than trying to update the present section, we refer the reader to the ASOF volume for more recent results. The North Atlantic Meridional Overturning Circulation (MOC) is discussed in Chap. 6 with reference to some diagnostic model calculations.

4.3.3.1 Fram Strait Transports

As the deepest connection between the Arctic Ocean and its surrounding seas, the passage between Greenland and Svalbard – Fram Strait –, has long been recognised as being of prime importance not only for the hydrography of the Arctic Ocean but also for the climate of the Arctic. It is the main (>90%) exit for the sea ice formed in the Arctic Ocean. It is also the passage where most of the oceanic sensible heat is advected into the Arctic Ocean. Although this transport is not large enough to keep the Arctic Ocean free of ice, as was speculated in the mid nineteenth century, the heat transport in the narrow meridional band occupied by the West Spitsbergen Current is comparable to the atmospheric heat transport across 80°N. In addition, the export of ice, or latent 'cold', further emphasises the importance of Fram Strait for the heat balance of the Arctic.

Fram Strait is also the only deep passage through which the Arctic Ocean deep waters may be advectively renewed, and for a long time, it was assumed that the Arctic Ocean deep waters derived from the Greenland Sea. When it was found that the Arctic Ocean deep waters to a large extent are locally produced, or at least locally modified, Fram Strait nevertheless remained the only passage, where an exchange of deep water could occur. A study of the water masses present in Fram Strait thus provides information of the integral effects of the water mass (trans) formation processes in the Arctic Ocean.

The main focus, however, has always been the transports. The inflow of Atlantic water was first estimated by geostrophic computations on hydrographic sections extending from Svalbard to the ice edge (e.g. Timofeyev 1962). Some hydrographic sections extended across the strait to the Greenland side, e.g. Ob in 1956 and Edisto in 1965 (Palfrey 1967). The northward transport was estimated to be 3–4 Sv (Timofeyev 1962). The outflow of polar surface water in the East Greenland Current has been more difficult to determine but has commonly been estimated to be 1–2 Sv (e.g. Mosby 1962; Vowinckel and Orvig 1970).

In 1971–1972, the first yearlong current measurements in the West Spitsbergen Current were obtained (Aagaard et al. 1973). They showed a much larger northward transport, 8 Sv, than previously assumed. The larger transport was due to a strong barotropic component of the current, which could not be assessed by the geostrophic computations. These observations formed the backbone of the mass, salt and heat budget for the Arctic Ocean made by Aagaard and Greisman (1975), where the inflow of 7.1 Sv of Atlantic water was assumed balanced by an outflow of 1.8 Sv of polar water and 5.3 Sv of returning, colder Atlantic water. The current measurements were continued for several years, and in 1984–1985 and 1985–1986, current metre arrays extending across the entire strait were deployed. The observations

showed a westward turning of the current in the central part of the strait, and the southward flow in the East Greenland Current above 600 m was estimated to be 3 Sv, 1 Sv polar water and 2 Sv Atlantic water (Foldvik et al. 1988).

In the 1980s, several complete sections were obtained across Fram Strait, and geostrophic transports were computed. The obtained transports of Atlantic water (1–2 Sv) were generally much lower than those estimated from direct current measurements, and a large recirculation of the West Spitsbergen Current was found in the strait (Rudels 1987; Bourke et al. 1988). That warmer Atlantic water is moving south beneath the polar water in the East Greenland Current has been known for a century, and its source had been deduced as the recirculation of the Atlantic water of the West Spitsbergen Current (Ryder 1891).

To allow for the unknown reference velocities, Rudels (1987) used a variational approach with constraints on the mass and salt transports imposed by requirement of mass and salt balance, estimates of the transports through the other passages and constraints on the deep circulation based on considerations of the Θ-S structure of the deep waters. The reference velocities were then calculated by minimising the total kinetic energy of the flow field. The obtained transports were about half of those estimated by Aagaard and Greisman (1975): The northward transport of Atlantic water was close to 2 Sv with 1 Sv recirculating in the strait. The applied mass balance also required a net southward flow of 1 Sv through the strait. Schlichtholz and Houssais (1999a, b) used the entire hydrographic data set from the MIZEX 1984 experiment but no other data and determined the circulation in the strait using a 3-dimensional variational model. They obtained a still smaller northward transport; less than 1 Sv of Atlantic water was found to enter the Arctic Ocean. By the end of the 1980s, the general opinion was that the transport estimates based on the direct current measurements had been too large and that the recirculation in the strait had been underestimated. Aagaard and Carmack (1989) in their new mass and freshwater balance of the Arctic Ocean gave 1 Sv as the inflow of Atlantic water through Fram Strait.

After a few years with less activity, the study of the Fram Strait exchanges took new life by the end of the 1990s. In connection with the VEINS (Variability of Exchanges in the Northern Seas) programme, a current metre array comprising 14 moorings was deployed across the strait along the sill at 79°N. This mooring array has, with small changes, additions and reductions, been in position ever since, first as a part of the ASOF programme and now within the DAMOCLES (Developing Arctic Modelling and Observing Capabilities for Long-term Environmental Studies). Hydrographic sections have been taken at least once every year in connection with the replacement of the moorings, but often more than one section have been taken in a year.

The results from the current measurements confirm the large northward transport and the barotropic flow obtained by the earlier moorings in the West Spitsbergen Current (Aagaard et al. 1973). The total, northward and southward, monthly mean transports have been around 10 Sv, with a net southward flow ranging from 1 to 3 Sv in the different years (Fahrbach et al. 2001; Schauer et al. 2004; Schauer et al. 2008). The estimated northward transport of Atlantic water has been around 4 Sv.

The transports have shown variations not only between the years but also seasonally with the strongest flow in winter. The northward heat flux has also varied between the years, but in 1999, the amount of heat entering the Arctic Ocean through Fram Strait was estimated to be sufficient to generate a temperature increase in the Atlantic layer comparable to that observed in the early 1990s (Schauer et al. 2004; Schauer et al. 2008).

The different streams of the West Spitsbergen Current have also become better known. In addition to the inflow stream over the shelf north of Svalbard, a second stream follows the western and northern slope around the Yermak Plateau. This stream transports Atlantic water and also intermediate and deep waters from the Nordic Seas into the Arctic Ocean (Aagaard et al. 1987; Rudels et al. 2000b; Rudels et al. 2005). The flow around the Yermak Plateau may be as strong as that closer to Svalbard (Schauer et al. 2004). Gascard et al. (1995) found from sub-surface drifters that a part of the West Spitsbergen Current may also cross the Yermak Plateau into the Sofia Deep along a smaller trough in the plateau. The recirculation in Fram Strait is clearly seen in the water mass properties, but it has been difficult to chart the recirculating branch(es), and it may be that the exchange between the West Spitsbergen Current and the East Greenland Current mainly takes place by the transfer of eddies (Gascard et al. 1988; Gascard et al. 1995; Rudels et al. 2005).

During VEINS and ASOF, the West Spitsbergen Current has been extensively explored during yearly expeditions with the sailing research vessel *Oceania*. Recently, the hydrography work has been augmented by current observations using ship-mounted ADCP as well as lowered (L)ADCP. These snapshots also show the large difference between geostrophically computed velocity and direct current measurements. Especially, the LADCP observations indicate transports in the West Spitsbergen Current that are even larger than those estimated from the mooring array (Walczowski et al. 2005). One complete CTD section made by *Polarstern* was complemented by current measurements from a ship mounted ADCP. Also, this estimate showed high transport and a net southward flow, 11.5 Sv to the north and 13.1 Sv to the south (Cisewski et al. 2003).

In the context of the ASOF programme, geostrophic transport computations were made also on historic sections. These, surprisingly, also show an increase in transports between the early 1980s and the late 1990s. A part, but not all, of this increase could be due to the closer station spacing on the more recent sections, which allows for the resolution of smaller eddies, which will add to the total northward and southward flows. The net southward flow ranged from 1.5 to above 4 Sv (Rudels et al. 2004b; Rudels et al. 2008). A net outflow is expected because of the Barents Sea inflow, but more than 3 Sv appears unrealistic. However, geostrophic computations, here combined with constraints on the deep salt and mass fluxes, are always susceptible to incomplete station spacing, not resolving the eddies, the effects of the sections not being synoptic, and to the unknown reference velocity. It is also likely that the geostrophic computations more severely underestimate the transports in the West Spitsbergen Current than in the more baroclinic East Greenland Current, resulting in a too large net outflow.

Rudels et al. (2000b) compared the water mass distributions on hydrographic sections taken in 1984 and in 1997 and found that the area occupied by recirculating

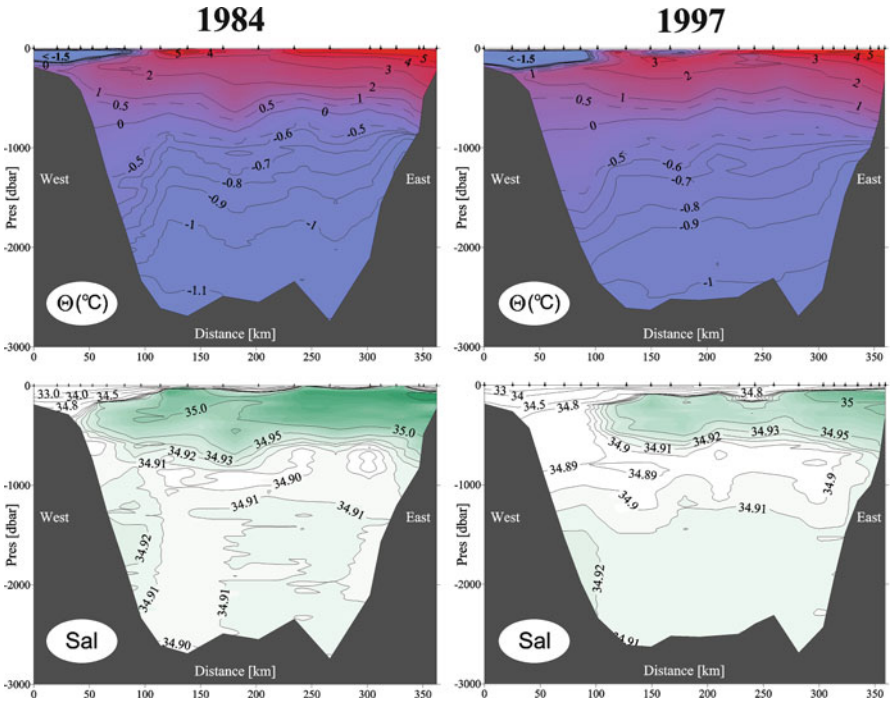

Fig. 4.13 Potential temperature and salinity sections at the sill in Fram Strait taken in 1984 and 1997. The recirculation, indicated by the lateral extent of the high salinity Atlantic water, was more confined to the central part of the strait in 1997 than in 1984, allowing a broader passage for the Arctic Ocean water masses to exit the Arctic Ocean and suggesting a closer coupling between the Arctic Ocean and the Nordic Sea in the 1990s. The outflow of Arctic Ocean intermediate and deep waters are seen by the larger separation of the +0.5°C and −0.5°C isotherms and the higher salinity at the Greenland slope. Recent years have shown a return to the 1980s situation with larger recirculation in the strait and the saline Atlantic water reaching to the Greenland slope (Adapted from Rudels 2001)

Atlantic water in 1984 extended up to the Greenland continental slope, while in 1997, it was more confined to the central part of the strait, opening a free passage for the Atlantic, intermediate and deep water of the Arctic Ocean (Fig. 4.13). This was interpreted as a change from a state with strong recirculation in the strait to one where more Atlantic water enters the Arctic Ocean and takes part in the circulation of the boundary current around the Arctic Ocean basins. A similar interpretation was made by Blindheim et al. (2000) in a discussion of the recent freshening trend occurring in the Nordic Seas, which could partly result from a larger presence of Arctic Ocean waters at the expense of the Recirculating Atlantic Water (RAW) in the Nordic Seas.

The ice export, although temporally varying, appears to have a fairly steady mean transport around 0.09 Sv (e.g. Dickson et al. 2008a). The estimates of the Fram Strait export of liquid freshwater, by contrast, seems to vary between less than half of the ice export (Aagaard and Carmack 1989) and as large, and perhaps larger, than the ice

export (Meredith et al. 2001). The presence in the East Greenland Current and the export of Pacific water through Fram Strait are also changing with time. After being present in the 1980s and 1990s up to the early 2000 (Anderson and Dyrssen 1981; Jones et al. 2003), Pacific water was not observed in 2004 (Falck et al. 2005). Falck et al. (2005) suggest that this change could be caused by changes in the state of the Arctic Oscillation, a more negative AO index would indicate a larger Beaufort Gyre and a westward shift of the Transpolar Drift, confining the Pacific water to north of the Canadian Arctic Archipelago (Steele et al. 2004, see also Fig. 4.12).

4.3.3.2 The Barents Sea

The widest entrance to the Arctic Ocean is over the Barents Sea. It is one of the Arctic shelf seas and thus considered a part of the Arctic Ocean. Its southern and western half is ice free and dominated by inflowing Atlantic water from the Norwegian Sea, while the northern and eastern half is more polar, and ice covered a large part of the year. In the early Russian literature, this difference was taken into account in the definition of the Polar Ocean, which included the deep Arctic Ocean and the Kara, Laptev, East Siberian and Chukchi Seas but only the part of the Barents Sea lying north of a line connecting the north-eastern part of Svalbard with the northern cape of Novaya Zemlya, excluding the mainly ice-free southern part of the Barents Sea.

The Norwegian Atlantic Current bifurcates when it reaches the latitudes of northern Norway, and the eastern stream enters the Barents Sea in the Bear Island Trough together with the Norwegian Coastal Current. The low-salinity ($S \approx 34.4$) coastal current flows eastward close to the coast, while the Atlantic water again splits with one branch continuing eastward south of the Central Bank in the middle of the Barents Sea and the second moving north into the Hopen Deep west of the bank. As it encounters the sill between Edgeøya and the Great Bank, the stream separates into 3 parts, one part turns eastward north of the Central Bank, a smaller part crosses the sill into the northern Barents Sea and the third part recirculates in the Hopen Deep towards the Norwegian Sea (Loeng 1991; Pfirman et al. 1994).

The Atlantic water is cooled and freshened by net precipitation and by ice melt. Few rivers enter the Barents Sea, and the main freshwater source is the Norwegian Coastal Current, carrying low-salinity water from the Baltic Sea augmented by runoff from the Norwegian coast. The cooling increases the density of the Atlantic water, and it occupies the main part of the water column above the deeper depressions. However, the densest water is formed over the shallow shelf areas in Storfjorden (see Sects. 4.2 and 4.3.1.5 above), close to Novaya Zemlya, and over the Central Bank. Here, less-saline surface water deriving, west of Novaya Zemlya from the Norwegian Coastal Current and from ice melt over the Central Bank, is cooled to freezing temperature. Ice is formed and the released brine convects into the water column. The convection eventually reaches the bottom and creates an almost homogenous water column at freezing temperature. Over the Central Bank, the water becomes less saline, but denser, than the Atlantic water in the Hopen Deep (Quadfasel et al. 1992), but on the shallow area west of Novaya Zemlya, the water

may occasionally become more saline than the Atlantic water in the eastern depression. This higher salinity is mainly due to the presence of a lee polynya close to Novaya Zemlya, while the ice remains above the Central Bank and the convection just homogenises the underlying water column and creates a dense anti-cyclonic vortex above the bank, trapping the ice. The water eventually drains from the shallow areas into the deeper depressions, entraining some Atlantic water forming a cold, dense bottom layer (Quadfasel et al. 1992).

Sea ice is advected with the wind and the surface currents and will ultimately melt, often at a position different from its formation. In the northern Barents Sea, this creates a less-saline upper layer on top of the Atlantic water. The stratification due to the separator effect caused by freezing and melting sea ice is augmented by the advection of sea ice and low-salinity surface water from the Arctic Ocean and from the Kara Sea into the northern Barents Sea. Aagaard and Woodgate (2001) proposed that ice melt was fundamental in lowering the salinity of the Atlantic water creating the less-saline deep-water masses of the Arctic Ocean that eventually also supply water to the Greenland–Scotland overflow. However, extremely strong wind mixing and/or a partial refreezing and convection are needed to mix the melt water against the stratification into the underlying Atlantic water.

The Atlantic water entering the Barents Sea from the west thus becomes transformed into three different waters: (1) less-saline and less-dense upper layer, (2) cooled and denser Atlantic water and (3) cold, dense and brine-enriched bottom water. The main outflow from the Barents Sea occurs between Franz Josef Land and Novaya Zemlya and then continues into the Arctic Ocean via the St. Anna Trough. A considerable mixing takes place between the denser water of the two inflow branches, but the less-dense upper layer of the Barents Sea branch remains distinct and eventually evolves into Barents Sea branch lower halocline water (Rudels et al. 2001, 2004a). Some less-saline water, mainly Norwegian Coastal Current water, enters the Kara Sea south of Novaya Zemlya, and a weaker outflow of dense water to the Arctic Ocean takes place in the Victoria Channel to the west of Franz Josef Land (Rudels 1986a; Schauer et al. 1997). The water that recirculates in the Hopen Deep returns as denser and colder water to the Norwegian Sea via the northern part of the Bear Island Trough (Blindheim 1989; Quadfasel et al. 1992). Here, an outflow of cold, less-saline and less-dense Arctic water is also present along the Svalbard Bank (Loeng 1991). This is partly a continuation of the Persey Current to the south of Franz Josef Land, which flows from the Kara Sea westward along the polar front and partly a southward transport of polar surface water from the Arctic Ocean. The waters entering the Norwegian Sea from the Barents Sea are carried northward into the Arctic Ocean by the West Spitsbergen Current.

In the early 1900s it was assumed that the main inflow to the Arctic Ocean occurred through the Barents Sea (Nansen 1906), and in Russian literature an inflow of 1.5 Sv was estimated (Nikiforov and Shpaiker 1980). Later, the strength of the Barents Sea inflow was assumed to be less, and Aagaard and Greisman (1975) gave a total flow of 0.7 Sv into the Kara Sea between Franz Josef Land and the Eurasian continent, only 10% of their estimated inflow through Fram Strait. In the 1980s, the transport estimates for the Barents Sea again began to increase.

Rudels (1987) derived 1.2 Sv from heat budget considerations, about the same as his estimate of the inflow of Atlantic water through Fram Strait, and Blindheim (1989) obtained a net transport of 1.9 Sv into the Barents Sea from a 3-week record from a current metre array deployed in the Bear Island Channel.

Loeng et al. (1993, 1997) and Schauer et al. (2002b) analysed the measurements from a yearlong deployment of a mooring array between Franz Josef Land and Novaya Zemlya in 1991. They found a net inflow to the Kara Sea of about 2 Sv. The largest transport occurred in the deeper southern part of the passage, and to the north, a weak westward flow of Atlantic water deriving from the Fram Strait inflow branch was observed, suggesting an anti-cyclonic circulation around Franz Josef Land. Schauer et al. (2002a, 2002b) also examined the hydrography in the St. Anna Trough and in the passage between Franz Josef Land and Novaya Zemlya and concluded that the high-density cold water present in the deepest part and at the eastern flank of the St. Anna Trough was a continuation of the flow passing eastward between Franz Josef Land and Novaya Zemlya.

The direct current measurements between Franz Josef Land and Novaya Zemlya have not been repeated yet, but since 1997, a current metre array has been deployed within the VEINS and ASOF programme in the western Barents Sea opening, being replaced every year. It has revealed a strong barotropic component and large short-time variability in the transport of Atlantic water. The flow is mainly eastward with a net transport around 1.5 Sv. However, not only days but also periods extended over almost a month (mostly April) with westward net transport through the Barents Sea opening have been recorded (Ingvaldsen et al. 2004a; Ingvaldsen et al. 2004b).

To get the total inflow over the Barents Sea, the transport of 0.7 Sv of the Norwegian Coastal Current has to be added (Blindheim 1989). A total transport of 2.2 Sv is in agreement with Blindheim (1989) and Loeng et al. (1993) and Schauer et al. (2002b). The Norwegian Coastal Current, as it enters the Barents Sea, still carries about half of the freshwater exported from the Baltic Sea and a large fraction of the runoff from the Norwegian coast. Its low salinity (34.4) and comparably large transport make it the largest freshwater source in the Barents Sea, and it contributes significantly to the freshwater balance of the other Siberian shelf seas and of the Arctic Ocean.

4.3.3.3 Bering Strait

Bering Strait connects the two opposite poles of the world ocean, the deeply ventilated North Atlantic and the almost stagnant North Pacific, and allows for a direct communication of surface waters between the two oceans. The flow is northward, into the Arctic Ocean, although southward flow may take place in the presence of strong northerly winds. In ‘The Oceans’, Sverdrup estimated the transport to be 0.3 Sv (Sverdrup et al. 1942). Russian work during the mid century indicated a larger transport and a significant seasonal variability, 1.2 Sv in summer and 0.4 Sv in winter (Maksimov 1945; Fedorova and Yankina 1964). The early direct measurements of the currents in and north of the strait suggested a somewhat larger flow 1.0–1.5 Sv, and no seasonal variation was reported (see e.g. Coachman et al. 1975).

The driving force for the flow was early realised to be the higher sea level in the North Pacific as compared to the Arctic Ocean, giving a pressure head that forces an essentially barotropic flow through the strait. The force balance becomes one-dimensional between the downstream pressure gradient, the field acceleration and the retarding friction (Coachman and Aagaard 1966). Coachman and Aagaard (1966) related the sea level slope to the local wind field and found a relation between the wind measured in Nome, Alaska and the sea level slope and thus the transport.

Stigebrandt (1984) took a more global view and showed that the cause for the higher sea level in the Pacific was the less-saline and less-dense water column in the North Pacific as compared to the water column in the North Atlantic. Assuming a level of compensating pressure at 1,600 m, the upper boundary of the North Atlantic Deep Water, which moves from the North Atlantic towards the Pacific, he obtained a value of the sea level slope and estimated the transport through Bering Strait to be 1.5 Sv, consistent with the current measurements. The higher sea level in the Pacific has partly been explained by the westward atmospheric transport of water vapour from the North Atlantic across the Isthmus of Panama to the North Pacific, making the Pacific water column less and the Atlantic water column more saline (Weyl 1968). The transport of low-salinity Pacific water through Bering Strait is thus a shortcut to correct this freshwater imbalance.

The observational work in the Bering Strait area has continued and has been especially intense in the last years. The more recent transport estimates vindicate the early Russian results (Coachman and Aagaard 1981; Coachman and Aagaard 1988; Roach et al. 1995). The transport varies seasonally with the strongest flow in summer. The yearly mean transport through the strait is about 0.8 Sv, less than what was believed in the 1970s and 1980s. The annual variability of the transport appears to be small, but the salinity as well as the temperature of the inflow varies both seasonally and annually (Roach et al. 1995). Woodgate et al. (2005) deduced from yearlong current measurements in 1991–1992 that the Pacific water leaves the Chukchi Sea at four main locations: (1) through De Long Strait into the East Siberian Sea, (2) along Herald Canyon, (3) through the Central Channel and (4) along the Barrow Canyon. These flows appeared to be equal in strength but with different properties. The outflow to the East Siberian Sea is likely compensated, in volume if not in salt, by an inflow of the Siberian Coastal Current. From current observations between 1990 and 2004 Woodgate and Aagaard (2005) also reported on the transport of the Alaskan Coastal Current, a strong, maximum velocity 1.7 m/s, and narrow low-salinity surface current present along the Alaskan coast from early summer to late fall. Woodgate and Aagaard (2005) estimated that this current, previously ignored, could add about 0.01–0.02 Sv or 20% to the freshwater transport through Bering Strait.

4.3.3.4 The Canadian Arctic Archipelago

The narrow channels of the Canadian Arctic Archipelago connect the Arctic Ocean with the Baffin Bay and the Labrador Sea and provide a second outlet for the less-dense Arctic Ocean waters to the North Atlantic, which does not pass through the

Nordic Seas. In the first half of the 1900s, it was assumed that the outflow through the archipelago was small, and in his mass balance for the Arctic Mediterranean, Sverdrup ignored the flow through the Canadian Arctic Archipelago and assumed that the water masses in Baffin Bay derived from the Labrador Sea with a deep water renewal by local convection (Sverdrup et al. 1942).

Baffin Bay is a deep (>2,300 m) narrow bay connected to the Labrador Sea and the North Atlantic by the 600 m deep Davis Strait. Baffin Bay is ice covered most of the year, and its upper layer has a temperature minimum close to freezing around 100 m with a salinity of ~33.6, indicating the depth of local winter convection. Below this low-salinity layer, a temperature maximum with temperatures of 2–3°C and a salinity of 34.5 is encountered, showing Atlantic water entering Baffin Bay from the south in the West Greenland Current. Below sill depth, the temperature decreases to −0.45°C at the bottom with a salinity of 34.45 (Riis-Carstensen 1936; Kiilerich 1939).

The channels in the Canadian Arctic Archipelago are shallow, 100 m to 230 m, and covered by land-fast ice most of the year, but the low-salinity surface water present in Baffin Bay suggests an inflow from the Arctic Ocean, and Sverdrup's view was later challenged. Several estimates, from geostrophic computations and occasionally from current observations (Day 1968; Sadler 1976), were made during the 1950s and 1960s, either in the individual straits or in Baffin Bay and Davis Strait, and have been summarised by Bailey (1957), Collin (1962), Collin and Dunbar (1963), Muench (1971) and Coachman and Aagaard (1974). A net southward flow of 1–2 Sv was obtained but with large temporal variations and with indications that changes in the transports through the different passages may compensate each other.

Bailey (1956) noticed that the characteristics of the Baffin Bay deep and bottom water were similar to those observed at 250 m in the Beaufort Sea and suggested that the deeper layers were supplied from the Arctic Ocean. This view has been contested by Bourke et al. (1990) and Bourke and Paquette (1991) who, during an expedition in 1986, did not observe any connection between the water found in the northern Nares Strait with the bottom water in Baffin Bay even though the characteristics were similar. They proposed, as did Sverdrup, that the Baffin Bay deep and bottom water is formed by local convection. Since neither an advective renewal of the Baffin Bay bottom water nor local convection has been observed in Baffin Bay, the question is still open. Should the Arctic Ocean supply the deep and bottom water of Baffin Bay, it would primarily be a contribution from the Barents Sea branch halocline water (Rudels et al. 2004a).

Simple model estimates of the outflow through the Archipelago have been provided by Stigebrandt (1981), who considered the entire Arctic Ocean and assumed a two layer geostrophically controlled outflow through Fram Strait and the Canadian Arctic Archipelago. He found the outflow through the archipelago to be larger (2 Sv) than that through Fram Strait (1.5 Sv). Rudels (1986b) assumed geostrophic two-layer flow through the channels in the archipelago as well as through Davis Strait and combined this with a heat, mass and salt balance for Baffin Bay, finding an outflow in the upper layers of 0.7 Sv and postulating an additional deeper outflow of 0.3 Sv. Steele et al. (1996) estimated the freshwater balance in different parts of the Arctic Ocean, assuming geostrophic transports across the boundaries between the different areas. They obtained an outflow of low-salinity water through the archipelago of 0.54 Sv.

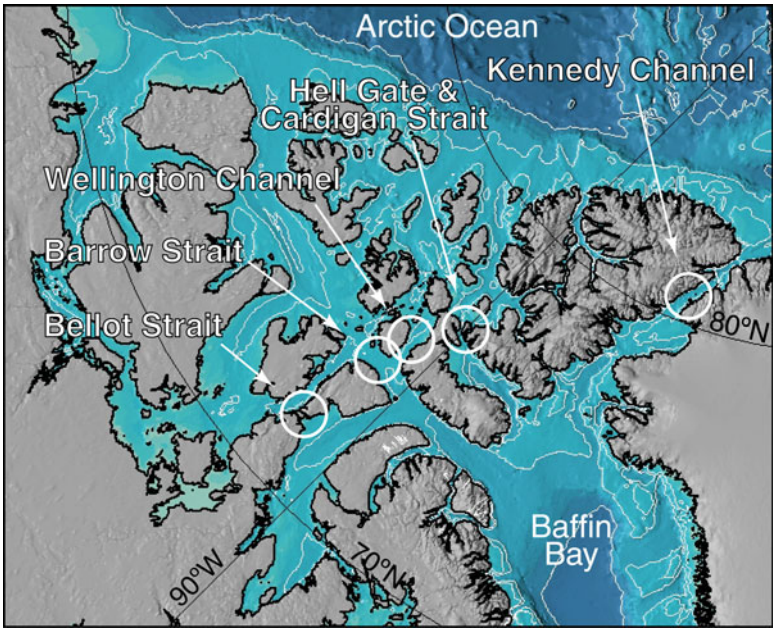

Fig. 4.14 Map showing the Canadian Arctic Archipelago and the main choke points

All transports through the Canadian Arctic Archipelago must cross the sills at one (or two) of six constrictions – Bellot Strait, Barrow Strait (Lancaster Sound), Wellington Channel, Cardigan Strait and Hell Gate (Jones Sound) and Kennedy Channel (Nares Strait). As Bellot Strait cross-section is small compared to the other straits and Wellington Channel enters into eastern Barrow Strait, monitoring surveys of the fluxes through the archipelago have been concentrated on the three main pathways: Kennedy Channel, Hell Gate and Cardigan Strait and eastern Barrow Strait (Fig. 4.14).

In the early 1980s, efforts were made to reference geostrophic calculations to measure currents in a number of channels (Prinsenberg and Bennett 1987; Fissel et al. 1988). Four factors posed significant challenges to the technology available at that time – unsatisfactory direction reference, small (less than 5 km) coherence scales for the flows, large seasonal variability and the logistics. However, a general pattern emerged from this study; currents near the surface flow towards Baffin Bay on the right-hand side of channels (looking south-east), and counter flow on the left-hand side creates a generally cyclonic circulation within the channels of the archipelago. In the late 1980s and early 1990s, the Bedford Institute of Oceanography ran a large hydrographic and mooring programme in Baffin Bay. The current metre moorings were mostly concentrated to Davis Strait, but deployments were also made in the central and northern Baffin Bay. The net volume transport through Davis Strait, based upon these current measurements, was 2.4 Sv (Tang et al. 2004).

Successful year-round use of acoustic Doppler profiling sonar in the Arctic (Melling et al. 1995) has stimulated new initiatives in measuring flow within the Archipelago. An RDI Work Horse ADCP was deployed on one of two moorings in

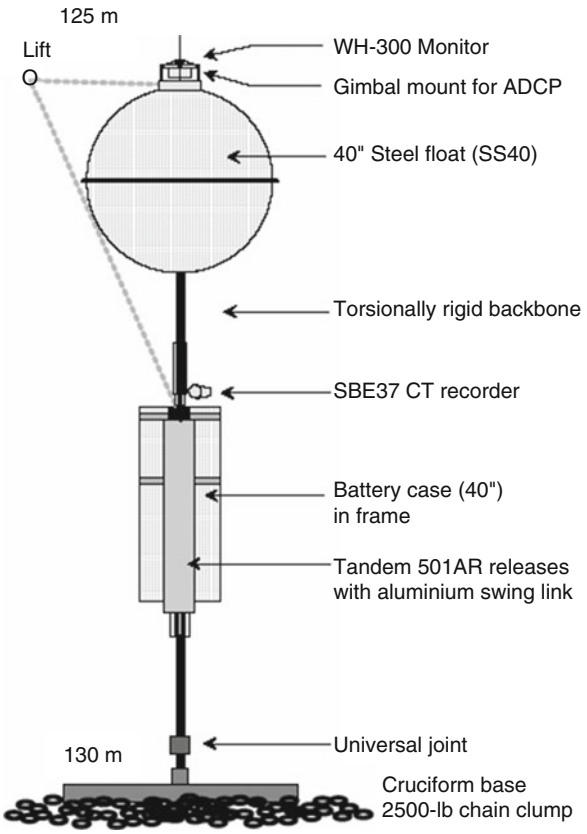

Fig. 4.15 Sketch of torsionally rigid mooring (Adapted from Melling 2004)

Smith Sound during the North Water Project, and in 1998, Fisheries and Oceans, Canada began a mooring study in Cardigan Strait and in eastern Barrow Strait. Along with the re-deployments in Cardigan Strait, the combined work established for the first time simultaneous observations in two of the three pathways through the archipelago with two goals: (1) to develop a reliable and cost-effective method of measuring current direction near the geomagnetic pole and (2) to acquire a better knowledge of the structure of Arctic channel flows.

For shallow straits, torsionally rigid moorings for ADCPs, holding the instrument at a fixed geographic heading so that a geomagnetic direction reference is not needed, have been successfully used. The unique mooring was designed to meet the special challenges of the environment. It is compact, rising less than 4 m from the seafloor to minimise vulnerability to icebergs and to reduce sensitivity to the strong, 2–3 ms^{-1}, currents. The Work Horse Monitor and in later years a 75-kHz Work Horse Long Ranger both of RD Instruments are mounted in gimbals to remain zenith-pointing despite lay-down of the mooring in strong current. A universal joint in the backbone permits the mooring to stand upright regardless of seabed roughness and slope (Melling 2004) (Fig. 4.15).

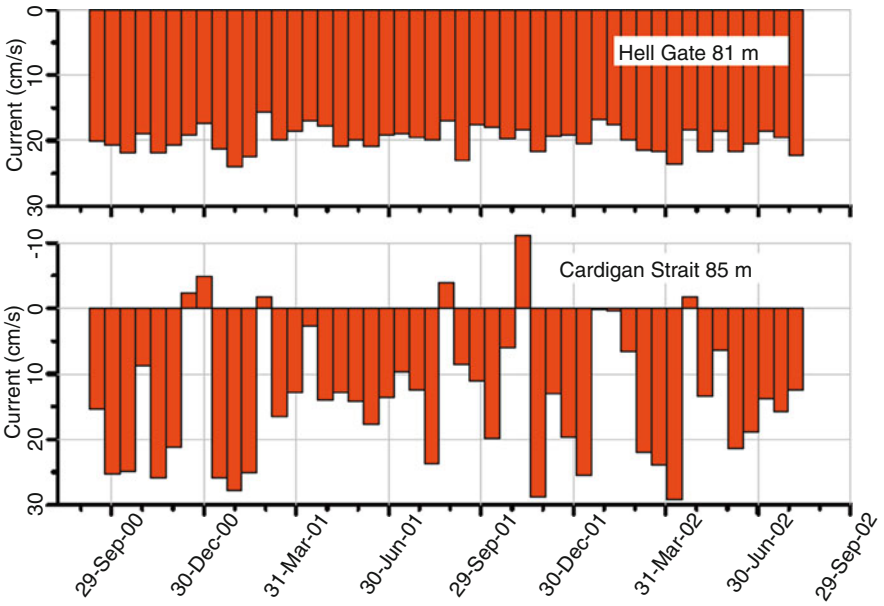

Fig. 4.16 15-day average of the current at 85 m depth in the Cardigan Strait and in the Hell Gate (Adapted from Melling 2004)

A second method to measure current direction near the magnetic pole especially for mid-water flow has been developed for the eastern Barrow Strait moorings (Hamilton 2001). The system uses precision heading reference systems to measure the orientation of ADCPs mounted in streamlined buoyancy packages. The measured magnetic heading is then adjusted for the varying declination with measurements from the Natural Resources Canada (NRCAN) geomagnetic observatory in Resolute to obtain direction relative to true north which, at the mooring site, varies by as much as ±30° over the course of a day. Thus, three commercially available products have been combined into a single package to provide reliable current direction and speeds in areas with any depths where the horizontal component of the earth's magnetic field is too low for conventional instrumentation to be useful.

Yearly mean flows through Cardigan Strait and Hell Gate during 1998–2002 show little year-to-year variations (Melling 2004). Shear is concentrated near the seabed and surface and suggested to be generated near the bottom by the benthic drag and by hydraulics at the sill. The surface shear is in part a consequence of wind, which accelerates between the high lands bordering the straits. The surface velocity is derived from tracking ice, which is sometimes land-fast, and the effect of annual averaging is not the same as for the current. Figure 4.16 displays the variation of a 15-day average current at 85 m depth for Hell Gate and Cardigan Strait. This measure of flow is clearly covariant in Cardigan Strait and Hell Gate, but the amplitude of the variation in Hell Gate is less than one seventh of that in Cardigan Strait, only 17 km away.

With support from the US National Science Foundation and from Fisheries and Oceans Canada, insights and technology from the study in Cardigan Strait and Hell Gate are being applied to the measurement of the fluxes of volume, freshwater and heat through Nares Strait, the third major pathway through the archipelago (Melling 2004). Twenty-three moorings were deployed during a 4-week expedition using the USCGC *Healy* in the summer of 2003. Eight torsionally rigid moorings carrying 75 kHz Long Ranger ADCPs were positioned at 5 km spacing across southern Kennedy Channel. These moorings were interleaved with eight taut-line moorings rising to 30 m depth and carrying SBE37 temperature-salinity-pressure recorders. In addition, two moorings carried ice-profiling sonar to measure the flux of freshwater by ice (Melling and Riedel 1996). Nestled into sheltered coastal locations were 5 very stable moorings carrying instruments to measure the total hydrostatic pressure (plus temperature and salinity). The deployment of the mooring array went according to plan, but the intended recovery from the ice in spring had to be cancelled, and the camp abandoned due to high-speed winds. This postponed the recovery by more than a year. However, the instruments were eventually recovered, and the measurements are being analysed (Müchow et al. 2006; Müchow et al. 2007; Müchow and Melling 2008; Melling et al. 2008).

At the mooring array in eastern Barrow Strait, the channel is 65 km wide and reaches a maximum depth of 285 m. Mobile and land-fast pack ice conditions are normally found for 10 months of the year. Salinity and temperature profiles collected during the August surveys showed that the coldest water (−1.7°C) was located at mid-depth, had a salinity of 32.8–33.0 and represented remnants of the winter-surface-mixed layer. Above this water mass, a very stable surface layer, diluted by ice melt and local runoff and warmed by summer heating, was found. The warmest and least saline water was observed at the surface along the two coasts, indicating the existence of coastal currents along both shores. Below the cold mid-depth water mass, the water became warmer and saltier with depth. This warmer deep water had entered the area from northern Baffin Bay. Geostrophic current field derived from the August 1998 density distribution shows an eastward-flowing current decreasing with depth that extends from the southern shore of Lancaster Sound to two-thirds of the way across the sound. A depth-varying current along the northern shore appears to be restricted to one-third of the northern part of the sound (Prinsenberg and Hamilton 2004).

Seasonal mean velocity profiles, derived from the daily mean along-strait data, show that different flow regimes exist at the two sides of the sound and that the currents exhibit seasonal and inter-annual variability. Along the southern shore, the yearly mean and seasonal flows are eastward, very homogeneous and mainly barotropic. Along the northern shore, the seasonal mean flow is weak, variable and baroclinic and generally westward in the surface and bottom layers. As was seen earlier in the geostrophic flow field, the strongest eastward flow along the southern shore occurs during the late summer, while along the northern shore, a definite three-layer flow regime exists.

To estimate fluxes from site-specific time series, it is assumed that the site-specific mooring data can represent, through weighting, the cross-sectional fluxes. Preliminary analysis of data from August 2001 to August 2002 of a modified array provided

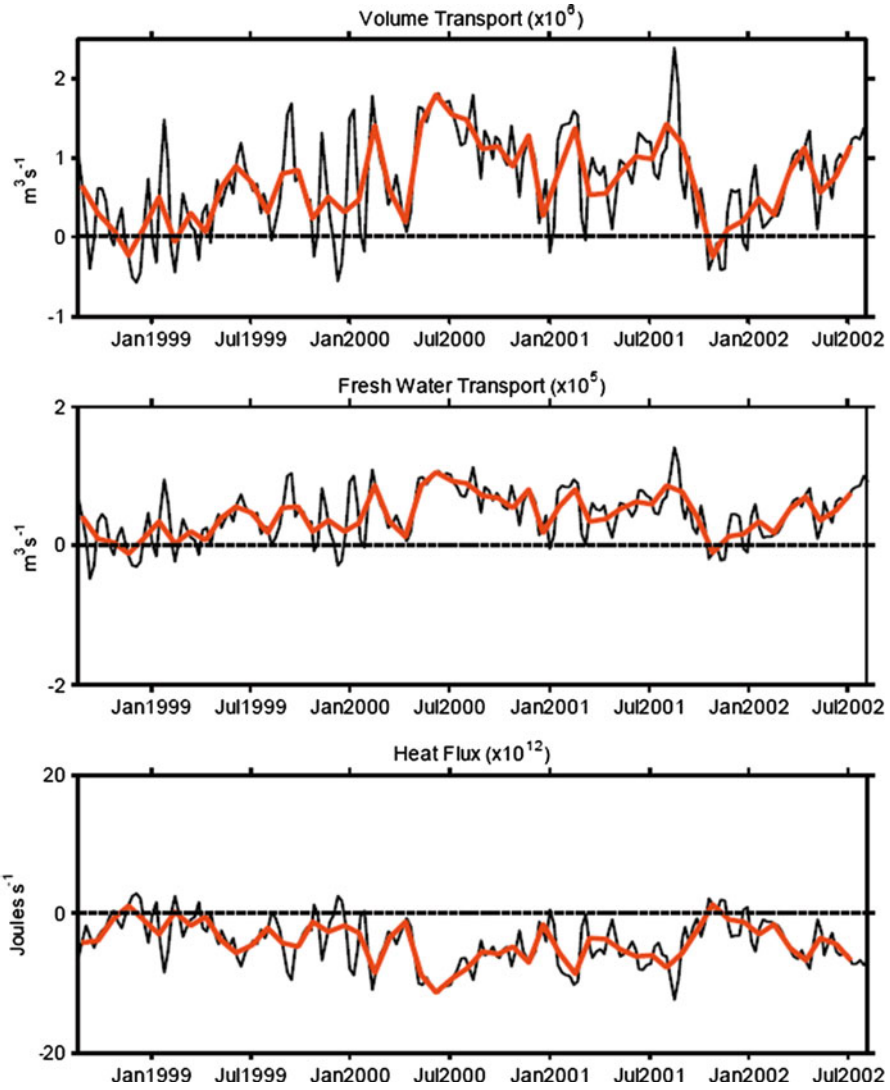

Fig. 4.17 Flux estimate through Barrow Strait over a 4-year period, August 1998 to August 2002 (Adapted from Prinsenberg and Hamilton 2004)

surface layer (0–60 m) current measurements from ¼ to ½ way across the strait as well as measurements at the southern and northern sites. A preliminary look at this data indicates that in winter and spring the eastward currents are similar across the southern two-thirds of the strait, while in summer and fall, the southern array should be reduced to 55% to represent the mean currents observed over two-thirds of the strait. The estimated transports of volume, heat and freshwater, calculated relative to 34.8 and −0.1°C, through Lancaster Sound during 3 years, are shown in Fig. 4.17.

A regional numerical model was developed for the Canadian Arctic Archipelago to provide a basis for evaluating the mooring programmes and to extrapolate oceanographic properties through the entire domain, as not all areas can be instrumented. The intent is to calibrate the model with the mooring observations to present day conditions and then to simulate changes in sea-ice regime and oceanography within the archipelago due to global climate change. The modelling work has successfully simulated the barotropic tidal heights and currents as well as the mean circulation (and fluxes) in response to sea level difference between the Arctic Ocean and Baffin Bay (Kliem and Greenberg 2003). The model is diagnostic, and the temperature and salinity fields are thus treated as fixed in time and used as forcing for the model. The open boundaries in the Arctic Ocean and Baffin Bay have both inflow and outflow regions. The inflow is given by prescribing the elevation along the boundary as specified for summer conditions by a large-scale ocean model (Holloway and Sou 2002). The simulations highlight the huge impact of the density field on the flow, emphasising the importance of the baroclinic forces. Secondly, the fluxes depend on the Arctic Ocean–Baffin Bay elevation difference, and a 5-cm Baffin Bay set-down can double the fluxes (Kliem and Greenberg 2003). The actual value is unknown but may be accessible once GPS referenced tide gauge data become available.

Fluxes derived from these observations in eastern Barrow Strait, and to a lesser extent in Cardigan Strait and Hell Gate, show large seasonal and inter-annual variability. Model simulations indicate that summer fluxes through the eastern Barrow Strait make up 35% of the flux through the Canadian Arctic Archipelago (Kliem and Greenberg 2003). Other models with different grid sizes and differently simulated physical processes indicate that fluxes through eastern Barrow Strait can be up to 50% of the total fluxes through the archipelago (Maslowski 2003). If these fractions also apply to the yearly mean fluxes (0.7 Sv), this indicates that the yearly mean volume flux through the archipelago would range from 1.4 to 2.0 Sv, similar to present literature values (Melling 2000; Prinsenberg and Bennett 1987). The archipelago model indicates 0.3 Sv through Jones Sound (sum of Hell Gate and Cardigan Strait). A 10-cm set-down is required to match the estimated summer flux of 1.0 Sv through eastern Barrow Strait (Kliem and Greenberg 2003). Both data sets thus indicate a Baffin Bay set-down in sea surface relative to the Arctic Ocean that is not simulated by existing coarse global models.

4.4 The Arctic Ocean as Part of the Arctic Mediterranean Sea

The larger Arctic Mediterranean Sea comprises not only the Arctic Ocean but also the Nordic Seas; the Greenland, Iceland and Norwegian Seas. In the first part of the twentieth century, the part played by the Arctic Mediterranean in the global circulation was assumed small, as was reflected in the mass balance for the Arctic Mediterranean compiled by Sverdrup in ‘The Oceans’ (Sverdrup et al. 1942). He estimated that 3 Sv entered the Arctic Mediterranean from the North Atlantic and 0.3 Sv from the North Pacific through Bering Strait. Net precipitation and runoff

were estimated to be 0.09 Sv and 0.16 Sv, respectively. The outflow, 3.55 Sv, was assumed to occur almost exclusively through Denmark Strait and to consist mainly of less-saline surface water. The amount of dense overflow water from the Arctic Mediterranean to the North Atlantic was considered negligible, and the North Atlantic Deep Water was believed to form in the North Atlantic southeast of Greenland.

This view has been completely revised. The inflow from the North Atlantic is now estimated to be 8 Sv, and most of it, 75%, returns as dense overflow water, 3 Sv between Scotland and Iceland and 3 Sv through Denmark Strait. The rest is transformed into less-dense water masses (Hansen and Østerhus 2000). The Bering Strait inflow is estimated to be 0.8 Sv, implying an outflow of 3 Sv of less-dense polar water, which likely is divided equally between Denmark Strait and the Arctic Archipelago (Hansen and Østerhus 2000). These findings indicate that the Arctic Mediterranean, together with the Southern Ocean, ventilates the deep world ocean. The Southern Ocean supplies the bottom waters and the Antarctic Intermediate Waters (AAIW), while the deep waters between 1,500 and 4,000 m derives from the Arctic Mediterranean, with less-dense additions from the Mediterranean outflow and from the Labrador Sea (Worthington 1976; Talley and McCartney 1982; McCartney and Talley 1984). In recent years, the possibility that the deep convection taking place in the Irminger Sea, in the northern limp of the subpolar gyre, also contributes to the North Atlantic Deep Water has again been revived (Pickart et al. 2003). However, the major contribution to the North Atlantic Deep Water are the overflows crossing the Greenland–Scotland Ridge, mainly in Denmark Strait and through the Faroe–Shetland Channel, and the ambient water entrained into the descending overflow plumes (Dickson and Brown 1994).

In the early 1980s, it was widely assumed that the intermediate convection in the Nordic Seas, especially in the Iceland Sea, supplied the Denmark Strait overflow water (Swift et al. 1980; Swift and Aagaard 1981), while the deep water formed in the Greenland Sea contributed to the deep waters of the Nordic Seas and the Arctic Ocean (Nansen 1906; Wüst 1941; Kiilerich 1945; Mosby 1959). The insights gained in the 1980s have shown that the Arctic Ocean is a source of deep water and that the Arctic Ocean and the Greenland Sea both contribute to the formation of the Norwegian Sea Deep Water (NSDW) (Aagaard et al. 1985; Rudels 1986a; Swift and Koltermann 1988). The deep flow through Fram Strait goes in both directions, exchanging deep waters between the two source regions. Since the depths of the basins are larger than the sill depth in Fram Strait, the bottom waters in the Arctic Ocean basins and in the Greenland Sea are locally produced and very distinct, the Arctic Ocean deep and bottom waters being warmer and more saline than the Greenland Sea bottom water. This deep circulation was, however, thought mainly confined to the Arctic Mediterranean.

During the Greenland Sea project in the late 1980s and the early 1990s, saline deep water from the Arctic Ocean was observed in Denmark Strait (Buch et al. 1996), and the possibility that the Arctic Ocean could contribute directly to the overflow was then considered seriously. This had been suggested earlier by Rudels (1986a) based on continuity arguments, and it had been implicit in all work on the deep circulation in the Arctic Mediterranean from the late 1980s (Aagaard et al.

1985; Smethie et al. 1988; Heinze et al. 1990). It is not possible to continuously produce deep and bottom water without allowing it to exit somewhere.

Mauritzen (1996a, 1996b), using an inverse box model, concluded that the Atlantic layer in the Arctic Ocean and the Atlantic water recirculating in Fram Strait were the main suppliers of the Denmark Strait overflow water. In this model, the contributions from the central gyres in the Greenland and Iceland seas were found almost negligible. Anderson et al. (1999) estimated the Arctic Ocean contribution to the overflow water using a plume entrainment model constraint with CFCs and concluded that the Arctic Ocean likely supplied about 40% of the overflow water.

The question of the importance of the different source areas is, however, far from settled. In addition to the time variability in the source waters, the overflow waters may also be drawn from different sources at different periods. This is especially the case for the Denmark Strait overflow water. Rudels et al. (2002) examined the different waters in the East Greenland Current and found that, in 1998, the Arctic and Recirculating Atlantic waters (AAW & RAW) and the upper Polar Deep Water (uPDW) were light enough to cross the Jan Mayen Fracture Zone and the sill in Denmark Strait. The Canadian Basin Deep Water was mostly too dense to cross the Jan Mayen Fracture Zone and remained in the Greenland Sea, while Arctic Intermediate Water from the Greenland Sea entered the East Greenland Current and crossed the sill into the Iceland Sea. Water masses too dense to cross the sill in Denmark Strait then flow eastward north of Iceland into the Norwegian Sea (Rudels et al. 1999c). The densest water crossing the sill appears to be transported by a narrow barotropic jet formed north of Iceland (Jónsson and Waldimarsson 2004), but whether this means that the jet carries waters formed in the Iceland Sea or the deeper part of the East Greenland Current is shifted towards Iceland north of the strait before it crosses the sill was not clarified by the end of the ACSYS decade.

The intensified observational activity during the decades at the turn of the millennium has revealed changes also in the characteristics of the deep waters in the Arctic Mediterranean, especially in the smaller basins in the Nordic Seas. Rudels et al. (1999c) examined data from the Greenland Sea taken in the late 1980s and concluded that, at least in 1988, a ventilation deeper than 2,000 m had occurred (see Fig. 4.18). The deep salinity maximum, deriving from the Eurasian Basin Deep Water (EBDW), had been reduced, and the Arctic Intermediate Water formed this year was denser than the Canadian Basin Deep Water (CBDW), which did not penetrate into the basin but remained at the slope, staying high enough to partly cross the Jan Mayen Fracture Zone and enter the Iceland Sea and then continue towards Denmark Strait (Rudels et al. 1999c). In 1993, the convection was limited to the upper 1,000 m, and the deep salinity maximum became more saline and shifted downward. Rudels (1995) and Meincke et al. (1997) suggested that the absence of deep convection relaxes the high-density dome in the central Greenland Sea. The isopycnals, and the salinity maximum, then move downward, and the EBDW at the rim can penetrate, isopycnally, into the central gyre without its salinity being reduced by the input of convecting, less-saline and colder water from above. The volume of the Greenland Sea Bottom Water (GSBW) below the salinity maximum has decreased, and its temperature and salinity have increased.

This agrees with the observations made on transient tracers, which suggest a reduction of the Greenland Sea deep water formation (Schlosser et al. 1991; Bönisch and Schlosser 1995; Bönisch et al. 1997). Meincke et al. (1997) used the changes in the salinity maximum to estimate the strength of the mechanically driven diapycnal mixing in the deep Greenland Sea and obtained a surprisingly large vertical diffusion coefficient, $K_v \approx 3.7 \times 10^{-3}$ m^2 s^{-1}. It should be emphasised that the EBDW and CBDW signals encountered in the Greenland Sea are much diluted by mixing in Fram Strait and along the Greenland slope from Fram Strait to the Greenland Sea, and probably less than 10% of the water in the temperature and salinity maxima comes from the Canadian and Eurasian basins.

After 1993, an intermediate temperature maximum started to develop in the Greenland Sea, indicating that Canadian Basin Deep Water (CBDW) was penetrating from the rim into the central gyre and that the convection in the Greenland Sea was producing intermediate water, less dense than the CBDW (Rudels 1995). This was a change from the 1980s, when the Arctic Intermediate Water (AIW) was denser than the CBDW and less CBDW entered the Greenland Sea Gyre, and the part that did enter the central basin was redistributed vertically by the deeper reaching local convection (Rudels et al. 1999c). The temperature and salinity of the CBDW-derived temperature maximum have gradually increased, and the maximum has been shifted towards deeper levels (Budéus et al. 1998). A possible cause for this downward displacement could be that the recent Greenland Sea convection has been confined to levels above the temperature maximum and that it is easier to bring water at the surface into the central Greenland Sea than remove it as AIW at intermediate levels, causing the storage and the thickness of the AIW layer in the Greenland Sea to increase with time (Fig. 4.18).

In 1996, low-salinity surface water was present in the Greenland Sea due to a large ice export through Fram Strait during the winter of 1994/1995, and ice formation occurred in the winter of 1996/1997. This led to a deepening of the convection from 800 to 1,200 m, and a less-saline, thick intermediate layer of Arctic Intermediate water was created. The winter of 1996/1997 was also the first winter after the Tracer Release Experiment in the Greenland Sea, when a cloud of SF_6 was injected at the 28.049 σ_θ surface. In the centre of the Greenland Sea Gyre, the convection reached deeper than this density surface, and the maximum tracer concentration was shifted to deeper (denser) levels, while outside of the gyre the SF_6, except for turbulent diffusion, remained on the initial density surface (Watson et al. 1999). This suggests that the convection in 1996/1997 was mainly haline, penetrating through the SF_6 cloud, entraining intermediate, SF_6 rich, water and bringing it to denser levels. The convection in the following years has been thermal and reached 1,600 m to 1,800 m, except locally within deeper vortices to be discussed below. The convecting water, the AIW, has been less dense than the CBDW, and the ventilated layer has remained above the temperature maximum.

A question, which has been ignored lately because of the presently almost ice-free conditions in the Greenland Sea, is the importance of ice formation for deep convection in the Greenland Sea. Most of the deep waters in the world ocean derive from high latitudes, where the stratification in the upper layers is in salinity, not in temperature, and ice formation is necessary to attain sufficiently high surface densities to induce convection, on the shelves and slopes as well as in the deep basins

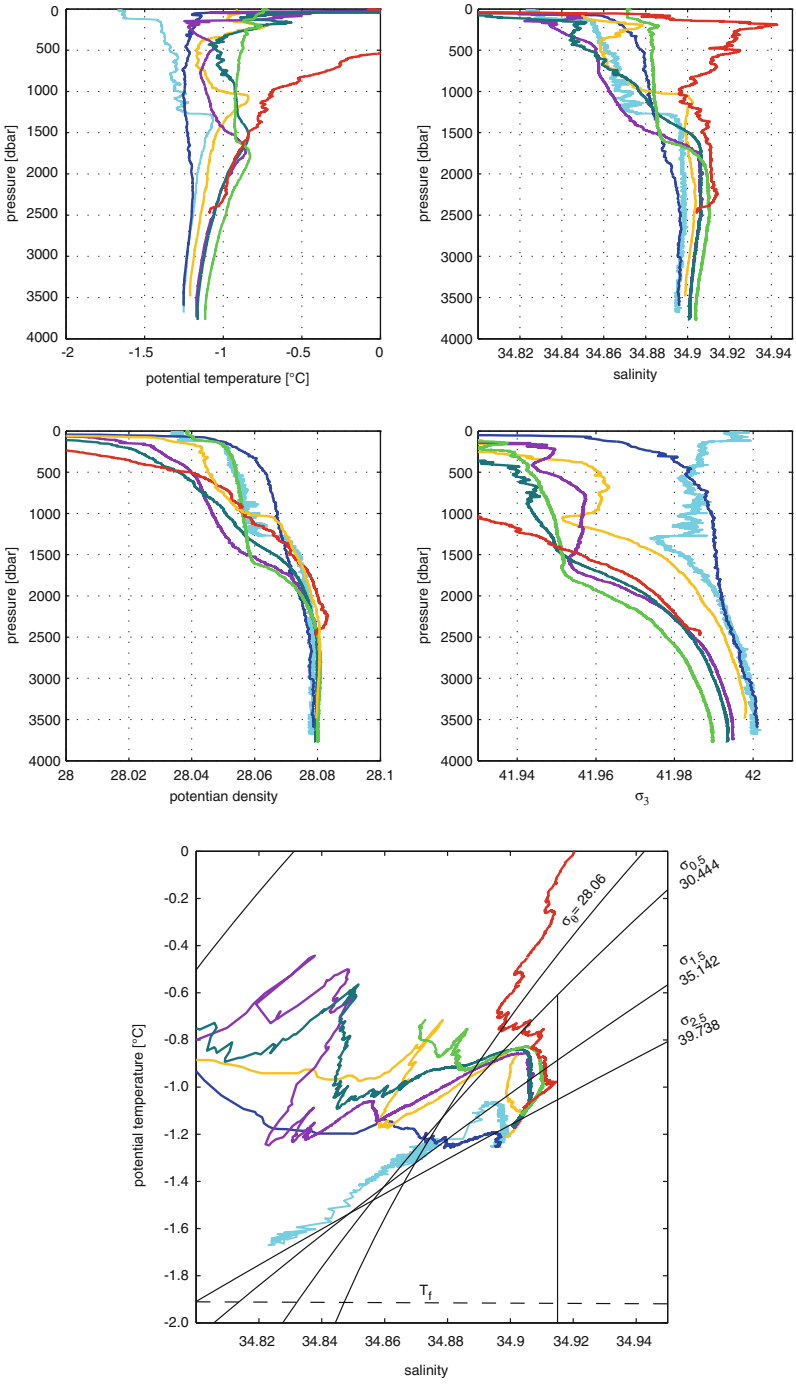
pressure [dbar]
potential temperature [°C]
salinity
potentian density
σ3
potential temperature [°C]
salinity
σ0= 28.06
σ0.5 30.444
σ1.5 35.142
σ2.5 39.738
Tf

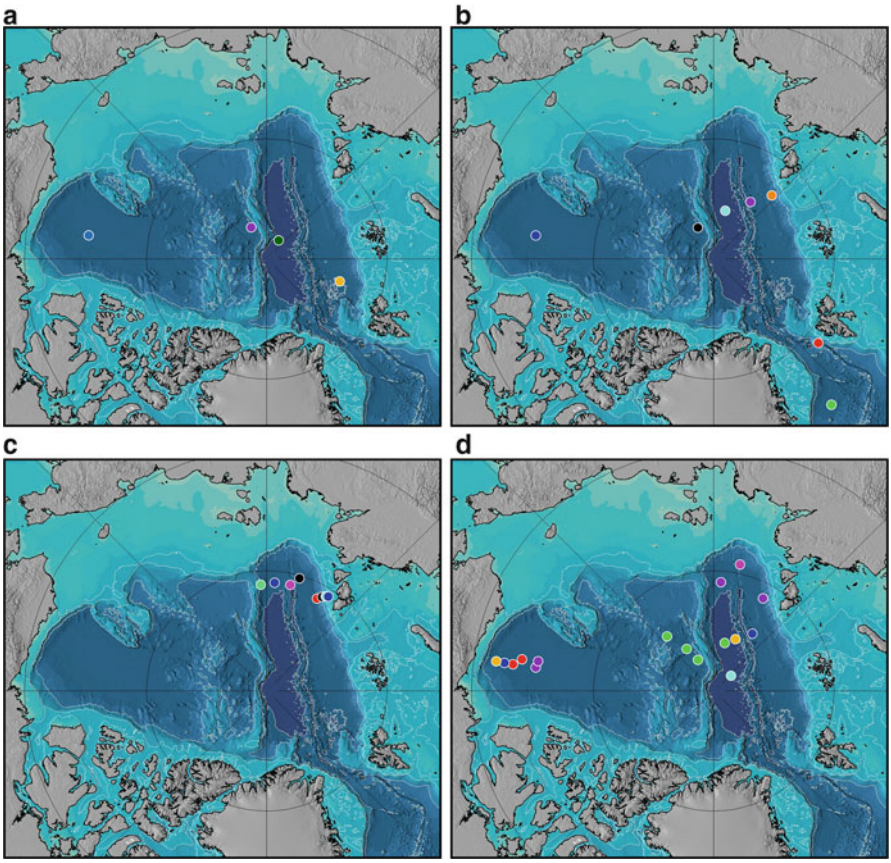

Fig. 4.19 (**a**) Positions of stations shown in Fig. 4.2. (**b**) Positions of stations shown in Fig. 4.4. (**c**) Positions of stations shown in Fig. 4.7. (**d**) Positions of stations shown in Fig. 4.9

Fig. 4.18 Changes in the ΘS properties in the water column in the central Greenland Sea between 1988 and 2002. (*upper left*) potential temperature profiles, (*upper right*) salinity profiles, (*centre left*) potential density profiles referenced to the sea surface, (*centre right*) potential density profiles referenced to 3,000db (*lower panel*) ΘS curves. The cyan station is from a winter station in 1988 with active convection down to 1,250 m (see also Rudels et al. 1989), while the *blue station* is from June the same year, indicating that the convection eventually reached deeper than 2,000 m. The *green station* is from 1993, the *violet* from 1997, the *grey-blue* from 1998 and the *yellow* from 2002, showing the advent and the deepening of the mid-depth temperature maximum derived from the Canadian Basin Deep Water, as well as the increase in temperature and salinity of the deeper layers due to inflow of EBDW. The red station is from the continental slope in 2002 showing the CBDW characteristics as it enters the Greenland Sea Gyre. The colder, less-saline layer found close to the bottom at the slope has the same characteristics as water at 3,300 m in the central Greenland Sea Gyre. This indicates that the previous doming of the isopycnals towards the surface in the central Greenland Sea, prominent in previous years, has now in the deeper layers been replaced by a depression of the isopycnals as a response to the inflow of Arctic Ocean deep waters and the accumulation of AIW in the upper part of the water column. The salinity and the temperature of the Arctic Intermediate Water have increased after the haline convection event in 1997. The upper, convectively ventilated part of the water column has become more homogenous and less stable during the thermal convection operating in recent years compared to the haline convection that occurred e.g. in 1988 (Adapted from Rudels 2010)

(Rudels 1993). Carmack (2000) separated the world ocean in a mid-latitude α-ocean and a high-latitude β-ocean, α and β being the coefficients of heat expansion and salt contraction, respectively, where the stability was determined by either heat or salt, and pointed out that the open ocean deep convection sites were mostly located at the boundary between these two oceans. Is the deepest convection expected to occur on the α-side or on the β-side of the boundary?

In the Greenland Sea, the common assumption has been that ice-free conditions lead to larger heat loss and to deep thermal convection into a weakly stratified water column, where the density surfaces dome upwards, preconditioned by the wind (Nansen 1906; Helland-Hansen and Nansen 1909; Mosby 1959; Killworth 1979). Rudels (1986a) and Aagaard and Carmack (1989) pointed out that for the same heat loss, the density increase of a water parcel due to ice formation and brine release is substantially larger than that due to cooling. If the ice cover never grows thick enough to significantly lower the heat flux to the atmosphere, ice formation would be more efficient in creating dense water.

Rudels (1986a) noted the deep salinity maximum always present in the Greenland Sea water column and suggested that the density anomalies created by brine rejection lead to a large-enough density increase in the upper layer that it could convect through and bypass the intermediate layers below, in the case of bottom water formation also through the salinity maximum, instead of gradually deepening into the underlying water. As the upper layer is emptied into the deep, warmer intermediate water is brought to the surface and starts to melt ice, re-forming the less-saline surface layer that again becomes cooled to freezing temperature. Ice formation recommences and a new deep convection event occurs. This would continue until so much freshwater is convected into the deeper parts of the water column that the surface layer does not reach the freezing point before the water column becomes unstable and convects (Rudels et al. 1999b). A stage of thermal convection with a slow deepening of the mixed layer then begins, which does not allow for any further deep convection events and for renewal of the deep and bottom waters, unless the thermal convection manages to homogenise the entire water column before the end of winter. The mainly ice-free conditions during the last 10 years have prevented any rigorous test of these ideas and they remain speculations.

There could be several causes behind the recent reduced convective deep and bottom water renewal in the Greenland Sea. The most obvious cause would be that the climate has become warmer, leading to less cooling and less dense water formation. The high NAO + state during the 1990s with warmer, windier winters and more precipitation could also reduce the salinity, and density, of the surface water in the Greenland Sea. Disregarding variability and changes in the atmospheric forcing, the largest difference between the 1980s and the present is the thick >1,000 m upper layer with higher temperature and initially a fairly low salinity, which likely was established after the large freshwater import from the Arctic Ocean in 1994/1995. The density difference between this layer and the temperature maximum below is so great that cooling of the entire layer to freezing temperature is required to reach the

density of the temperature maximum. The heat content in the upper layer is too large for this to occur during one winter, and in the last years the convection in the Greenland Sea has been thermal and confined to above the intermediate temperature maximum.

During the last few years, several, deep homogenous vortices have been observed in the Greenland Sea. These vortices are 10–20 km in diameter, and some have penetrated down to 2,400 m. They are denser than their surroundings in their upper part and less dense in their lower part, and the isopycnals below the vortices are depressed (Gascard et al. 2002; Wadhams et al. 2002; Budéus et al. 2004). Apart from a much larger vertical extent, they are similar to the mesoscale eddies observed in the Arctic Ocean (see above, Sect. 4.2). The water mass characteristics of the eddies can be reproduced by a mixing of about 1/3 surface water with 2/3 intermediate water (Gascard et al. 2002). This suggests a homogenisation of the water column by convection. However, the scales of the meteorological forcing are larger than 20 km, and to create such a localised convection, the water column must be preconditioned on that scale. Wadhams et al. (2002) proposed that the passage of intermediate water between the Boreas Basin and the Greenland Basin through a narrow gap in the Greenland Fracture Zone might spin up the intermediate water and bring it closer to the surface. This is somewhat similar to the suggestion by D'Asaro (1988) for formation of the Arctic eddies by a frictional spin-up of dense Bering Strait inflow water in the Barrow Canyon. The possibility for the convection to locally break through the surface layer and homogenise a narrow water column thus increases. Once the convection has commenced, the surface water from a larger area may convect down the funnel, increase the depth of the convection and depress the isopycnals below the maximum convection depth. In summer, the eddy will be covered by a less-dense surface layer, which will be rapidly removed the next fall, and the eddy will be further cooled and 'recharged' thus being able to survive several seasons. Because their density is lower than that of the mid-depth temperature maximum, these vortices do not appear to be the mode by which the deep and bottom waters of the Greenland Sea might locally be renewed. It is also not known how much they contribute to the formation of Arctic Intermediate Water that presently takes place in the Greenland Sea. The nature of these eddies and of the convection is presently subject to intense research.

Contrary to the earlier situation, when the isopycnals domed upwards toward the sea surface, the density surfaces in the Greenland Sea below the AIW now are depressed downwards (Budéus and Ronski 2009). The wind stress curl, which has commonly been assumed to cause the doming of the isopycnals, has not, except during some years in the mid 1980s, shown any sign of decreasing (Jakobsen et al. 2003) and should be as effective in creating a doming of the density surfaces in the Greenland Sea as in the 1970s. This suggests that the dome of dense deep water observed earlier would rather be due to the active formation and convection of denser water than an effect of wind forcing.

The formation of Arctic Intermediate Water (AIW) has also led to a freshening of the Norwegian Sea (Blindheim et al. 2000; Mork and Blindheim 2000). The intermediate and deep waters have become less dense, and the isopycnals crossing

the Iceland–Scotland Ridge at the Faroe–Shetland Channel have been displaced downwards. The pressure head driving dense water through the Faroe–Shetland Channel then becomes reduced, which could lead to a decrease in the overflow. A possible slowing down of the Faroe–Shetland overflow has also been reported (Hansen et al. 2001). However, this trend appears to have been reversed in recent years (Hansen and Østerhus 2007). The strength of the Denmark Strait overflow has remained unaffected, and a slowdown of the Meridional Overturning Circulation has not been documented (Dickson et al. 2008b).

The importance of the Arctic Ocean freshwater balance for the Atlantic Overturning Circulation has been the focus of much recent research (Peterson et al. 2006; Serreze et al. 2006; Dickson et al. 2007). The freshwater discharged into the Arctic Ocean is exported as ice and as liquid water within the water column. Will a reduced ice cover affect the distribution of the fluxes between these two routes and will this lead to a change in the residence time of the freshwater in the Arctic Ocean, and in what direction? Will such a change influence the convection in the downstream ventilation sites, the Greenland Sea and the Labrador Sea? Will the freshwater be only temporarily stored in the Nordic Seas and then continue with the overflow water into the North Atlantic, causing changes like the recently documented freshening of the North Atlantic Deep Water (Curry et al. 2003)?

Many sources, in the Arctic Ocean as well as in the Nordic Seas, contribute to the overflow (Rudels et al. 2002; Rudels et al. 2003), and also the Arctic Intermediate Water presently created in the Greenland Sea, in spite of its reduced density, is still dense enough to barely pass the sill in the Denmark Strait. SF_6, which has become an identifier of the AIW and its spreading into the Iceland and Norwegian seas and into the Arctic Ocean through Fram Strait, has been followed. The main export appears to be towards the Arctic Ocean, not towards the Norwegian and Iceland seas and the Greenland–Scotland Ridge (Messias et al. 2008; but see also Marnela et al. 2008). This suggests that the main part of the AIW makes a loop into the Arctic Ocean, or at least into Fram Strait, before it joins the East Greenland Current and becomes transported southward. The direct southward transport of SF_6 reached the Greenland–Scotland Ridge first in Denmark Strait and later in the Faroe–Shetland Channel. It appears, however, that the SF_6 first crossed the ridge into the North Atlantic through the Faroe–Shetland Channel and only later through Denmark Strait (Messias et al. 2008). In the Arctic Mediterranean Sea, the overall production and storage of water dense enough to supply the Greenland–Scotland overflow thus do not appear to have diminished, and the renewal of the North Atlantic Deep Water and the forcing of the Meridional Overturning Circulation are not presently threatened.

Acknowledgement The writing and revision of this study have extended over a considerable period of time, and economic support has been obtained from various sources during various phases of the writing process. The more important of these sources are: ASOF-N (contract No EVK2-CT-2002–00139) (BR, PE, EF, US), DAMOCLES (Contract No 018509) (BR, LA, PE, EF, US,) The Academy of Finland (No. 210551) (BR), the Canadian Panel of Energy Research and Development (EPJ).

References

Aagaard K (1968) Temperature variations in the Greenland Sea deep water. Deep Sea Res 15:281–296
Aagaard K (1980) On the deep circulation in the Arctic Ocean. Deep Sea Res 27:251–268
Aagaard K, Carmack EC (1989) The role of sea ice and other freshwater in the Arctic circulation. J Geophys Res 94:14485–14498
Aagaard K, Carmack EC (1994) The Arctic Ocean and climate: a perspective. In: Johannessen OM, Muench RD, Overland JE (eds) The polar oceans and their role in shaping the global climate. American Geophysical Union, Washington, DC, pp 5–20
Aagaard K, Coachman LK (1975) Toward an ice-free Arctic Ocean. Eos 56:484–486
Aagaard K, Greisman P (1975) Towards a new mass and heat budget for the Arctic Ocean. J Geophys Res 80:3821–3827
Aagaard K, Woodgate RA (2001) Some thoughts on the freezing and melting of sea ice and their effects on the ocean. Ocean Model 3:127–135
Aagaard K, Darnall C, Greisman P (1973) Year-long measurements in the Greenland-Spitsbergen passage. Deep Sea Res 20:743–746
Aagaard K, Coachman LK, Carmack EC (1981) On the halocline of the Arctic Ocean. Deep Sea Res 28:529–545
Aagaard K, Swift JH, Carmack EC (1985) Thermohaline circulation in the Arctic Mediterranean Seas. J Geophys Res 90:4833–4846
Aagaard K, Foldvik A, Hillman SR (1987) The West Spitsbergen Current: disposition and water mass transformation. J Geophys Res 92:3778–3784
Aagaard K, Barrie LA, Carmack EC, Garrity C, Jones EP, Lubin D, Macdonald RW, Swift JH, Tucker WB, Wheeler PA, Whritner RH (1996) U.S., Canadian researchers explore the Arctic Ocean. Eos 177:209–213
Anderson LG, Dyrssen D (1981) Chemical constituents of the Arctic Ocean in the Svalbard area. Oceanol Acta 4:305–311
Anderson LG, Jones EP (1992) Tracing upper waters of the Nansen Basin in the Arctic Ocean. Deep Sea Res 39:425–443
Anderson LG, Jones EP, Lindegren R, Rudels B, Sehlstedt P-I (1988) Nutrient regeneration in cold, high salinity bottom water of the Arctic shelves. Cont Shelf Res 8:1345–1355
Anderson LG, Jones EP, Koltermann K-P, Schlosser P, Swift JH, Wallace DWR (1989) The first oceanographic section across the Nansen Basin in the Arctic Ocean. Deep Sea Res 36:475–482
Anderson LG, Björk G, Holby O, Jones EP, Kattner G, Koltermann K-P, Liljeblad B, Lindegren R, Rudels B, Swift JH (1994) Water masses and circulation in the Eurasian Basin: results from the Oden 91 expedition. J Geophys Res 99:3273–3283
Anderson LG, Jones EP, Rudels B (1999) Ventilation of the Arctic Ocean estimated from a plume entrainment model constrained by CFCs. J Geophys Res 104:13423–13429
Anderson LG, Jutterström S, Kaltin S, Jones EP, Björk G (2004) Variability in river runoff distribution in the Eurasian Basin of the Arctic Ocean. J Geophys Res 109:C01016. doi:10.1029/2003JC00173
Backhaus JO, Fohrmann H, Kämpf J, Rubino A (1997) Formation and export of water masses produced in Arctic shelf polynyas – process studies of oceanic convection. ICES J Mar Sci 54:366–382
Bailey WB (1956) On the origin of Baffin Bay deep water. J Fish Res Board Can 13(3):303–308
Bailey WD (1957) Oceanographic features of the Canadian archipelago. J Fish Res Board Can 14:731–769
Bauch D, Schlosser P, Fairbanks RG (1995) Freshwater balance and the source of deep and bottom waters in the Arctic Ocean inferred from the distribution of $H_2{}^{18}O$. Prog Oceanogr 35:53–80
Baumgartner A, Reichel E (1975) The world water balance. Elsevier, Amsterdam, 179 pp
Belyakov LN, Volkov VA (1980) Doklady Akad. Nauk SSR 254(3):752–754

Björk G (1989) A one-dimensional time-dependent model for the vertical stratification of the upper Arctic Ocean. J Phys Oceanogr 19:52–67
Björk G, Winsor P (2006) The deep waters of the Eurasian Basin, Arctic Ocean: geothermal heat flow, mixing and renewal. Deep Sea Res I 53:1253–1271
Björk G, Söderqvist J, Winsor P, Nikolopoulos A, Steele M (2002) Return of the cold halocline to the Amundsen Basin of the Arctic Ocean: implication for the sea ice mass balance. Geophys Res Lett 29(11):1513. doi:10.1029/2001GL014157
Björk G, Jakobsson M, Rudels B, Swift JH, Anderson L, Darby DA, Backman J, Coakley B, Winsor P, Polyak L, Edwards M (2007) Bathymetry and deep-water exchange across the central Lomonosov Ridge at 88–89°N. Deep Sea Res I 54:1197–1208. doi:10.1016/j.dsr.2007.05.010
Blindheim J (1989) Cascading of Barents Sea bottom water into the Norwegian Sea. Rapp P-v Réun Cons Int Explor Mer 188:49–58
Blindheim J, Borovkov V, Hansen B, S-Aa M, Turrell WR, Østerhus S (2000) Upper layer cooling and freshening in the Norwegian Sea in relation to atmospheric forcing. Deep Sea Res I 47:655–680
Bönisch G, Schlosser P (1995) Deep water formation and exchange rates in the Greenland/ Norwegian Seas and the Eurasian Basin of the Arctic Ocean. Prog Oceanogr 35:29–52
Bönisch G, Blindheim J, Bullister JL, Schlosser P, Wallace DWR (1997) Long-term co-ordinated trends of temperature, density and transient tracers in the central Greenland Sea. J Geophys Res 102:18553–18577
Bourke RH, Paquette RG (1991) Formation of Baffin Bay bottom and deep waters. In: Chu PC, Gascard J-C (eds) Deep convection and deep water formation in the oceans. Elsevier, Amsterdam, pp 135–155
Bourke RH, Weigel AM, Paquette RG (1988) The westward turning branch of the West Spitsbergen Current. J Geophys Res 93:14065–14077
Bourke RH, Addison VG, Paquette RG (1989) Oceanography of Nares Strait and Northern Baffin Bay in 1986 with emphasis on deep and bottom water formation. J Geophys Res 94:8289–8302
Boyd TJ, D'Asaro EA (1994) Cooling of the West Spitsbergen Current: wintertime observations west of Svalbard. J Geophys Res 99:22597–22618
Boyd TJ, Steele M, Muench RD, Gunn JT (2002) Partial recovery of the Arctic Ocean halocline. Geophys Res Lett 29(14). doi:10.1029/2001GL014047
Buch E, S-Aa M, Kristmannsson SS (1996) Arctic Ocean deep water masses in the western Iceland Sea. J Geophys Res 101:11965–11973
Budéus G, Ronski S (2009) An integral view of the hydrographic development in the Greenland Sea over a decade. The Open Oceanogr J 3:8–39
Budéus G, Schneider W, Krause G (1998) Winter convection events and bottom water warming in the Greenland Sea. J Geophys Res 103:18513–18527
Budéus G, Cisewski B, Ronski S, Dietrich D, Weitere M (2004) Structure and effects of a long lived vortex in the Greenland Sea. Geophys Res Lett 31:L05304. doi:10.1029/2003GL017983
Buinitsky VKH (1951) Ice formation and drift in the Arctic Basin. In: Proceedings of the drifting expedition of Glavsevmorput onboard the Icebreaker "G. Sedov" 1937–149, V.4M-L, pp 74–179
Carmack EC (1986) Circulation and mixing in ice covered waters. In: Untersteiner N (ed) The geophysics of sea ice. Plenum, New York, pp 641–712
Carmack EC (1990) Large-scale physical oceanography of polar oceans. In: Smith WO Jr (ed) Polar oceanography, Part A. California Academic Press, San Diego, pp 171–212
Carmack EC (2000) The Arctic Ocean's freshwater budget: sources, storage and export. In: Lewis EL et al (eds) The freshwater budget of the Arctic Ocean, vol 70, NATO science series 2 environmental security. Kluwer, Dordrecht, pp 91–126
Carmack EC, Kulikov YA (1998) Wind-forced upwelling and internal wave generation in Mackenzie Canyon, Beaufort Sea. J Geophys Res 103:18447–18458
Carmack EC, MacDonald RW (2002) Oceanography of the Canadian shelf of the Beaufort Sea: a setting for marine life. Arctic 55(Supp 1):29–45

Carmack EC, Macdonald RW, Perkin RG, McLaughlin FA (1995) Evidence for warming of Atlantic water in the southern Canadian Basin. Geophys Res Lett 22:1961–1964
Carmack EC, Aagaard K, Swift JH, Macdonald RW, McLaughlin FA, Jones EP, Perkin RG, Smith JN, Ellis KM, Killius LR (1997) Changes in temperature and tracer distributions within the Arctic Ocean: results from the 1994 Arctic Ocean section. Deep Sea Res II 44:1487–1502
Cavalieri DJ, Martin S (1994) The contribution of Alaskan, Siberian and Canadian coastal polynyas to the cold halocline layer of the Arctic Ocean. J Geophys Res 99:18343–18362
Chapman DC, Gawarkiewicz G (1997) Shallow convection and buoyancy equilibrium in an idealized coastal polynya. J Phys Oceanogr 27:555–566
Cisewski B, Budéus G, Krause G (2003) Absolute transport estimates of total and individual water masses in the northern Greenland Sea derived from hydrographic and acoustic Doppler current profiler measurements. J Geophys Res 108(C9):3298. doi:10.1029/2002JCC001530
Coachman LK, Aagaard K (1966) On water exchange through Bering Strait. Limnol Oceanogr 44–59 pp
Coachman LK, Aagaard K (1974) Physical oceanography of the arctic and subarctic seas. In: Herman Y (ed) Marine geology and oceanography of the arctic seas. Springer, New York, pp 1–72
Coachman LK, Aagaard K (1981) Reevaluation of water transports in the vicinity of Bering Strait. In: Wood DW, Calder JA (eds) The eastern Bering Sea shelf: Oceanography and resources, vol 1. University of Washington Press, Seattle, pp 95–110
Coachman LK, Aagaard K (1988) Transports through Bering Strait: annual and interannual variability. J Geophys Res 93:15535–15539
Coachman LK, Barnes CA (1961) The contribution of Bering Sea water to the Arctic Ocean. Arctic 14:147–161
Coachman LK, Barnes CA (1962) Surface waters in the Eurasian Basin of the Arctic Ocean. Arctic 15:251–277
Coachman LK, Barnes CA (1963) The movement of Atlantic water in the Arctic Ocean. Arctic 16:8–16
Coachman LK, Aagaard K, Tripp R (1975) Bering Strait: the regional physical oceanography. University of Washington Press, Seattle, 172 pp
Collin AE (1962) Oceanographic observations in the Canadian Arctic and the adjacent Arctic Ocean. Arctic 15:194–201
Collin AE, Dunbar MJ (1963) Physical oceanography in Arctic Canada. In: Barnes HE (ed) Oceanography and biology: an annual review. G. Allen & Unwin, London, pp 45–77
Curry R, Dickson RR, Yashayaev I (2003) A change in the freshwater balance of the Atlantic over the past four decades. Nature 426:826–829
D'Asaro EA (1988a) Observations of small eddies in the Beaufort Sea. J Geophys Res 93:6669–6684
D'Asaro EA (1988b) Generation of submesoscale vortices: a new mechanism. J Geophys Res 93:6685–6693
Day CG (1968) Current measurements in Smith Sound, summer 1963. USCG Oceanogr Rep 16:75–84
Dickson RR, Brown J (1994) The production of North Atlantic Deep Water. Sources, rates and pathways. J Geophys Res 99:12319–12341
Dickson R, Rudels B, Dye S, Karcher M, Meincke J, Yashayaev I (2007) Current estimates of freshwater flux through the Arctic and Subarctic seas. Prog Oceanogr 73:210–230. doi:10.1016/j.pocean.2006.12.003
Dickson RR, Meincke J, Rhines P (2008a) Arctic-Subarctic Ocean fluxes. Springer, Dordrecht, X + 736 pp
Dickson RR, Dye S, Jónsson S, Köhl A, Macrander A, Marnela M, Meincke J, Olsen S, Rudels B, Valdimarsson H, Voet G (2008b) The overflow flux west of Iceland: variability, origins and forcing. In: Dickson RR, Meincke J, Rhines P (eds) Arctic-Subarctic Ocean fluxes. Springer, Dordrecht, pp 443–474

Ekman VW (1905) On the influence of earth's rotation on ocean currents. Arch Math Astron Phys 2(11)
Ekwurzel B, Schlosser P, Mortlock RA, Fairbanks RG, Swift JH (2001) River runoff, sea ice melt water, and Pacific water distribution and mean residence times in the Arctic Ocean. J Geophys Res 106:9075–9092
Environmental Worging Group (EWG) (1997) Joint U.S. Russian atlas of the Arctic Ocean: oceanography atlas for the Winter period. National Snow and Ice Data Center, Boulder
Environmental Worging Group (EWG) (1998) Joint U.S. Russian atlas ofthe Arctic Ocean: oceanography atlas for the Summer period. National Snow and Ice Data Center, Boulder
Fahrbach E, Meincke J, Østerhus S, Rohardt G, Schauer U, Tverberg V, Verduin J (2001) Direct measurements of volume transports through Fram Strait. Polar Res 20:217–224
Falck E, Kattner G, Budéus G (2005) Disappearance of Pacific water in the northwestern Fram Strait. Geophys Res Lett 32:L14169. doi:10.1029/2005GL023400
Fedorova AP, Yankina AS (1964) The passage of Pacific Ocean water through the Bering Strait into the Chukchi Sea. Deep Sea Res 11:427–434
Fer I, Skogseth R, Haugan PM (2003a) Mixing of the Storfjorden (Svalbard Archipelago) overflow inferred from density overturns. J Geophys Res 109:C01005. doi:10.1029/2003JC001968
Fer I, Skogseth R, Haugan PM, Jaccard P (2003b) Observations of the Storfjorden overflow. Deep Sea Res I 50:1283–1303
Fissel DB, Birch JR, Melling H, Lake RA (1988) Non-tidal flows in the Northwest Passage. Canadian technical report of hydrography and ocean sciences 8, Institute of Ocean Sciences, Sidney, Canada, V8L 4B2, 143 pp
Fjeldstad JE (1936) Results of tidal observations. Norwegian North Polar Expedition "Maud" 1918–1925. Sci Results 4(4):88pp
Foldvik A, Aagaard K, Törresen T (1988) On the velocity field of the East Greenland Current. Deep Sea Res 35:1335–1354
Frank M, Smethie WM, Bayer R (1998) Investigation of subsurface water flow along the continental margin of the Eurasian Basin using transient tracers tritium, ^{3}He, and CFCs. J Geophys Res 103:30773–30792
Friedrich H, Houssais M-N, Quadfasel D, Rudels B (1995) On Fram Strait water masses. In: Extended abstract, Nordic seas symposium, Hamburg, 7/3–9/3 1995, pp 69–72
Gascard J-C, Kergomard C, Jeannin PF, Fily M (1988) Diagnostic study of the Fram Strait marginal ice zone during summer from Marginal Ice Zone Experiment 84 and 84 Lagrangian observations. J Geophys Res 93:3613–3641
Gascard J-C, Richez C, Roaualt C (1995) New insights on large-scale oceanography in Fram Strait: the West Spitsbergen Current. In: Smith WO Jr, Grebmeier JM (eds) Arctic oceanography, marginal ice zones and continental shelves, vol 49. American Geophysical Union, Washington, DC, pp 131–182
Gascard J-C, Watson AJ, Messias M-J, Olsson KA, Johannessen T, Simonsen K (2002) Long-lived vortices as a mode of deep ventilation in the Greenland Sea. Nature 416:525–527
Gawarkiewicz G (2000) Effects of ambient stratification and shelf-break topography buoyancy equilibrium in an idealised coastal polynya. J Geophys Res 105:3307–3324
Gawarkiewicz G, Chapman DC (1995) O numerical study of dense water formation and transport on a shallow, sloping continental shelf. J Geophys Res 100:4489–4508
Gawarkiewicz G, Weingartner T, Chapman DC (1998) Sea-ice processes and water mass modification and transports over Arctic shelves. In: Brink KH, Robinson AR (eds) The Sea, vol 10. Wiley, New York, pp 171–190
Goldner DR (1999a) Steady models of Arctic shelf-basin exchange. J Geophys Res 104:29733–29755
Goldner DR (1999b) On the uncertainty of the mass, heat and salt budgets of the Arctic Ocean. J Geophys Res 104:29757–29770
Gorshov SG (1980) World Ocean Atlas 3. The Arctic Ocean. Leningrad USSR Ministry of Defence XIV, 180 pp
Guay CK, Falkner KK (1998) A survey of dissolved barium in the estuaries of major Arctic rivers and adjacent seas. Cont Shelf Res 18:859–882

Guay CK, Falkner KK, Muench RD, Mensch M, Frank M, Bayer R (2001) Wind-driven transport pathways for Eurasian Arctic river discharge. J Geophys Res 106:11469–11480
Haarpainter J (1999) The Storfjorden polynya: ERS-2 SAR observations and overview. Polar Res 18:175–182
Haarpainter J, O'Dwyer J, Gascard J-C, Haugan PM, Schauer U, Østerhus S (2001) Seasonal transformations of water masses, circulation and brine formation observed in Storfjorden, Svalbard. Ann Glaciol 33:437–443
Hamilton JM (2001) Accurate ocean current direction measurements near magnetic poles. The 11th international offshore and polar engineering conference proceedings. ISOPE, Stavanger, vol I:815–846
Hansen B, Østerhus S (2000) North Atlantic – Nordic Seas exchanges. Prog Oceanogr 45:109–208
Hansen B, Østerhus S (2007) Faroe bank Channel overflow 1995–2005. Prog Oceanogr 75:817–856. doi:10.1016/j.pocean.2007.09.004
Hansen B, Turrell WT, Østerhus S (2001) Decreasing overflow from the Nordic seas into the Atlantic Ocean through the Faroe Bank Channel since 1950. Nature 411:927–930
Hanzlick D, Aagaard K (1980) Freshwater and Atlantic Water in the Kara Sea. J Geophys Res 85:4937–4942
Harris RA (1911) Arctic tides. US Printing Office, Washington, DC, 103 pp
Hart JE, Killworth PD (1976) On open ocean baroclinic instability in the Arctic. Deep Sea Res 23:637–645
Heinze C, Schlosser P, Koltermann K-P, Meincke J (1990) A tracer study of the deep water renewal in the European polar seas. Deep Sea Res 37:1425–1453
Helland-Hansen B, Nansen F (1909) The Norwegian Sea. Its physical oceanography based upon the Norwegian researches 1900–1904. Kristiania, Report on Norway fishery and marine investigations II(1):390 pp
Holloway G (2001) Is the arctic sea ice rapidly thinning? Ice and climate news, the Arctic Climate System Study/Climate and Cryosphere project newsletter 1:2–5
Holloway G, Sou T (2002) Has the arctic sea-ice rapidly thinned? J Clim 15:1691–1701
Hunkins K (1966) Ekman drift currents in the Arctic Ocean. Deep-Sea Res 13:607–620
Hunkins K (1974) Subsurface eddies in the Arctic Ocean. Deep-Sea Res 21:1017–1033
Hurrell JW (1995) Decadal trends in the North Atlantic Oscillation: regional temperatures and precipitation. Science 269:677–679
Ingvaldsen RB, Asplin L, Loeng H (2004a) Velocity field of the western entrance to the Barents Sea. J Geophys Res 109:C03021. doi:101029/2003JC001811
Ingvaldsen RB, Asplin L, Loeng H (2004b) The seasonal cycle in the Atlantic transport to the Barents Sea during the years 1997–2001. Cont Shelf Res 24:1015–1032
Jakobsen PK, Nielsen MH, Quadfasel D, Schmith T (2003) Variability of the surface circulation of the Nordic Seas during the 1990s. In: Hydrobiological variability in the ICES area 1990–1999. ICES Marine Science Symposia, vol 219, pp 367–370
Jakobson M, Macnab R, Mayer L, Anderson R, Edwards M, Hatzky J, Schenke HW, Johnson P (2008) An improved bathymetric portrayal of the Arctic Ocean: implications for ocean modelling and geological, geophysical and oceanographic analyses. Geophys Res Lett 35:L07602. doi:10.1029/2008GL033520
Jakobsson M, Grantz A, Kristoffersen Y, MacNab R (2004a) Bathymetry and physiography of the Arctic Ocean and its constituent seas. In: Stein R, Macdonald RW (eds) The organic carbon cycle in the Arctic Ocean. Springer, Berlin, pp 1–6
Jakobsson M, MacNab R, Cherkis N, Schenke H-W (2004b) The international bathymetric chart of the Arctic Ocean (IBCAO). Research Publication RP-2, National Geophysical Data Center, Boulder
Jones EP, Anderson LG (1986) On the origin of the chemical properties of the Arctic Ocean halocline. J Geophys Res 91:10759–10767
Jones EP, Coote AR (1980) Nutrient distributions in the Canadian Archipelago: indictors of summer water mass and flow characteristics. Can J Fish Aquat Sci 37(4):589–599
Jones EP, Anderson LG, Wallace DWR (1991) Tracers of near-surface, halocline and deep waters in the Arctic Ocean: implications for circulation. J Mar Syst 2:241–255

Jones EP, Rudels B, Anderson LG (1995) Deep waters of the Arctic Ocean: origins and circulation. Deep-Sea Res 42:737–760
Jones EP, Anderson LG, Swift JH (1998) Distribution of Atlantic and Pacific waters in the upper Arctic Ocean: implications for circulation. Geophys Res Lett 25:765–768
Jones EP, Swift JH, Anderson LG, Lipizer M, Civitarese G, Falkner KK, Kattner G, McLaughlin FA (2003) Tracing Pacific water in the North Atlantic Ocean. J Geophys Res 108(C4):3116. doi:10.1029/2001JC001141
Jónsson S, Waldimarsson H (2004) A new path for the Denmark Strait overflow water from the Iceland Sea to Denmark Strait. Geophys Res Lett 31:L03305. doi:10.1029/2003GL019214
Jungclaus JH, Backhaus JO, Fohrmann H (1995) Outflow of dense water from the Storfjord in Svalbard: a numerical model study. J Geophys Res 100:24719–24728
Kiilerich A (1939) The Godthaab Expedition 1928. A theoretical treatment of the hydrographical observational material. Medd. om Grönland 78(5):149 pp
Kiilerich A (1945) On the hydrography of the Greenland Sea. Medd om Grönland 144(2):63 pp
Killworth PD (1979) On chimney formations in the oceans. J Phys Oceanogr 9:531–554
Kinney P, Arhelger ME, Burrell DC (1970) Chemical characteristics of water masses in the Amerasian basin of the Arctic Ocean. J Geophys Res 75:4097–4104
Kliem N, Greenberg DA (2003) Diagnostic simulations of the summer circulation in the Canadian Arctic Archipelago. Atmosphere-Ocean 41(4):273–289. doi:10.3137/ao.410402
Krümmel O (1907) Handbuch der Ozeanographie. Band I, Stuttgart, 526 pp
Kulikov EA, Carmack EC, MacDonald RW (1998) Flow variability at the continental shelf break of the Mackenzie shelf in the Beaufort Sea. J Geophys Res 104:12725–12741
Lemke P (1993) Modelling sea ice – mixed layer interaction. In: J Willebrandt, DLT Anderson (eds) Modelling oceanic climate interactions. Proceedings of the NATO advanced study institute on modelling of oceanic climate interactions, Les Houches, 17–28 Feb 1992. NATO ASI series I: global environmental change, vol 11. Springer, Berlin, pp 243–269
Libin YaS (1946) Hydrological observations/expedition onboard "H-169" air plane to the "pole of inaccessibility" scientific results.-M-L, Izdatelstvo Glavsevmorputi, pp 74–123
Livingston HD, Kufferman SL, Bowen VT, Moore RM (1984) Vertical profile of artificial radionuclide concentration in the central Arctic Ocean. Geochim Cosmochim Acta 48:2195–2203
Loeng H (1991) Features of the physical oceanographic conditions in the central parts of the Barents Sea. Polar Res 10:5–18
Loeng H, Ozhigin V, Ådlandsvik B, Sagen H (1993) Current measurements in the northeastern Barents Sea. ICES C.M. 1993/C:41 Hydrographic Committee, 22 pp
Loeng H, Ozhigin V, Ådlandsvik B (1997) Water fluxes through the Barents Sea. ICES J Mar Sci 54:310–317
MacDonald RW (2000) Arctic estuaries and ice: a positive-negative estuarine couple. In: Lewis EL et al (eds) The freshwater budget of the Arctic Ocean. NATO science series 2: environmental security – vol 70. Kluwer, Dordrecht, pp 383–407
Macdonald RW, Carmack EC (1991) Age of Canada Basin deep waters: a way to estimate primary production for the Arctic Ocean. Science 254:1348–1350
Macdonald RW, Paton DW, Carmack EC, Omstedt A (1995) The freshwater budget and under-ice spreading of the Mackenzie River water in the Canadian Beaufort Sea based on salinity and $^{18}O/^{16}O$ measurements in water and ice. J Geophys Res 100:895–919
Macdonald RW, Carmack EC, McLaughlin FA, Falkner KK, Swift JH (1999) Connections among ice, runoff and atmospheric forcing in the Beaufort Gyre. Geophys Res Lett 26: 2223–2226
Maksimov IV (1945) Determining the relative volume of the annual flow of Pacific water into the Arctic Ocean through Bering Strait. Probl Arktiki 2:51–58
Marnela M, Rudels B, Olsson KA, Anderson LG, Jeansson E, Torres DJ, Messias MJ, Swift JH, Watson AJ (2008) Transport of Nordic Sea water masses and excess SF_6 through Fram Strait to the Arctic Ocean. Prog Oceanogr 78:1–11
Martin S, Cavalieri DJ (1989) Contributions of the Siberian shelf polynyas to the Arctic Ocean intermediate and deep water. J Geophys Res 94:12725–12738

Martinson DG (1990) Evolution of the southern Ocean winter mixed layer and sea ice: open ocean deep water formation and ventilation. J Geophys Res 95:11641–11654
Martinson DG, Steele M (2001) Future of the Arctic sea ice cover: implications of an Antarctic analog. Geophys Res Lett 28:307–310
Maslowski W (2003) High resolution modelling of the Arctic Ocean: a decade of progress. In: ACSYS final science conference, St. Petersburg, Russia, 11–14 Nov 2003: WCRP-118(CD) WMO/TD(1232)
Maslowski W, Newton B, Schlosser P, Semtner A, Martinson D (2000) Modelling recent climate variability in the Arctic. Geophys Res Lett 27:3743–3746
Mauritzen C (1996a) Production of dense overflow waters feeding the North Atlantic across the Greenland Sea-Scotland Ridge. Part 1: evidence for a revised circulation scheme. Deep Sea Res 43:769–806
Mauritzen C (1996b) Production of dense overflow waters feeding the North Atlantic across the Greenland Sea-Scotland Ridge. Part 2: an inverse model. Deep Sea Res 43:807–835
May BD, Kelley DE (2001) Growth and steady state stages of thermohaline intrusions in the Arctic Ocean. J Geophys Res 106:783–794
McCartney MS (1977) Subantarctic mode water. In: Angel M (ed) A voyage of discovery. Pergamon Press, Oxford, pp 103–119
McCartney MS, Talley LD (1984) Warm-to-cold water conversions in the Northern North Atlantic Ocean. J Phys Oceanogr 14:922–935
McLaughlin FA, Carmack EC, Macdonald RW, Bishop JKB (1996) Physical and geochemical properties across the Atlantic/Pacific water mass boundary in the southern Canada Basin. J Geophys Res 101:1183–1197
McLaughlin FA, Carmack EC, MacDonald RW, Weaver AJ, Smith J (2002) The Canada Basin 1989–1995: upstream events and far-field effects of the Barents Sea branch. J Geophys Res 107. doi:1029/2001JC000904
McLaughlin FA, Carmack EC, Macdonald RW, Melling H, Swift JH, Wheeler PA, Sherr BF, Sherr EB (2004) The joint roles of Pacific and Atlantic-origin waters in the Canada Basin, 1997–1998. Deep Sea Res I 51:107–128
McPhee MG (1990) Small-scale processes. In: Smith WO Jr (ed) Polar oceanography, Part A: physical science. Academic, San Diego, pp 287–334
McPhee MG, Stanton TP, Morison JH, Martinson DG (1998) Freshening of the upper ocean in the Arctic: is the perennial sea ice disappearing? Geophys Res Lett 25:1729–1732
Meincke J, Rudels B, Friedrich H (1997) The Arctic Ocean-Nordic Seas thermohaline system. ICES J Mar Sci 54:283–299
Melling H (2000) Exchanges of freshwater through the shallow straits of the North American Arctic. In: EL Lewis et al (eds) The freshwater budget of the Arctic Ocean. Proceedings of a NATO advanced research workshop, Tallinn, Estonia, 27 Apr–1 May 1998. Dordrecht, Kluwer Academic, Dordrecht, pp 479–502
Melling H (2004) Fluxes through the northern Canadian Arctic Archipelago. ASOF Newsl 2:3–7
Melling H, Lewis EL (1982) Shelf drainage flows in the Beaufort Sea and their effect on the Arctic Ocean pycnocline. Deep Sea Res 29:967–985
Melling H, Moore RM (1995) Modification of halocline source waters during freezing on the Beaufort Sea shelf: evidence from oxygen isotopes and dissolved nutrients. Cont Shelf Res 15:89–113
Melling H, Riedel DA (1996) Development of seasonal pack ice in the Beaufort Sea during the winter of 1991–1992: a view from below. J Geophys Res 101(C5):11975–11991
Melling H, Johnston PH, Riedel DA (1995) Measurement of the underside topography of sea ice by moored subsea sonar. J Atmos Ocean Technol 12(3):589–602
Melling H, Agnew TA, Falkner KK, Greenberg DA, Craig ML, Münchow A, Petrie B, Prinsenberg SJ, Samelson RM, Woodgate RA (2008) In: Dickson RR, Meincke J, Rhines P (eds) Arctic-Subarctic ocean fluxes. Springer, Dordrecht, pp 193–247
Meredith MP, Heywood KJ, Dennis PF, Goldson LE, White R, Fahrbach E, Østerhus S (2001) Freshwater fluxes through the western Fram Strait. Geophys Res Lett 28:615–618

Merryfield WJ (2000) Origin of thermohaline staircases. J Phys Oceanogr 30:1046–1068
Merryfield WJ (2002) Intrusions in double-diffusively stable Arctic waters: evidence for differential mixing? J Phys Oceanogr 32:1452–1459
Messias M-J, Watson AJ, Johannessen T, Oliver KIC, Olsson KA, Fogelqvist E, Olafsson J, Bacon S, Balle J, Bergman N, Budéus G, Danielsen M, Gascard J-C, Jeansson E, Olafsdottir SR, Simonsen K, Tanhua T, Van Scoy K, Ledwell JR (2008) The Greenland Sea tracer experiment 1996–2002: horizontal mixing and transport of Greenland Sea intermediate water. Prog Oceanogr 78:85–105. doi:1016/jpocean.2007.06.005
Midttun L (1985) Formation of dense bottom water in the Barents Sea. Deep Sea Res 32:1233–1241
Melling H (2004) Fluxes through the northern Canadian Arctic Archipelago. ASOF Newsl 2:3–7
Moore RM, Wallace DWR (1988) A relationship between heat transfer to sea ice and temperature-salinity properties of the Arctic Ocean waters. J Geophys Res 93:565–571
Moore RM, Lowings MG, Tan FC (1983) Geochemical profiles in the central Arctic Ocean. Their relation to freezing and shallow circulation. J Geophys Res 88:2667–2674
Morison JH, Steele M, Anderson R (1998) Hydrography of the upper Arctic Ocean measured form the nuclear submarine USS Pargo. Deep Sea Res I 45:15–38
Mork K-A, Blindheim J (2000) Variations in the Atlantic inflow to the Nordic Seas, 1955–1996. Deep Sea Res I 47:1035–1057
Mosby H (1959) Deep water in the Norwegian Sea. Geofys Publ 21, 62 pp
Mosby H (1962) Water, mass and heat balance of the North Polar Sea and of the Norwegian Sea. Geofys Publ 24(II):289–313
Müchow A, Melling H (2008) Ocean current observations from Nares Strait to the west of Greenland: interannual to tidal variability and forcing. J Mar Res 66:801–833
Müchow A, Melling H, Falkner KK (2006) An observational estimate of volume and freshwater flux leaving the Arctic Ocean through Nares Strait. J Phys Oceanogr 36:2025–2041
Müchow A, Falkner KK, Melling H (2007) Spatial continuity of measured seawater and tracer fluxes through Nares Strait, a dynamically wide channel bordering the Canadian Archipelago. J Mar Res 65:759–788
Muench RD (1971) The Physical oceanography of the northern Baffin Bay region. The Baffin Bay – North Water Project. Scientific report no 1, Arctic Institute of North America, Washington, DC, 150 pp
Münchow A, Weingartner TJ, Cooper LW (1999) The summer hydrography and surface circulation of the East Siberian Shelf Sea. J Phys Oceanogr 29:2167–2182
Nansen F (1902) Oceanography of the North Polar Basin. The Norwegian North polar expedition 1893–1896. Sci Res (9):427 pp
Nansen F (1906) Northern waters, Captain Roald Amundsen's oceanographic observations in the Arctic Seas in 1901. Videnskab-Selskabets Skrifter 1. Matematisk-Naturvidenskabelig Klasse 1, Kristiania, pp 1–145
Nansen F (1915) Spitsbergen waters. Videnskabs-selskabets skrifter I. Matematisk-Naturvidenskabelig klasse I(3):145 pp
Neal VT, Neshyba S, Denner W (1969) Thermal stratification in the Arctic Ocean. Science 166:373–374
Neshyba S, Neal VT, Denner W (1971) Temperature and conductivity measurements under Ice Island T-3. J Geophys Res 76:8107–8120
Newton JL, Sotirin BJ (1997) Boundary undercurrent and water mass exchanges in the Lincoln Sea. J Geophys Res 102:3393–3403
Newton JL, Aagaard K, Coachman LK (1974) Baroclinic eddies in the Arctic Ocean. Deep Sea Res 21:707–719
Nikiforov EG, Shpaiker AO (1980) Principles of large-scale variations of the Arctic Ocean hydrography. Hydrometeizdat, Leningrad, 269 pp
Östlund HG (1982) The residence time of the freshwater component in the Arctic Ocean. J Geophys Res 87:2035–2043
Östlund HG, Hut G (1984) Arctic Ocean water mass balance from isotope data. J Geophys Res 89:6373–6381

Padman L (1995) Small-scale physical processes in the Arctic Ocean. In: Smith WO Jr, Grebmeier JM (eds) Arctic oceanography, marginal ice zones and continental shelves, vol 49. American Geophysical Union, Washington, DC, pp 131–182
Padman L, Dillon TM (1987) Vertical heat fluxes through the Beaufort Sea thermohaline staircases. J Geophys Res 92:10799–10806
Padman L, Dillon TM (1988) On the horizontal extent of the Canada Basin thermohaline steps. J Phys Oceanogr 18:1458–1462
Padman L, Dillon TM (1989) Thermal microstructure and internal waves in an oceanic diffusive staircase. Deep Sea Res 36:531–542
Palfrey KM (1967) Physical oceanography in the northern part of the Greenland Sea in summer of 1964. MS thesis, University of Washington, 101 pp
Pease CH (1987) The size of wind-driven polynyas. J Geophys Res 92:7049–7059
Perkin RG, Lewis EL (1984) Mixing in the West Spitsbergen Current. J Phys Oceanogr 14:1315–1325
Petermann A (1865) Der Nordpol und Südpol, die Wichtigkeit ihrer Erforschung in geographischer und kulturhistorischer Beziehung. Mit Bemerkungen über die Strömungen der Polar-Meere. Pet Mitt Gotha, pp 146–160
Peterson BJ, McClelland J, Curry R, Holmes RM, Walsh JE, Aagaard K (2006) Trajectory shifts in the Arctic and Subarctic freshwater cycle. Science 313:1061–1066
Pfirman SL, Bauch D, Gammelsröd T (1994) The northern Barents Sea: water mass distribution and modification. In: Johannessen OM, Muench RD, Overland JE (eds) The polar oceans and their role in shaping the global environment. American Geophysical Union, Washington, DC, pp 77–94
Pickart RS, Spall MA, Ribergaard MH, Moore GWK, Milliff RF (2003) Deep convection in the Irminger Sea forced by the Greenland tip jet. Nature 424:152–156
Polyakov IV, Proshutinsky AY, Johnson MA (1999) Seasonal in the two regimes of Arctic Climate. J Geophys Res 104:25761–25788
Polyakov IV, Johnson MA (2000) Arctic decadal and interdecadal variability. Geophys Res Lett 27:4097–4100
Polyakov IV, Alekseev GV, Timokhov LA, Bhatt US, Colony RL, Simmons HL, Walsh D, Walsh JE, Zakharov VF (2004) Variability of the Intermediate Atlantic water of the Arctic Ocean over the last 100 years. J Clim 17:4484–4494
Polyakov IV, Beszczynska A, Carmack EC, Dmitrenko IA, Fahrbach E, Frolov IF, Gerdes R, Hansen E, Holfort J, Ivanov VV, Johnson MA, Karcher M, Kauker F, Morison J, Orvik KA, Schauer U, Simmons HL, Skagseth Ø, Sokolov VT, Steele M, Timokhov LA (2005) One more step toward a warmer Arctic. Geophys Res Lett 32(17):1–4. doi:101029/2005GL023740
Prinsenberg SJ, Bennett EB (1987) Mixing and transports in Barrow Strait, the central part of the Northwest passage. Cont Shelf Res 7:913–935
Prinsenberg SJ, Hamilton J (2004) The oceanic fluxes through Lancaster Sound of the Canadian Arctic Archipelago. ASOF Newsl 2:8–11
Proshutinsky AY, Johnson MA (1997) Two circulation regimes of the wind-driven Arctic Ocean. J Geophys Res 102:12493–12514
Quadfasel D, Gascard J-C, Koltermann K-P (1987) Large-scale oceanography in Fram Strait during the 1984 marginal ice zone experiment. J Geophys Res 92:6719–6728
Quadfasel D, Rudels B, Kurz K (1988) Outflow of dense water from a Svalbard fjord into the Fram Strait. Deep Sea Res 35:1143–1150
Quadfasel D, Sy A, Wells D, Tunik A (1991) Warming in the Arctic. Nature 350:385
Quadfasel D, Rudels B, Selchow S (1992) The Central Bank vortex in the Barents Sea: water mass transformation and circulation. ICES Mar Sci Symp 195:40–51
Quadfasel D, Sy A, Rudels B (1993) A ship of opportunity section to the North Pole: upper ocean temperature observations. Deep Sea Res 40:777–789
Redfield AC, Ketchum BH, Richard FA (1963) The influence of organisms on the composition of sea water. In: Hill MN (ed) The Sea, vol 2. Interscience, New York, pp 26–77
Riis-Carstensen E (1936) The "Godthaab" expedition 1928. The hydrographic work and material. Meddeleser om Grönland 78(3):101 pp

Roach AT, Aagaard K, Pease CH, Salo A, Weingartner T, Pavlov V, Kulakov M (1995) Direct measurements of transport and water properties through the Bering Strait. J Geophys Res 100:18443–18457

Rothrock DA, Yu Y, Maykut GA (1999) Thinning of the Arctic sea-ice cover. Geophys Res Lett 26:3469–3472

Ruddick B (1992) Intrusive mixing in a Mediterranean salt lens: intrusion slopes and dynamical mechanisms. J Phys Oceanogr 22:1274–1285

Ruddick B, Walsh D (1995) Observation of the density perturbations which drive thermohaline intrusions. In: Brandt A, Fernando HJS (eds) Double-diffusive convection. American Geophysical Union, Washington, DC, pp 329–334

Rudels B (1986a) The θ-S relations in the northern seas: implications for the deep circulation. Polar Res 4 ns:133–159

Rudels B (1986b) The outflow of polar water through the Arctic Archipelago and the oceanographic conditions in Baffin Bay. Polar Res 4 ns:161–180

Rudels B (1987) On the mass balance of the Polar Ocean, with special emphasis on the Fram Strait. Norsk Polarinstitutt Skrifter 188, 53 pp

Rudels B (1989) The formation of polar surface water, the ice export and the exchanges through the Fram Strait. Prog Oceanogr 22:205–248

Rudels B (1993) High latitude ocean convection. In: Stone DB, Runcorn SK (eds) Flow and creep in the solar system: observations, modeling and theory. Kluwer, Dordrecht, pp 323–356

Rudels B (1995) The thermohaline circulation of the Arctic Ocean and the Greenland Sea. Philos Trans R Soc Lond A 352:287–299

Rudels B (2001) Arctic basin circulation. In: Steele JH, Turekian KK, Thorpe SA (eds) Encyclopedia of ocean sciences. Academic, San Diego, pp 177–187. doi:10.1016/rwos.2001.0372

Rudels B (2009) Arctic Ocean circulation. In: Steele JH, Turekian KK, Thorpe SA (eds) Encyclopedia of ocean sciences 2nd ed. Academic, San Diego, pp 211–225. doi:016/B978–012374473–9.00601–9

Rudels B (2010) Constraints on the exchanges in the Arctic Mediterranean – do they exist and can they be of use? Tellus 62A:109–122

Rudels B, Friedrich HJ (2000) The transformations of Atlantic water in the Arctic Ocean and their significance for the freshwater budget. In: Lewis EL et al (eds) The freshwater budget of the Arctic Ocean. NATO science series 2: environmental security – vol 70. Kluwer, Dordrecht, pp 503–532

Rudels B, Quadfasel D, Friedrich H, Houssais M-N (1989) Greenland Sea convection in the winter of 1987–1988. J Geophys Res 94:3223–3227

Rudels B, Larsson A-M, Sehlstedt P-I (1991) Stratification and water mass formation in the Arctic Ocean: some implications for the nutrient distribution. Polar Res 10:19–31

Rudels B, Jones EP, Anderson LG, Kattner G (1994) On the intermediate depth waters of the Arctic Ocean. In: Johannessen OM, Muench RD, Overland JE (eds) The role of the polar oceans in shaping the global climate. American Geophys Union, Washington, DC, pp 33–46

Rudels B, Anderson LG, Jones EP (1996) Formation and evolution of the surface mixed layer and the halocline of the Arctic Ocean. J Geophys Res 101:8807–8821

Rudels B, Björk G, Muench RD, Schauer U (1999a) Double-diffusive layering in the Eurasian Basin of the Arctic Ocean. J Mar Syst 21:3–27

Rudels B, Friedrich HJ, Hainbucher D, Lohmann G (1999b) On the parameterisation of oceanic sensible heat loss to the atmosphere and to ice in an ice-covered mixed layer in winter. Deep Sea Res II 46:1385–1425

Rudels B, Friedrich HJ, Quadfasel D (1999c) The Arctic circumpolar boundary current. Deep Sea Res II 46:1023–1062

Rudels B, Muench RD, Gunn J, Schauer U, Friedrich HJ (2000a) Evolution of the Arctic Ocean boundary current north of the Siberian shelves. J Mar Syst 25:77–99

Rudels B, Meyer R, Fahrbach E, Ivanov VV, Østerhus S, Quadfasel D, Schauer U, Tverberg V, Woodgate RA (2000b) Water mass distribution in Fram Strait and over the Yermak Plateau in summer 1997. Ann Geophys 18:687–705

Rudels B, Jones EP, Schauer U, Eriksson P (2001) Two sources for the lower halocline in the Arctic Ocean. ICES CM 2001/W:15, 18 pp

Rudels B, Fahrbach E, Meincke J, Budéus G, Eriksson P (2002) The East Greenland Current and its contribution to the Denmark Strait overflow. ICES J Mar Sci 59:1133–1154

Rudels B, Eriksson P, Buch E, Budéus G, Fahrbach E, Malmberg S-Aa, Meincke J, Mälkki P (2003) Temporal switching between sources of the Denmark Strait overflow water. ICES marine science symposia: hydrobiological variability in the ICES area, 1990–1999, Edinburgh, 8–10 Aug 2001: Actes du symposium: posters presented at the symposium, vol 219, pp 319–325

Rudels B, Jones EP, Schauer U, Eriksson P (2004a) Atlantic sources of the Arctic Ocean surface and halocline waters. Polar Res 23:181–208

Rudels B, Marnela M, Eriksson P, Schauer U (2004b) Variability of volume, heat and freshwater transports through Fram Strait. In: ACSYS final science conference, St. Petersburg, Russia, 11–14 Nov 2003, extended abstracts. WCRP-118(CD)WMO/TD(1232)

Rudels B, Björk G, Nilsson J, Winsor P, Lake I, Nohr C (2005) The interactions between waters from the Arctic Ocean and the Nordic Seas north of Fram Strait and along the East Greenland Current: results from the Arctic Ocean-02 Oden expedition. J Mar Syst 55:1–30. doi:10.1016/j.jmarsys.2004.06.008

Rudels B, Marnela M, Eriksson P (2008) Constraints on estimating mass, heat and freshwater transport in the Arctic Ocean: an exercise. In: Dickson RR, Meincke J, Rhines P (eds) Arctic-Subarctic ocean fluxes. Springer, Dordrecht, pp 315–341

Ryder C (1891–1892) Tidligere Ekspeditioner til Grønlands Østkyst nordfor 66° Nr Br Geogr Tids Board 11, København, pp 62–107

Sadler HE (1976) Water, heat and salt transports through Nares Strait, Ellesmere Island. J Fish Res Board Can 33(10):2286–2295

Salmon DK, McRoy CP (1994) Nutrient-based tracers in the Western Arctic: a new lower halocline defined. In: Johannessen OM, Muench RD, Overland JE (eds) The polar oceans and their role in shaping the global environment, AGU geophysical monographs 85. American Geophysical Union, Washington, DC, pp 47–61

Schauer U (1995) The release of brine-enriched shelf water from Storfjord into the Norwegian Sea. J Geophys Res 100:16015–16028

Schauer U, Fahrbach E (1999) A dense bottom water plume in the western Barents Sea: downstream modification and interannual variability. Deep Sea Res I 46:2095–2108

Schauer U, Muench RD, Rudels B, Timokhov L (1997) Impact of eastern Arctic shelf water on the Nansen Basin intermediate layers. J Geophys Res 102:3371–3382

Schauer U, Loeng H, Rudels B, Ozhigin VK, Dieck W (2002a) Atlantic water flow through the Barents and Kara Seas. Deep Sea Res I 49:2281–2298

Schauer U, Rudels B, Jones EP, Anderson LG, Muench RD, BjörkG SJH, Ivanov V, Larsson A-M (2002b) Confluence and redistribution of Atlantic water in the Nansen, Amundsen and Makarov basins. Ann Geophys 20:257–273

Schauer U, Fahrbach E, Østerhus S, Rohardt G (2004) Arctic Warming through the Fram Strait: oceanic heat transports from 3 years of measurements. J Geophys Res 109:C06026. doi:10.1029/2003JC001823

Schauer U, Beszczynska-Möller A, Walczowski W, Fahrbahr E, Piechura J, Hansen E (2008) Variation of measured heat flow through the Farm Strait between 1997 and 2006. In: Dickson RR, Meincke J, Rhines P (eds) Arctic-Subarctic ocean fluxes. Springer, Dordrecht, pp 65–85

Schlichtholz P, Houssais M-N (1999a) An inverse modeling study in Fram Strait. Part I: dynamics and circulation. Deep Sea Res II 46:1083–1135

Schlichtholz P, Houssais M-N (1999b) An inverse modeling study in Fram Strait. Part II: water mass distribution and transport. Deep Sea Res II 46:1137–1168

Schlosser P, Bönisch G, Kromer B, Münnich KO, Koltermann K-P (1990) Ventilation rates of the waters in the Nansen Basin of the Arctic Ocean derived from a multi-tracer approach. J Geophys Res 95:3265–3272

Schlosser P, Böhnisch G, Rhein M, Bayer R (1991) Reduction of deep water formation in the Greenland Sea during the 1980s: evidence from tracer data. Science 251:1054–1056

Schlosser P, Bauch D, Fairbanks R, Bönisch G (1994a) Arctic river-runoff: mean residence time on the shelves and in the halocline. Deep Sea Res Part A 41:1053–1068

Schlosser P, Kromer B, Östlund G, Ekwurzel B, Bönisch G, Loosli HH, Purtschert R (1994b) On the ^{14}C and ^{39}Ar distribution in the central Arctic Ocean: implications for deep water formation. Radiocarbon 36:327–343

Schlosser P, Bönisch G, Kromer B, Loosli HH, Büler B, Bayer R, Bonan G, Koltermann K-P (1995) Mid 1980s distribution of tritium, ^{3}He, ^{14}C, ^{39}Ar, in the Greenland/Norwegian seas and in the Nansen Basin of the Arctic Ocean. Prog Oceanogr 35:1–28

Schlosser P, Kromer B, Ekwurzel B, Bönisch G, McNichol A, Schneider R, von Reden K, Östlund HG, Swift JH (1997) The first trans-Arctic ^{14}C section: comparison of the mean ages of the deep waters in the Eurasian and Canadian basins of the Arctic Ocean. Nucl Instrum Methods Phys Res Sect B 123:431–437

Serreze MC, Barrett A, Slater AJ, Woodgate RA, Aagaard K, Steele M, Moritz R, Meredith M, Lee C (2006) The large-scale freshwater cycle in the Arctic. J Geophys Res 111:C11010. doi:10.1029/2005JC003424

Shirshov PP (1944) Scientific results of the drift of station “North Pole”. Doklad na obshchem sobr. AN SSSR, Moscow, 14–17, fevralya

Skogseth R, Haugan PM, Jakobsson M (2005) Water mass transformations in Storfjorden. Cont Shelf Res 25:667–695. doi:10.1016/j.csr.2004.10.005

Smethie WM, Swift JH (1989) The tritium:krypton −85 age of the Denmark Strait overflow water and Gibbs Fracture zone water just south of Denmark Strait. J Geophys Res 94:8265–8275

Smethie WM, Chipman DW, Swift JH, Koltermann K-P (1988) Chlorofluoromethanes in the Arctic Mediterranean seas: evidence for formation of bottom water in the Eurasian Basin and the deep-water exchange through Fram Strait. Deep Sea Res 35:347–369

Smethie WM, Schlosser P, Bönisch G (2000) Renewal and circulation of intermediate waters in the Canadian Basin observed on the SCICEX 96 cruise. J Geophys Res 105:1105–1121

Smith JN, Ellis KM, Boyd T (1999) Circulation features in the central Arctic Ocean revealed by nuclear fuel reprocessing tracers from Scientific Ice Expeditions 1995 and 1996. J Geophys Res 104:29663–29667

Steele M, Boyd T (1998) Retreat of the cold halocline layer in the Arctic Ocean. J Geophys Res 103:10419–10435

Steele M, Morison JH, Curtin TB (1995) Halocline water formation in the Barents Sea. J Geophys Res 100:881–894

Steele M, Thomas D, Rothrock D, Martin S (1996) A simple model study of the Arctic Ocean freshwater balance, 1979–1985. J Geophys Res 101:20833–20848

Steele M, Morison JH, Ermold W, Rigor I, Ortmeyer M (2004) Circulation of summer Pacific water in the Arctic Ocean. J Geophys Res 109:C02027. doi:10.1029/2003JC002009

Stern ME (1967) Lateral mixing of water masses. Deep Sea Res 14:747–753

Stigebrandt A (1981) A model for the thickness and salinity of the upper layers of the Arctic Ocean and the relation between the ice thickness and some external parameters. J Phys Oceanogr 11:1407–1422

Stigebrandt A (1984) The North Pacific: a global-scale estuary. J Phys Oceanogr 14:464–470

Sverdrup HU, Johnson MW, Fleming RH (1942) The oceans: their physics, chemistry and general biology. Prentice-Hall, New York, 1042 pp

Swift JH, Aagaard K (1981) Seasonal transitions and water mass formation in the Icelandic and Greenland Seas. Deep Sea Res 28:1107–1129

Swift JH, Koltermann K-P (1988) The origin of the Norwegian Sea deep water. J Geophys Res 93:3563–3569

Swift JH, Aagaard K, S-Aa M (1980) The contribution of the Denmark Strait overflow to the deep North Atlantic. Deep Sea Res 27:29–42

Swift JH, Jones EP, Carmack EC, Hingston M, Macdonald RW, McLaughlin FA, Perkin RG (1997) Waters of the Makarov and Canada Basins. Deep Sea Res II 44:1503–1529

Swift JH, Aagaard K, Timokhov L, Nikiforov EG (2005) Long-term variability of Arctic Ocean water: evidence from a reanalysis of the EWG data set. J Geophys Res 110:C03012. doi:10.1029/2004JC002312

Talley LD, McCartney MS (1982) Distribution and circulation of Labrador sea water. J Phys Oceanogr 12:1189–1205
Tan FC, Strain PM (1980) The distribution of sea ice melt water in the eastern Canadian Arctic. J Geophys Res 85:1925–1932
Tang CCL, Ross C-K, Yao T, Petrie B, DeTracey BM, Dunlap E (2004) The circulation, water masses and sea-ice of Baffin Bay. Prog Oceanogr 63:183–228
Thompson DWJ, Wallace JM (1998) The Arctic oscillation signature in the wintertime geopotential height and temperature fields. Geophys Res Lett 25:1297–1300
Timmermans M-L, Garrett C, Carmack E (2003) The thermohaline structure and evolution of the deep waters in the Canada Basin, Arctic Ocean. Deep Sea Res I 50:1305–1321. doi:10.1016/S0967(03), 00125-0
Timofeyev VT (1960) Water masses of the Arctic basin. Gidromet. Izdat, Leningrad
Timofeyev VT (1962) The movement of Atlantic water and heat into the Arctic sea basin. Deep Sea Res 9:358–361
Toole JM, Georgi DT (1981) On the dynamics and effects of double-diffusively driven intrusions. Prog Oceanogr 10:121–145
Treshnikov AF (ed) (1985) Atlas of the Arctic. GUGiK, Moscow, 204 pp
Vowinckel E, Orvig S (1970) The climate of the North Polar Basin. In: Orvig S (ed) World climate survey, vol 14. Climates of the polar regions, vol 14. Elsevier, Amsterdam, 370 pp
Wadhams P, Holfort J, Hansen E, Wilkinson JP (2002) A deep convective chimney in the winter Greenland Sea. Geophys Res Lett 29. doi:0.1029/2001GL014306
Walczowski W, Piechura J (2006) New evidence of warming propagating toward the Arctic Ocean. Geophys Res Lett 33:L12601. doi:10129/2006GL025872
Walczowski W, Piechura J, Osinski R (2005) The West Spitsbergen Current volume and heat transport from synoptic observations in summer. Deep Sea Res I 52:1374–1391. doi:1016./j.dsr.2005.03.009
Walin G (1993) On the formation of ice on deep weakly stratified water. Tellus 45A:143–157
Wallace DWR, Schlosser P, Krysell M, Bönisch G (1992) Halocarbon ratio and tritium/^{3}He dating of water masses in the Nansen Basin, Arctic Ocean. Deep Sea Res A 39:443–458
Walsh D, Carmack E (2002) A note on the evanescent behavior of Arctic thermohaline intrusions. J Mar Res 60:281–310
Watson AJ, Messias M-J, Fogelqvist E, Van Scoy KA, Johannessen T, Oliver KIC, Stevens DP, Tanhua T, Olsson KA, Carse F, Simonsen K, Ledwell JR, Jansen J, Cooper DJ, Kruepke JA, Guilyardi E (1999) Mixing and convection in the Greenland Sea from a tracer release experiment. Nature 401:902–904
Weingartner TJ, Cavalieri DJ, Aagaard K, Sasaki Y (1998) Circulation, dense water formation and outflow on the northeast Chukchi Sea shelf. J Geophys Res 103:7647–7662
Weingartner TJ, Danielson S, Sasai Y, Pavlov V, Kulakov M (1999) The Siberian Coastal Current: a wind and buoyancy-forced arctic coastal current. J Geophys Res 104:29697–29713
Weyl PK (1968) The role of the oceans in climate change. Meteorol Monogr 8:37–62
Winsor P (2001) Arctic sea ice thickness remained constant during the 1990s. Geophys Res Lett 28:1039–1041
Winsor P, Björk G (2000) Polynya activity in the Arctic Ocean from 1958 to 1997. J Geophys Res 105:8789–8803
Winsor P, Chapman DC (2002) Distribution and interannual variability of dense water production from coastal polynyas on the Chukchi shelf. J Geophys Res 107(C7):3079. doi:10.1029/2001JC000984
Woodgate RA, Aagaard K (2005) Revising the Bering Strait freshwater flux into the Arctic Ocean. Geophys Res Lett 32:L02602. doi:1029/204GL021747
Woodgate RA, Aagaard K, Muench RD, Gunn J, Björk G, Rudels B, Roach AT, Schauer U (2001) The Arctic Ocean boundary current along the Eurasian slope and the adjacent Lomonosov Ridge: water mass properties, transports and transformations from moored instruments. Deep Sea Res I 48:1757–1792

Woodgate RA, Aagaard K, Weingartner T (2005) A year in the physical oceanography of the Chukchi Sea: Moored measurements from autumn 1990–1991. Deep Sea Res II 52:3116–3149. doi:10.1016/j.dsr2.2005.10.016

Worthington LV (1953) Oceanographic results of Project Skijump I and II. Trans Am Geophys Union 34(4):543–551

Worthington LV (1976) On the North Atlantic circulation, Johns Hopkins oceanographic studies no 6. The Johns Hopkins University Press, Baltimore, 110 pp

Wüst G (1941) Relief und Bodenwasser in Nordpolarbecken. Zeitschrift der Gesellschaft für Erdkunde zu Berlin 5(6):163–180